Spectroscopy to derive Engineering Parameters of Expansive Soils

Fekerte Arega Yitagesu

March, 2006

Spectroscopy to derive Engineering Parameters of Expansive Soils

by

Fekerte Arega Yitagesu

Thesis submitted to the International Institute for Geo-information Science and Earth Observation in partial fulfilment of the requirements for the degree of Master of Science in Geo-information Science and Earth Observation, Specialisation: geo-engineering.

Thesis Assessment Board

Prof. Dr. F.D. van der Meer	Chairman (and 1st supervisor)
Prof. Dr. S.B. Kroonenberg	External examiner
Ir. Wolter Zigterman	2nd supervisor
Drs. H.M.A van der Werff	3rd supervisor
Dr. P.M van Dijk	Programme Director

INTERNATIONAL INSTITUTE FOR GEO-INFORMATION SCIENCE AND EARTH OBSERVATION
ENSCHEDE, THE NETHERLANDS

Disclaimer

This document describes work undertaken as part of a programme of study at the International Institute for Geo-information Science and Earth Observation. All views and opinions expressed therein remain the sole responsibility of the author, and do not necessarily represent those of the institute.

Abstract

Expansive soils give rise to major problems that need due attention in geotechnical investigations. This is because of their characteristic to undergo large volume changes upon wetting and drying which have serious implications on the planning, design, construction, maintenance, and overall performance of civil engineering infrastructure.

Several researches have been done and various methods & techniques have been proposed and developed for the identification and characterization of expansive soils. However, the conventional testing methods are expensive, time consuming, labour intensive and continuous representation of sites is not possible. Hence, it is not uncommon to take a limited number of samples for analyses and interpolate the results as representative of the whole site. This under-sampling of sites can lead to a situation that the presence and types of expansive soils are overlooked. A great deal of effort, from the remote sensing society, has gone to developing a more reliable supporting method of conventional testing methods to help in avoiding such problems.

For this study, 80 soil samples were collected from the eastern part of Addis Ababa city. Much construction activities are taking place here and problems due to expansive soils are frequently reported. We measured specific expansive soil engineering parameters namely; Atterberg limits (liquid limits, plastic limits and plasticity indices), free swell and cation exchange capacity in a soil mechanics laboratory. We also acquired the reflectance spectra of each soil sample using the ASD fieldspec and PIMA spectrometers to establish a relationship between the engineering parameters and the soil reflectance spectra. Analyzing the engineering parameters as well as the spectral characteristics of the soil samples has revealed that the soil samples have a large variation in their expansion and shrinkage potential. Examination of the soil's plasticity nature resulted in grouping them into the five classes of the Casagrande soil plasticity classes (low, intermediate, high, very high and extremely high). Examination of their reflectance spectra resulted in grouping them into three mineralogical classes; Kaolinites, Mixtures and Smectites. Among the Smectites are Montmorillonite and Nontronite; and of the Kaolinites groups are Halloysite and Kaolinites.

We used a multivariate calibration method, partial least squares regression (PLSR) analysis to construct empirical prediction models to enable the estimation of engineering parameters of expansive soils from their reflectance spectra. Absorption feature parameters and simple wave length approaches were employed in establishing the empirical relation between the engineering parameters and the reflectance spectra of the soil samples. Correlation coefficients obtained showed that a large portion of the variation in the engineering parameters can be accounted for by the spectral parameters. The results of the prediction models are high, indicating the potential of spectroscopy in deriving engineering parameters of expansive soils from their respective reflectance spectra, and hence its potential applicability in the geotechnical investigations of such soils.

Key words: Expansive soils, spectroscopy, reflectance spectra, engineering parameters, absorption feature parameters, PLSR etc.

Acknowledgements

I would like to thank the Netherlands fellowship programme (NFP) and my employing organisation the Ethiopian Roads Authority (ERA) for giving me this opportunity to study at ITC.

My deepest gratitude goes to my supervisors, Prof. Freek van der Meer, Ir. Wolter Zigterman and Drs. Harald van der Werff. You have been of active support and assistance throughout the whole duration of this thesis research. Thank you for your advice, guidance, patience and encouragement; and the friendliness that you showed to me. I have learned a lot from you; above all the essence of a scientific research, to explore why things are as they are.

I would also like to acknowledge Ir. Siefko Slob for the valuable comments that he gave me. I am grateful to the staff and Programme Director of the AES programme, under whom I have learnt a lot for the past 18 months.

I am greatly indebted to Mr. Bekele Negussie, the Planning and Programming Division manager of the Ethiopian Roads Authority for he arranged my field work in Addis and offered a great deal of support to make it successful. I am also grateful to my friends and colleagues (Tadelle, Abdissa, Daniel, and Awoke…..) in ERA who also contributed towards the success of my field work. My heartfelt thanks go to Mr. Thsgaye, Tefera and Haileab who worked with me during the sampling and laboratory testing. I would also like to thank Mr. Tekeste of SUR Construction Company who kindly arranged some laboratory testing to be done in their laboratory, and Mr. Aderajew and his colleagues for performing the laboratory tests.

I would like to extend my sincere gratitude to Ing. W. Verwall & his family, and Mr. A. Mulder for their assistance and supervision in the laboratory during the CEC determination in Delft. I am also thankful to Drs. de Smeth who kindly arranged and helped in the laboratory work in ITC and TU Delft, also gave many valuable ideas. Drs. Frank van Ruitenbeek is thanked for his comments on spectral interpretations; Dr. D. J. Rossiter for his comments and the moral support; and Drs. J.K Kooistra for his help during acquiring the soil spectra.

My special thanks will go to my family; Abuye, Ruthi, Teni, for your love, constant support, understanding and encouragement. I love you. Getch, Efe, Nati, Dere, Marthi & Dave, Abeba, Gash Tade, thank you for being there for me.

Finally, my classmates and friends…I thank you all and wish you the best.

Dedicated to Abuye, Ruth and Teni.

Table of contents

List of figures

List of tables

List of Acronyms

AASHTO	American society of state highway and transportation officials
AAU	Addis Ababa University
ASD	Analytical spectral device
ASTER	Advanced Spaceborne and Thermal Emission Reflection Radiometer
ASTM	American society for testing materials
CEC	Cation Exchange Capacity
DTA	Differential thermal analysis
ERA	Ethiopian Roads Authority
FS	Free Swell
GSE	Geological survey of Ethiopia
LL	Liquid Limit
MB	Methylene blue
MBA	methylene blue absorption
MDC	Minimum distance to mean classification
meq	Millequivallents
MSC	Multiplicative scatter correction
PCA	Principal component analysis
PI	Plasticity Index
PIMA	Portable infrared mineral analyzer
PL	Plastic Limit
PLS	Partial Least Squares
PLSR	Partial Least Squares Regression
RMSEC	Root mean square error of calibration
RMSEP	Root mean square error of prediction
SEC	Standard error of calibration
SEP	Standard error of prediction
SL	Shrinkage limit
SWIR	Shortwave infrared
VNIR	Visible near infrared
XRD	X-ray diffraction

1. Introduction

1.1. Background

Among the different and most important engineering geological and / or geotechnical properties of clayey soils that have got critical implications on the planning, designing, performance and maintenance of civil engineering infrastructure are their potential to expand and shrink with varying amount of moisture content. Expansive soils occur in many parts of the world. However, the problem of expansion and shrinkage is associated with high moisture changes. Hence it is restricted in areas where the seasonal variation in climatic conditions is high (Bell, 1983). The large volume change with the periodic cycle of wetting and drying can cause extensive damages to civil engineering infrastructure; mainly on small buildings, shallow foundations and other lightly loaded structures including roads & airport pavements, pipelines etc (e.g. Chen, 1988; Day, 2001; Gourley et al., 1993; Kariuki, 2003; Nelson and Miller, 1992; Wilson, 1987).

The severity and magnitude of expansion and shrinking, and hence the damage associated varies depending among other things on clay mineralogy (Day, 2001). Many authors and researchers have confirmed the importance of mineralogical composition of clayey soils in governing their expansive nature (e.g. Chen, 1988; Day, 2001; Gourley et al., 1993; Mitchell, 1993). On the order of problems that these soils are capable of inducing smectite group clays ranked first followed by illite and kaolinite groups (Nelson and Miller, 1992). While smectite groups can exhibit tremendous volume changes, illites show moderate swell and kaolinites almost none.

In Ethiopia the occurrence and spatial distribution of expansive soils is significant (e.g. Chen, 1988; Mekonnen, 2004). Thus, the damage caused and restrictions posed by these soils on different activities mainly in engineering (which is our concern in this thesis research) and agriculture are high. In developing countries like Ethiopia, the time consuming and high costs of conventional site investigation and materials testing methods, can lead to proceedings of the main construction activities prior to getting adequate information on the occurrences and spatial distribution, types and constituents of expansive soils, etc. Goetz et al. (2001) mentioned that under-sampling of sites because of the high costs of standard testing techniques makes the problem worse.

Knowing the occurrence of expansive soils together with their spatial distribution and identification of the types of clay minerals involved is of utmost concern in the early stages of site investigation processes. This is to obtain information on the extent and magnitude of problems that should be expected. Hence, to enable the planning and formulation of the necessary counteracting measures and inclusions of appropriate design parameters and precautions possible. This will help to avoid or minimize the magnitude of damage on civil engineering infrastructure. Hawkins (1986) discussed the advantages of obtaining as much information as possible about a site in question before

proceeding into a detailed geotechnical investigation and testing procedures. He attributed this with getting more reliable information for producing environmentally compatible and economically sound designs of civil engineering infrastructure as follows:

"The more that is known about the site before examining it in the field, the more usefully can the time in the field be spent and attention can be concentrated on the important locations from an engineering point of view" (Hawkins, 1986).

It has been indicated in several studies (e.g. Gourley et al., 1993) that the conventional geotechnical investigation and materials testing methods should be supported by other methods. This aids for better understanding and identification of expansive soils and also to avoid some inaccuracies. Owing to this, a great deal of effort has gone into developing ways and techniques for supporting existing methods. Successful and promising results have been found for example by the use of remote sensing methods (e.g. Goetz et al., 2001; Kariuki, 2003; Van der Meer, 1999a).

Remote sensing methods are employed in the geotechnical investigation processes for obtaining information (e.g. geological, geomorphological, hydrological etc) about construction sites and materials (e.g. Bowles, 1984; Hawkins, 1986; Johnson and Pettersson, 1988). Use of remote sensing methods have an extra advantage of large area coverage, are rapid and less costly (Van der Meer, 2004a). Besides, continuous sampling is possible for identification of clay mineralogy (e.g. Goetz et al., 2001; Kariuki, 2003). Hence, it is an attractive and indispensable option that should be employed in the site investigation processes for supporting the geotechnical investigation of expansive soils.

1.2. Problems due to expansive soils in Ethiopia

Expansive soils cover a large portion of Ethiopia. According to information obtained from literature about 10 % of the country's land is covered by Vertisols (Berhanu, 1983) or by their commonly known name 'Black cotton soils' alone. The dominant clay minerals of these soils are indicated to be the smectite groups and are mainly nontronite & montmorillonite clays (Berhanu, 1983). According to Berhanu (1983) illitic minerals also constitute significant portion of these soils. Others (e.g. Mekonnen, 2004; Netterberg, 2001) have reported the occurrences of clay soils of mixed mineral composition with significant smectite contents in various parts of the country. At places where expansive soils are abundant, they are well known by their adverse property which poses difficulties of different types in fields mainly engineering and agriculture.

Expansive soils are known to pose severe problems on construction activities; which can lead to expensive design and construction costs, mitigation measures as well as repeated and costly maintenance works. The following are the major engineering difficulties that are apparent due to the adverse properties (large changes in their volume with variation in moisture content which is related to periodic cycle of drying and wetting) of these expansive soils.

1.2.1. Differential settlement

This can cause cracking, rutting and deformations in general distresses on road and runway pavements, failure of drainage structures (bridges, culverts) etc. Similar cracking and deformation problems can also be induced on foundation slabs and walls of small buildings, pipe lines & sewerage systems and other similar light weight structures.

As far as the road infrastructure are concerned, the differential settlement creates series of bumps or corrugations, potholes & patches on different road sections in various parts of the country which in turn reduces the riding quality of roads. Thus the owner of the country's road network, the Ethiopian Roads Authority (ERA) was forced to decrease the maximum speed limits below the original design speeds at many localities for instance on the main road connecting Addis Ababa and Jimma town (Netterberg, 2001). Costly and repeated maintenance requirements were also frequently demanded as a result of such problems.

A similar problem has resulted in reconstruction of the runway at the Bole international airport during the upgrading and extension of the runway few years ago. Signs of failures and cracking of the runway pavement were apparent immediately following the first rainy season after completion of the construction.

Figure 1-1: Problems of deformation and cracks on Addis Ababa - Jimma road sections (Netterberg 2001) due to the presence of expansive soils beneath the sub-grade.

1.2.2. Instability of cut slopes

Cut slopes on these soils are prone to instabilities and slope movements due to erosion, heaving and slumping. In places where they are overlain by stiff material the stiffness contrast can lead to even larger problems. Problems of clogging of road side ditches and culverts are common difficulties that demanded the allocation of high budgets for the clearing and maintenance of such drainage structures every year (Ethiopian Roads Authority, 2001).

1.2.3. Gully formations

Gully formation is associated with the poor permeability and erosion susceptibility nature of these soils. This poses negative and serious economical as well as environmental problems. Scouring of drainage structures seriously affects the overall performance of road infrastructure in many localities. Erosion of soils and hence degradation of environment is also another issue of great national concern that is associated with the properties of these types of soils. There are lots of claim cases from farmers every year (EMSB, 2000) complaining that concentrated runoff from road drainage structures are causing severe erosion on their farm lands and grazing plots etc., which in turn demands extensive as well as expensive erosion control and mitigation requirements out of the right-of-way of the road alignments. This raises the cost of constructing road networks in those places where the occurrence of expansive soils is dominant.

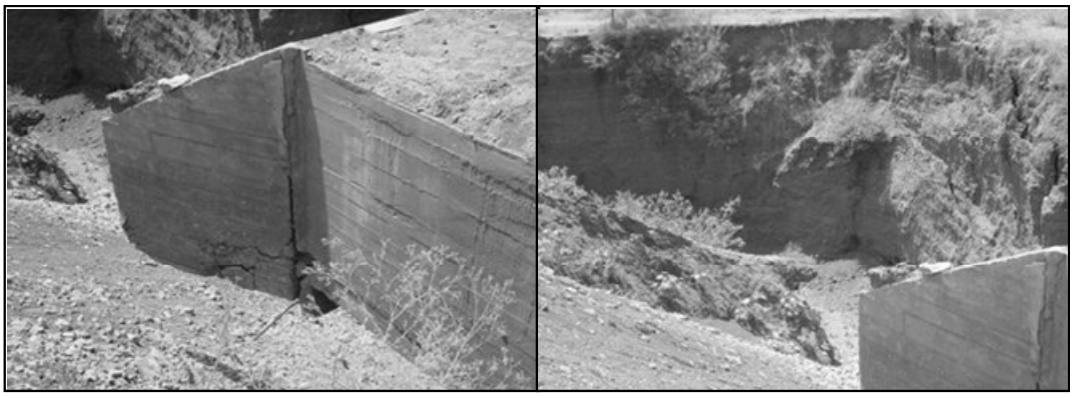

Figure 1-2: Gully formation which leads to scouring and subsequent failure of a box culvert that was founded on expansive soil on the Awash – Hirna feeder road section (EMSB, 2000).

1.2.4. Difficult ground operations

Due to their sticky and slippery character when saturated with water, the workability of these soils is poor. This in turn is attributed to the difficulty in excavating them, accessibility restrictions to sites of construction and material production (borrow pits and quarry sites), hence time delays in construction activities. This has a negative implication on the cost of construction activities.

"When clay soils are wet, they swell and become plastic- thick, slick and heavy. During the dry season, which lasts from late October to late May (with occasional rain in between), these once-waterlogged soils lose their moisture and shrink. Cracks, some as large as 10 centimetres and 1 meter deep are not uncommon." (SINET, 1987)

In general, engineering problems due to expansive soils have remained one of the biggest challenges in the construction sector in Ethiopia. Even if there is no statistics available on the cost consequences and the amount of damage caused by this problem, there have been serious economical losses and substantial increases in cost of constructions which in many times exceeds the initial cost estimates of construction projects and the allocated budgets & available fund. The

failure of the main road connecting Addis Ababa to one of the biggest coffee producing district centre Jimma town was among those. Various portions of this road have suffered from failure which is attributed to the expansion and shrinkage of active clayey soils beneath the sub-grade (Netterberg, 2001). The presence of these expansive soils and their high expansion potential was overlooked during the site investigation period and the problem was not properly addressed in the design.

In this thesis research, the focus is on the engineering behaviour and the associated problems of expansive soils in an attempt to establish a relationship between engineering parameters of these soils and their reflectance spectra determined in the laboratory. However it should also be noted that clay soils of certain mineral composition and physical properties that have the ability to achieve low hydraulic conductivity; and capacity to remove certain toxic materials (the presence of iron oxide and organic matter enhances the retention capacity of heavy metals or contaminants like Pb, Zn, Mn, Cd) have important engineering uses such as land fill liner, drilling mud, construction materials etc (Gillott, 1968). Expansive soils can be used to seal landfills storing hazardous wastes to avoid for example, the downward migration of contaminants to ground water. Gillott (1968) has also mentioned some other commercial uses of certain clay minerals and soils.

1.3. Specific problems

- Clay soils having a potential to undergo significant volume changes (expansion and shrinkage) with periodic cycle of drying and wetting, pose difficulties and damage on civil engineering infrastructures in the study area.

- Conventional standard methods of assessing the geotechnical properties of these soils are expensive, labour intensive, time consuming and it is not possible to get continuous representation of soil masses in space. Hence, the presence & spatial distribution of these soils can be overlooked and their types not precisely determined.

- Thus there is a need to identify these expansive soil types & their constituents, and to determine their respective engineering parameters that can indicate their expansion potential in a method that is cheaper, rapid and continuous as compared to the conventional methods of assessing geotechnical properties of these soils.

1.4. Research objectives

The main objective of this thesis research will be to derive empirical models from reflectance spectra of soils for predicting engineering parameters and characterizing different types of expansive soils and their constituents.

1.4.1. Specific objectives

- To establish a relationship between laboratory determined expansive soil engineering parameters and soil reflectance spectra.

- To identify characteristic spectral features diagnostic of engineering parameters that can be used in identification of expansive soils such as Atterberg limits, cation exchange capacity and free swell.

- To determine the applicability of reflectance spectroscopy in identifying different types of potentially expansive soils, and their constituents. And investigate its contribution to geotechnical investigation processes in identifying expansive soils and predicting their expansion potential.

- To re-sample the laboratory determined soil spectra into ASTER band passes and see whether they can be linked with engineering parameters of expansive soils.

1.5. Research questions

- Is it possible to establish a relationship between the laboratory determined engineering parameters of expansive soils & their spectral reflectance, and develop prediction models to estimate the expansion potential of these soils?

- Is it possible to determine engineering parameters, recognize and hence discriminate between different types of expansive soils using reflectance spectroscopy?

- Which spectral parameters can best describe or are diagnostic of engineering parameters of expansive soils such as Atterberg limits (PL, LL, and PI), cation exchange capacity (CEC) and free swell?

- How can reflectance spectroscopy contribute to site investigation?

- How much information can be obtained from the spectra that are re-sampled to ASTER band passes?

1.6. Research hypotheses

Clay soils that have mineral composition & physical properties causing significant volume changes (a potential of expansion and shrinking) due to variation in moisture contents pose engineering difficulties and damage on civil engineering infrastructures. The difficulty and damage posed by these soils depend on their mineralogy and physical properties together with their abundance in space.

Hypothesis 1:

Based on differences in mineral composition and the different responses & spectral characteristics (peak reflectance & distinct absorption features) which are a function of wavelength (Clark, 1999), it is possible to identify different types of clay soils and also their constituents. The applicability of reflectance spectroscopy in the determination of mineralogy and providing information on the chemical composition is discussed by many researchers (e.g. Clark, 1999; Van der Meer, 2004a, b).

"Photons are absorbed in minerals by several processes. The variety of absorption processes and their wavelength dependence allows us to derive information about the chemistry of a mineral from its reflected or emitted light" (Clark, 1999)**.**

Hypothesis 2:

A relationship can be established between laboratory determined expansive soil engineering parameters and soil reflectance spectra. Hence models can be derived to predict the various engineering parameters (those that are indictors of expansion potential) and constituents of the soils. Models can explain a large portion of the total variation in engineering parameters.

Kariuki (2003) showed that clay mineralogy is a major factor in determining soil physiochemical and spectral characteristics. He also developed empirical models to estimate the expansion potential of such soils from spectral data. Farshad and Farifteh (2002) on the other hand found high correlations between soil reflectance and soil properties including mineralogy. But the question here is whether models that are developed in one place are universally applicable or not. It is unlikely that these models are universally applicable due to environmental specific soil forming factors; parent materials, climate, topography, organic matter & human activity, and also time (Fitzpatrick, 1980; Gray and Murphy, 2002) differences in different environment.

Hypothesis 3:

It is possible to determine engineering parameters of expansive soils using reflectance spectroscopy with a reasonable degree of certainty.

Van der Meer (1999) discussed characteristic spectral features of clay minerals that will enable to discriminate among the different varieties. Kariuki (2003) described major absorption features that characterize the reflectance spectra of clay minerals in the SWIR wavelength region. He also demonstrated linear regression models linking soil properties indicating expansion potential with absorption feature parameters.

Hypothesis 4:

Reflectance spectroscopy can contribute to site investigation process by providing with a cost effective & rapid information of large area coverage (e.g. Goetz et al., 2001; Van der Meer, 2004a) on engineering parameters of expansive soils. It can also support the conventional geotechnical testing methods by providing with additional or complementing information (e.g. mineralogical identification) and hence help to avoid under-sampling of sites.

1.7. Methodology and thesis structure

This thesis research encompassed field work preparation, field work data collection and post field work data analysis stages. Prior to the field work, one of our major tasks was the identification of

engineering parameters of expansive soils that are good indicators of their expansive potential together with proper sampling methodology designing that should be employed in the collection of soil samples so as to obtain soil samples of variable expansion potential from low to high. Literature review and gathering of as much information as possible about the study subject and the study area were also some of the major activities in the pre-field work stage.

During the field work stage soil samples were collected for subsequent laboratory analysis. In addition, any other data of relevance (maps, reports and previous studies) were also collected. After obtaining the laboratory results of engineering parameters and the soil reflectance spectra we proceeded into the data preparation & compilation, processing, integration, analysis and interpretation stages. The different stages & the methods employed are elaborately described in chapter 4. The following figure, figure 1.3 shows a briefly summarized schematic work flow of the various steps that were undertaken to achieve the objectives of the research.

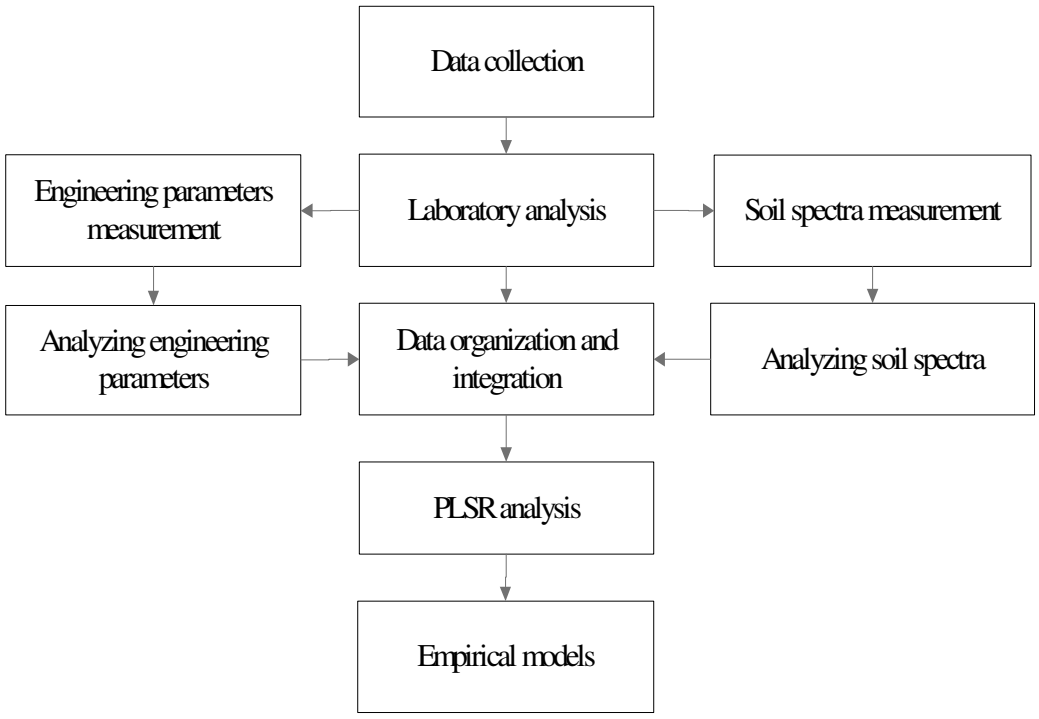

Figure 1-3: Schematic work flow diagram.

The thesis is divided into seven separate chapters. This chapter (chapter one) provides an introduction to the topic. It also discussed the engineering problems and difficulties that are associated with potentially expansive soils, and the overall objectives of the thesis including a brief description of the research methodology. Chapter two dealt with relevant literature review and summarizes various aspects related to the research topic. In this chapter, some conventional geotechnical techniques that are useful for identification of potentially expansive soils are presented. The roles of remote sensing techniques in this respect are also reviewed. Chapter three gave description of the study area and its location. We also described why this particular area was found

to be of interest with respect to this thesis research. Chapter four reviewed the materials and methods for this thesis research. It also included details of field work sample collection, laboratory analysis of engineering parameters and spectral measurements followed by subsequent interpretation and analysis of the results. The data exploration and preliminary analysis using different statistical tools is presented in chapter five. Partial least squares regression (PLSR) analysis to predict expansive soil engineering parameters from their reflectance spectra is illustrated in chapter six. The conclusions and recommendations for future prospect are summarized in the last chapter, chapter seven.

2. Literature review

2.1. Expansive soils

Detailed geotechnical investigation of the ground mass and determination of engineering properties of construction materials are the most important components of any civil engineering design work. This is to ensure the stability, cost effectiveness, overall performance and environmental compatibility of the designed structures (e.g. Hawkins, 1986). In doing so identification and characterization of expansive soils and determining their expansion potential is one of the major concerns (Day, 2001). This is specially the case when dealing with light weight structures like road infrastructures, airfields, and small buildings etc.

Gourley et al. (1993) defined expansive soils as soils of clay composition that have got a characteristic property to undergo significant volume changes upon wetting and drying. Such soils expand or swell when moistened and shrink & crack when dried. Some terrain and surface morphological features associated with the occurrences of expansive soils for example surface crusting, gilgai, polygonal cracks and popcorn structures etc. are mentioned. Figure 2.1 shows polygonal cracking & popcorn structures exhibited by expansive soils in dry periods. Expansive soils are largely recognised, among other things, for the problems and considerable damage that they can pose in construction sector. The damage is adverse and is mainly restricted to light weight structures (e.g. Chen, 1988; Gourley et al., 1993; Kariuki, 2003; Thomas, 1998) where the downward pressure exerted from the structure is exceeded by the uplift pressure from the soil swell. Goetz (2001) mentioned that the damage from expansive soils exceeds the damage caused by all other natural hazards combined together. It has been reported that the damage caused by these soils contributes significantly to the burden that natural hazards pose on the economy (Nelson and Miller, 1992) of countries where the occurrence of these soils is significant. Ethiopia is among the list of countries in which the occurrence and spatial distribution of expansive soils (e.g. Chen, 1988; Thomas, 1998) is recognised as significant.

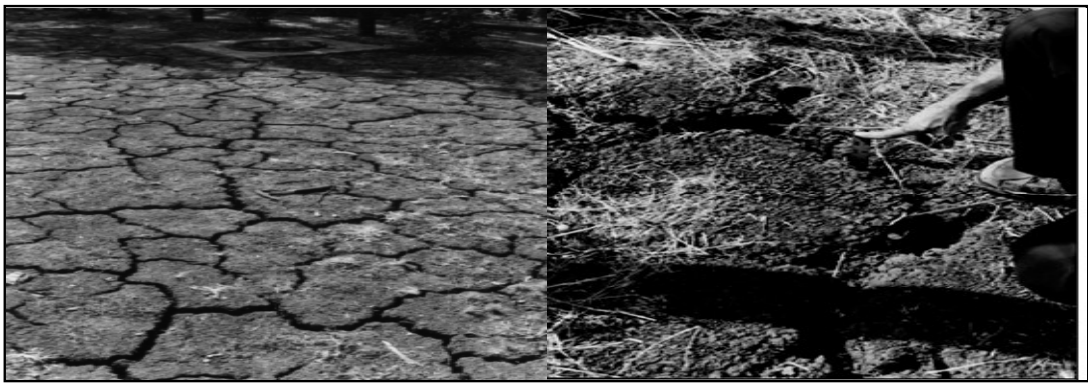

Figure 2-1: Cracking of expansive soil during dry periods (Rogers et al., 2000), note the polygonal cracking patterns and popcorn structures formed.

Different factors are attributed to be responsible for causing the change in volumes of these soils. These include the presence, amount and type of clay minerals in the soil (e.g. Chen, 1988; Day, 2001; Mitchell, 1993) which are also found to be the major ones coupled with significant changes in climatic condition between wet and dry seasons. Perloff and Baron (1976) stated that most of the properties associated with expansive soils are the result of the electrochemical properties of clay minerals. Clays have large specific surface area and net negative charge. Hence, when they come in contact with water they can absorb a great deal of water which is subsequently coupled with a great deal of volume change. Rogers et al. (2000) demonstrated cases of foundation distresses due to uplift pressure and the mechanism of swelling and shrinking phenomena. Other factors include soil water chemistry contained within voids, soil structure & fabric, dry density, grain size, state of stress, magnitude of loading and other environmental factors (Nelson and Miller, 1992).

Three groups of clay minerals are often described as important for engineering purposes (Nelson and Miller, 1992) namely; kaolinite groups, mica like groups which includes illites and vermiculites, and smectite groups. Researchers have developed relations between clay mineralogy and soil expansion or swelling potential, and grouped various clay minerals into different swelling classes (Chen, 1988).

2.2. Identification and classification

Various methods and techniques are developed by soil scientists and geotechnical engineers to obtain information on the physical, chemical and mineralogical properties of expansive soils. This is to help in the recognition and characterization of these soils, and to estimate the magnitude of damage that might be faced. Chen (1988), and Nelson and Miller (1992) grouped the methods into three categories; namely mineralogical identification, indirect measurements (index properties) and direct measurements.

Among the mineralogical identification methods are x-ray diffraction (XRD), differential thermal analysis (DTA), dye absorption, chemical analysis and electron microscope resolution methods. These methods are important in research laboratories in exploring the basic properties of clays. But they are costly and hence not commonly used in soil mechanics laboratories (Chen, 1988).

Researchers have established thresholds of some chemical properties of soils for instance cation exchange capacity (CEC) of different clay types, and established relationship with soil expansion potential (e.g. Chen, 1988). Table 2.1 shows the range of CEC in different clay minerals with their respective expansion potential.

Clay mineral	CEC (meq/ 100g)	Expansion potential
Kaolinite	3-15	Low
Illite	10-40	Moderate
Smectite (montmorillonite)	60-100	High

Table 2-1: Ranges of cation exchange capacity of the three main clay minerals and the respective expansion potential that they can exhibit (Bell, 1983; Chen, 1988).

Cation exchange capacity is used as a measure of soil expansion and shrinkage potential in engineering applications. Clay minerals have high capacity to hold exchangeable cations due to their chemical structure (e.g. Chen, 1988; Perloff and Baron, 1976). However, various types of clay minerals are observed to exhibit different magnitudes of cation exchange capacities (e.g. Chen, 1988; Bell, 1983, Day, 2001; Nelson and Miller, 1992; Wilson, 1987 etc). While the smectite group clays show the highest CEC, the kaolinite group clays exhibit the lowest CEC.

Under the indirect methods are Atterberg limits (liquid limit (LL), plastic limit (PL), plasticity index (PI), and shrinkage limit (SL)), free swell, colloid contents and linear shrinkage tests etc. These methods are the most widely used in engineering work for purposes of classification of soils and assessment of their expansion potential (e.g. Chen, 1988; Day, 2001; Nelson and Miller, 1992). Brief explanation about these indirect methods (Atterberg limits and free swell tests) and their determination is included in chapter 4.

Especially the Atterberg limits are considered very popular indicators of soil swelling potential. Atterberg limits are related to the amount of water attracted to the surfaces of the soil particles. Hence, they show the various states of consistency of cohesive soils in relation to their moisture content. Water has a significant influence on the physical properties of cohesive soils. Therefore, knowing the different states at which soils exist with varying amount of moisture content is of geotechnical interest. For example plasticity indices show the range of moisture content over which the soil remains plastic (Lambe and Whitman, 1979). The higher the plasticity index the higher the plasticity and compressibility of the soils, also the greater the change in volume that they can exhibit. Atterberg limits are of high importance not only because they are indicators of soil expansion potential. They are also used in identifications and classifications of cohesive soils for engineering purposes. Besides, there is a good correlation between Atterberg limits and strength of cohesive soils (e.g. Perloff and Baron, 1976). Perloff and Baron (1976) have also mentioned the work of Skempton and Northey (1952) which showed that Atterberg limits can give an indication of sensitivity of soils when they are coupled with measurements of natural moisture contents of soils. Owing to these relevance, Atterberg limits are directly used in construction specifications for controlling the quality of construction materials that will be used in fill, embankment and sub-base constructions etc (e.g. AASHTO, 2002; ASTM, 1989; British Standard Institution, 1981 etc.).

Thresholds are developed and relations are established between Atterberg limits and expansion potential of soils as well as the types of clay minerals in the soils (e.g. Nelson and Miller, 1992). Table 2.2 shows some of the established relationships. Researchers have observed an increase in the

liquid limit and plasticity indices of soils with an increase in soil expansion potential (e.g. Chen, 1988; Lambe and Whitman, 1979). Whereas no specific conclusions were given about the plastic limits of soils on this respect; instead wide range of overlapping numbers are common for different types of clays with variable expansion potential.

	Atterberg limits			
Clay mineral type	**LL %**	**PL%**	**SL%**	**Expansion potential**
Kaolinite	10-20	30-100	25-29	Low
Illite	60-120	35-60	15-17	Moderate
Smectite (Montmorillonite)	100-900	50-100	8.5-15	High

Table 2-2: Relationships between soil expansion potential, Atterberg limits and types of clay minerals (Nelson and Miller, 1992).

There is no single characteristic value of LL, PL and PI for a particular type of clay mineral. This is due to the inherent structure and composition within the crystal lattice of clay minerals and variations in the exchangeable cation compositions (Bell, 1983). For example Bell (1990) and, Perloff and Baron (1976) indicated differences in Atterberg limits of montmorillonite clays having different types of exchangeable cations. They reported that Li and Na montmorillonite showed the highest liquid limits and hence plasticity indices followed by Ca, Mg, K, Al montmorillonite respectively. They also mentioned that the plasticity indices of Li and Na montmorillonite range between 300-600 %. Whereas montmorillonite with other cations have plasticity indices between the ranges of 40-300 % (e.g. Bell, 1983; Bowles, 1984; Perloff and Baron, 1976). As far as crystal lattice structure and particle sizes are concerned, it is reported that they can influence for example the liquid limit and plasticity indices of kaolinite clays. Higher values of LL are indicated for poorly crystallised & fine grained kaolinites while very low values were coupled with well crystallised and coarser grained kaolinite clays. Plasticity indices of 8-40 % are reported for kaolinite clays (Grim, 1992 cited in Perloff et al 1993). The same kind of influence is also recognised in case of illite clays. Presence of smectites was in general noted to cause substantial increase in the Atterberg limit values of clays (e.g. Bell, 1983; Bowles, 1984; Gourley et al., 1993; Perloff and Baron, 1976).

Bell (1983) discussed the importance of free swell tests in assessing volume changes of soils and indicated the free swell ranges of different clay minerals. Kaolinite clays were reported to show the smallest free swell. Illite may swell up to 15 %, whereas inter-mixed illite and montmorillonite was observed to swell up to 60-100 %. The montmorillonite clays were mostly found to exhibit larger free swell percentages. But there are also variations in the free swell of different kinds of montmorillonite clays. For example Ca montmorillonite was noted to show lesser swelling (50-100 %) than the Na variety (Bell, 1983) which is characterized by a much higher free swell values. Nelson and Miller (1992) indicated that soils showing a free swell value of 100 % and above might exhibit considerable expansion and shrinkage properties under light loadings. Hence such soils should be viewed with caution. Soils with a free swell value of 50 % and less were mentioned to be less prone to significant volume changes. However, free swell tests can only give a crude estimate of soil expansion potential and are not considered as such reliable for they suffer from certain limitations. Examples are the difficulty to measure a loose volume of exactly 10 cm^3 of soil (because

of the higher sensitivity of the volume to hygroscopic moisture) and the methods of pouring (Head, 1980). Hence the use of free swell tests is somehow limited to the preliminary geotechnical investigation stages to get an overall picture of the characteristic expansion potential of soils.

Direct measurement involves the use of consolidation apparatus or oedometer to measure the swelling pressure that can be exerted by the soil expansion. This method should be done in a sophisticated and controlled conditions with all the anticipated environmental conditions fulfilled. It gives an opportunity of directly observing the effects of soil expansion on different scale or magnitude of loadings that resembles the actual conditions. It is the most common and useful swell & heave prediction test method (Nelson and Miller, 1992). However, it might take several days and loading steps before the swell pressure is determined even for a single sample which in turn makes it an expensive and labour intensive testing method.

Even though researchers have succeeded in formulating methods and developing standard techniques for characterization of expansive soils, all these conventional methods are hampered by one common problem. The methods are costly and time consuming. Hence, it is not uncommon to take a limited number of samples per a given area (e.g. Goetz et al., 2001; Seed et al., 1962) and interpolate the results for the un-sampled parts. It is also impossible to obtain a continuous representation of soil masses in the geographic space. Thus, the identification of soils requiring further detailed geotechnical investigation and analysis remains difficult. Engineers have for long been claiming that the major reason which contributes to the damage caused by expansive soils is a tendency to overlook their presence. They attributed this to the under-sampling of sites followed by underestimation of their expansion potential rather than lack of proper design.

The problem of overlooking the presence of expansive soils and lack of obtaining continuous representation has motivated researchers to look for another method that can offer an easy, inexpensive and continuous way of representation & identification of these soils (e.g. Goetz et al., 2001; Kariuki, 2003; Van der Meer, 1999a). These methods are required for a better understanding of their nature and properties of the soils, to assist in assessing the suitability of sites for construction purposes and develop a reliable way of estimating soil expansion potential.

2.3. The role of remote sensing

It has long been known that remote sensing plays a vital role and have got a wide range of applications in geotechnical investigations. Use of aerial photographs have stayed and will remain to be an integral part of reconnaissance surveys for construction site selections (e.g. British Standard Institution, 1981). Geotechnical investigation is benefiting a lot from the use of satellite images too. Johnson and Pettersson (1988) illustrated case studies on some of the applications of satellite imagery (e.g. Landsat/MSS and radar images) in this respect. Much information about the sites of interest can be obtained from aerial photograph and image interpretation. Examples are delineating tectonic features like faults, lineaments, folds, subsidence etc. Also, identifying geomorphic features for instance landslides, erosional features and other kinds of ground instabilities, in general

engineering geological hazards. Remote sensing has also proved to be useful in the allocation of potential construction material sites.

With the current development in technology, remote sensing methods allow the possibility of identification and mapping of different mineral types. Of which reflectance spectroscopy is found to be an excellent tool in deriving information about clay mineralogy (Clark, 1999).

2.3.1. Spectroscopy

Clark (1999) defined spectroscopy as a study of light as a function of wavelength that is emitted, absorbed, reflected or scattered from materials either solid, liquid or gas. When light interacts with a mineral, some of it is reflected from the grain surfaces, some pass through the grain and some are absorbed. Reflectance spectroscopy is a study of light reflected from materials to get qualitative or quantitative information of their nature and properties.

"Light is absorbed in minerals by several processes. The variety of absorption processes and their wavelength dependence allows us to derive information about the chemistry of a mineral from its reflected or emitted light." (Clark, 1999)

Spectroscopy is found to be sensitive to specific chemical bonds in materials. Researchers have observed shifts in position and variation in shape of absorption features with variation in chemical composition of materials (e.g. Clark, 1999; Kariuki, 2003; Van der Meer, 1995). Spectroscopy can be used in laboratories & field where one will be able to take close measurements using laboratory and field spectrometers. It is also possible to acquire hyperspectral images for hyperspectral imaging devices are available.

Kruse et al. (1990) showed the potential applicability of imaging spectroscopy in mineral mapping and pointed out that it can be a powerful tool in the future. Van der Meer (2004) discussed the contribution of field and laboratory reflectance spectroscopy in mineralogical and chemical compositional analysis in various disciplines; soil science, mineralogy and vegetation science. He demonstrated the vital role that reflectance spectroscopy can play in surface compositional mapping. He also cited numerous other research works that were done on this respect in an attempt to extract quantitative information of mineralogy and other chemical properties of materials from spectral data.

The application of spectroscopy lies on analysing spectral features or parameters named absorption feature parameters: absorption feature position, depth, area, width and asymmetry. Figure 2.2 shows absorption feature parameters on a continuum removed spectra.

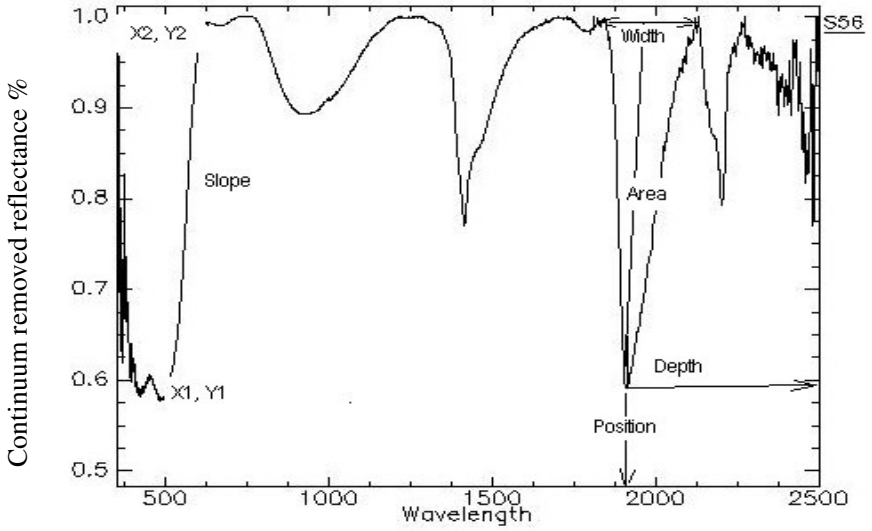

Figure 2-2: Absorption feature parameters (after Van der Meer, 1995).

- Absorption feature position is the wave length at which minimum reflectance is observed.
- Relative absorption depth is the depth of the absorption feature.
- Relative absorption area is the area of the absorption feature.
- Relative absorption width is the distance between the left and right shoulder of wave length band.
- Asymmetry is the ratio of the area left of the absorption centre to the area right of the absorption centre.

Van der Meer (1995) also mentioned that a slope parameter can be calculated as the slope of the spectral curve at any wavelength of interest.

Slope is calculated as; $\frac{y2 - y1}{x2 - x1}$ where Y is reflectance and X is wavelength.

2.3.2. Reflectance properties of soils and clay minerals

Van der Meer (2001) mentioned that spectral reflectance characteristics of soils are the result of their physical and chemical properties, and they are largely influenced by their composition. Electronic and vibrational processes are responsible for the prevalence of absorption bands in the spectra of minerals (Clark, 1999).

Reflectance spectra of minerals are dominated by the presence or absence of transition metal ions in the visible to near infrared wavelength regions of the electromagnetic spectrum. The presence or absence of iron oxides and hydroxides in soils are important since these can influence some properties of soils for example their cation exchange capacity (McSweeney, 1999). Especially if such minerals occur in amorphous form rather than being in crystalline form, the large specific surface area & porous structure can amplify the cation exchange capacity of the soils. Researchers

were able to identify Fe- related characteristic spectral features and hence spectrally discriminate various iron oxide and hydroxide minerals from spectral data (e.g. Crowley et al., 2003).

Reflectance spectra of minerals in the SWIR region of the electromagnetic spectrum are dominated by the presence or absence of water and hydroxyl molecules. As far as clay minerals are concerned, there is a well established observation of their spectral characteristics in this wavelength region. For example it is documented that the water bearing clay mineral groups, smectites produce absorption features due to the OH stretching at ~1400 nm & due to the combination of H-O-H bending and OH stretching near ~1900 nm. Combination of fundamental OH stretching and bending with Al, Mg, or Fe ions are known to produce absorption features at ~2200 – 2300 nm , and these are diagnostic of clay minerals (Clark, 1999).

It has been found that absorption feature parameters such as depth, position, width, area and asymmetry are influenced by the chemistry of minerals (e.g. Chabrillant and Goetz, 1997-2000; Kariuki, 2003; Van der Meer, 2004a). Hence, analysing these parameters can give qualitative compositional information of minerals as well as quantitative estimates of certain properties.

Researches have been done to establish relationship between properties of minerals and absorption feature parameters of which clay minerals were also of concern. Table 2.3 shows the major clay mineral related absorption feature positions and the causes of the absorptions coupled with the type of clay minerals involved.

Major feature position	Molecule	Clay mineral
1400 nm	OH & H_2O	Kaolinite/ Smectites / Illites
1900 nm	H_2O	Smectites/ Illites
2170 nm	Al-OH	Kaolinites
2200 nm	Al-OH	Kaolinite/ Smectites / Illites
2290 nm	Fe-OH	Smectites (Nontronite)
2300 nm	Mg-OH	Smectites (Hectorite)
2340 nm	Fe-OH/ Mg-OH	Illite
2384 nm	Fe-OH	Kaolinite

Table 2-3: Major clay mineral related absorption feature positions, molecules causing the absorption and the types of clay minerals (after Hauff, 2000 cited in Kariuki, 2004).

3. Study area

3.1. Description of the study area

The study area is located on the eastern part of the Capital city of Ethiopia, Addis Ababa and lies between latitudes 9^0 00' 05.01" N and 9^0 05' 10.14" N and 38^0 52' 04.87" E and 38^0 47' 18.79" E. Location map of the study area is shown in figure 3.1.

The climate of Addis Ababa is cool to temperate with a mean annual temperature of 16 degrees centigrade, and a mean annual rainfall of 1200-1600 mm (EMA, 1988). The main rainy season in the area falls between June and mid September which is winter. While the lesser rains of autumn fall between February and April which sometimes extends up to mid May. Heavy and torrential rains that last from few minutes to several hours are common during both rainy seasons.

The topography of the study area is variable, that is rugged, hilly and mountainous at the north and northeastern parts whereas flat towards the south & southwest. Elevation ranges from 2700 m (northern parts) to 2300 m (southern parts) above sea level.

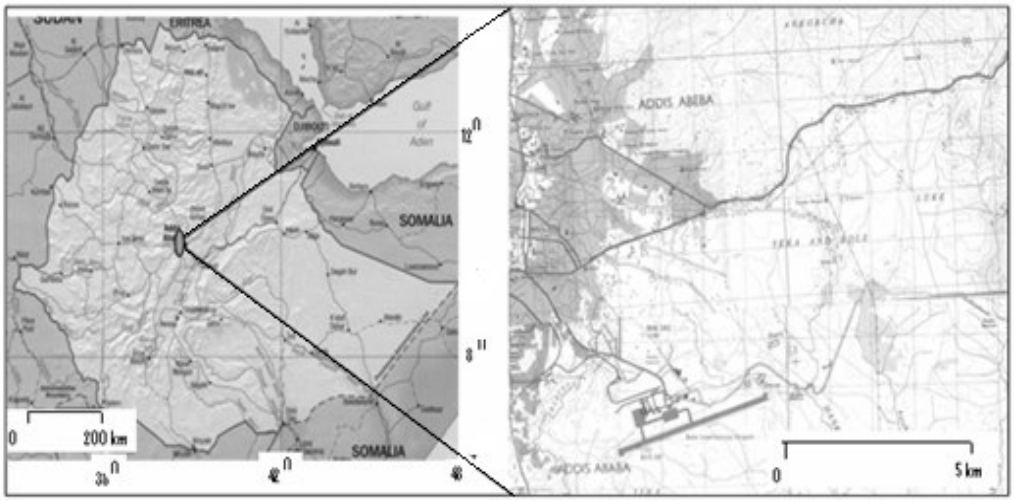

Figure 3-1: Location Map of the study area.

The main geologic formation in Addis Ababa is the Cenozoic Tertiary volcanics of Trap series that were formed by lava and debris ejected from fissure eruptions. Basalts, Trachyte, Rhyolite, and Ignimbrite are the major rock types that belong to the Trap series formation. Tuff and Alluvials are also found in few amounts at different localities. According to the geological survey of Ethiopia, GSE (1990) the city is predominantly covered by alkaline basalts with interbedded pyroclastics, trachytes and rhyolites. The eruptions took place at intervals and in some locations there was sufficient time between different episodes to allow interbedded soil layers to form.

The geology of Addis Ababa is shown in figure 4.1 which is a map produced by the collaboration of GSE and the department of Geology and Geophysics of Addis Ababa University (Tamiru, 2001).The study area is covered by four of the above mentioned rock types namely Basalt, Rhyolite, Trachyte and Ignimbrite.

Addis Ababa is not only the capital city of Ethiopia, but also the biggest and the most highly populated city in the country. The city is situated in the main high land plateau with an average elevation of 2440 m above sea level. According to recent census the inhabitants of the city are more than 2.3 million (CSA, 2004). Due to the rapid expansion of the city and the need to build more houses, currently there is an extensive construction activity going on in every direction of the city including and mostly on parts of the study area.

Extensive areas to the south and southwestern part of the study area are covered by soils of expansive nature (GSE, 1990; Lulseged, 1990). Soil expansion and shrinkage is a big problem posing damage to buildings and other infrastructure like roads, pipelines, and sewerage systems etc in areas of construction activities where such soils exist. Most of the damages are reported from the south & south western part (CMC and Bole) of the study area. Figure 3.2 shows some damages to houses and a road that goes from CMC to Ayat village.

Figure 3-2: Damages to buildings and road infrastructures (field pictures) in the study area due to soil expansion and shrinking.

In an engineering geological study conducted by GSE (1990) which had included some parts of the study area, soils covering Addis Ababa city are classified into four classes namely; Residual soils, Alluvial soils, Colluvial soils and Lacustrine soils.

Detailed geotechnical studies and investigations have been conducted particularly on soils of Bole area following the failure of the runway of the Bole international airport. GSE (1990) reported that the thickness of expansive soils in the Bole area varies from 2 - 10 m with an increase in thickness towards the south and west of the airport. The average clay content of soils in this area is mentioned to be around 76 %, while their swelling potential is reported to be exceeding 100 %. Whereas the swelling potential of the other soil types (Residual, Colluvial, and Alluvial) in the city is reported to

be on the order of 50 % and less. According to GSE (1990) it is likely that, during the Pleistocene these low lying flat parts of the city were covered by a water body that was fed by sediments brought by rivers coming from the higher altitudes.

Natural vegetation cover in the study area is trees (mainly Eucalyptus and conifers) and grasses. The northern part is mainly forested; the built up area is fewer than the central, south and southwest which currently is the main expansion area of the Addis Ababa city where plenty of new construction activities are going on. Construction materials sources are mainly from the northern & central portions where many quarries of basalt, trachyte and rhyolite are present.

4. Materials and methods

4.1. Data collection

The data collection stage involved gathering of relevant information from literature followed by field work soil sampling. Sampling sites were selected within and at the outskirt of the city of Addis Ababa based on information from previous studies conducted by the Geological Survey of Ethiopia (GSE, 1990) and Addis Ababa University (AAU, 2004). Within the selected area a stratified random sampling strategy was employed. The study area was first divided into two more or less homogenous areas with respect to the expansion potential of the soils within each area. One part is the CMC and Bole area where frequent problems due to soil expansion are reported. Different types of damages on different types of structures have been reported. These are mainly; deformation of road pavements, cracking of foundation slabs and walls of small houses, jamming of doors and windows of houses, and dislocation of pipe lines. During the time of the field work data collection, we were also able to note such damages in this part of the study area. The other area is the Kotebe and Ferensay area where problems due to soil expansion are rarely reported. Finally a third area was added from a place close to the international airport to represent extreme cases. Soils within the vicinity of this particular area are documented to be composed of highly active clay minerals (AAU, 2004; GSE, 1990; Lulseged, 1990).

The field work data collection was conducted from the 12th of September to the 13th of October, 2005. During the time of the sampling the climatic condition was rainy and cloudy. The samples taken were all in wet condition. Most parts of the study area were covered by grasses; only at few places exposed bare soil were found (e.g. gullies and river sides). The grass cover was removed by spade before taking the soil samples. Disturbed soil samples were then taken from the top 0-30 cm of the surface soil fulfilling the aim of representing mass properties of the ground (e.g. British Standard Institution, 1981). For this study a total of eighty soil samples were taken by excavating the ground using hand digging equipment like a spade and shovel. Each soil sample was taken from one stratum and is representative of that same stratum. Appendix C shows the summary of description of the soil samples. Soil samples were not taken from areas where construction works and man made deposits are suspected to impose effects on the nature of the soils. In addition to this, sample locations falling on bare rocks, inaccessible valleys, marshy areas and protected sites (e.g. cemeteries) were rejected and substituted by other locations. Figure 4.1 shows the distribution of sampling points within the study area.

Some soil samples (eighteen) were also taken from the sub soil (30-60 cm depth). This helped to see if there are significant variations in soil properties between the top and the sub soils. A pit of one meter by one meter was dug at one randomly selected location (UTM 477913569 and 1000511980 i.e. sample number 19). However, for soil samples obtained from the subsoil only the Atterberg limits tests were done; hence for further analysis we used only the eighty soil samples from the surface soil.

Visual examination and description of fresh soil samples as well as character and variability of the ground mass was done together with describing the engineering properties. Notes were taken and descriptions have been made where soil strata were observed to change. Changes in soil strata were noted at different localities where soil horizons are seen exposed (e.g. river cuts, gullies, construction sites and material production sites etc). In addition, there was a chance of observing the vertical variation in soil profile in areas of construction activities where cuttings and open excavations were apparent. From results obtained from the laboratory analysis and the field observations made, the soils seems to have less variability in their expansion potential between the top soil and the subsoil.

Approximately 10-15 Kg of soil samples were taken from each sampling location. The samples were properly labelled and stored as per the requirements of AASTHO (2002) standards of handling soil samples. Prior to proceeding to the laboratory analysis, the samples were air dried except for the samples obtained from the Bole area. Samples from the Bole area were very wet, hence oven dried.

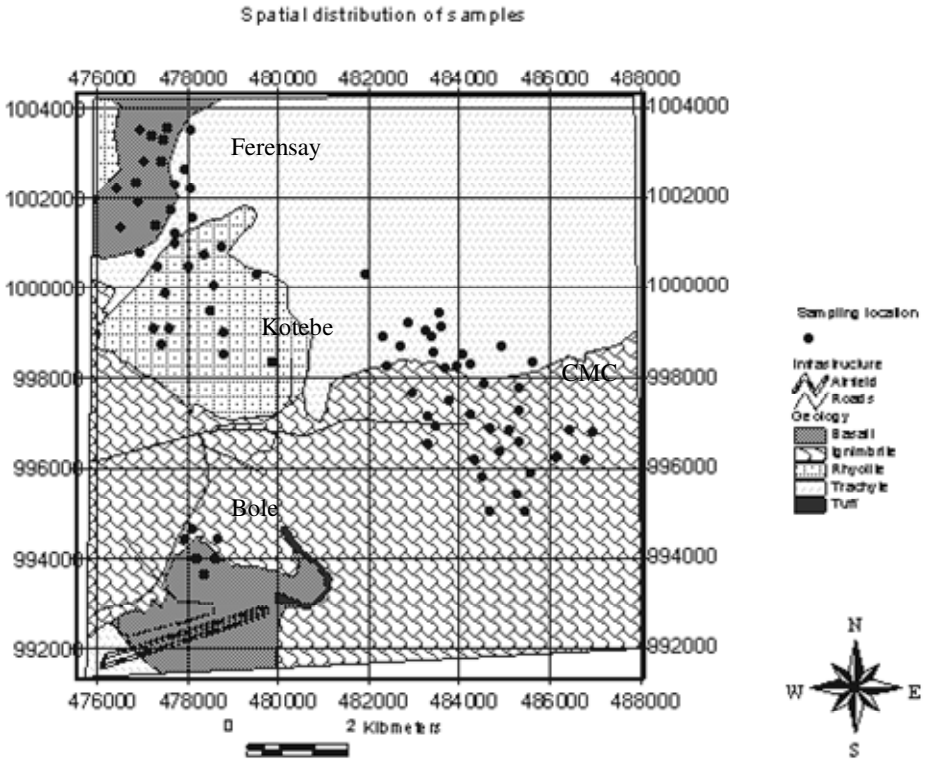

Figure 4-1: Distribution of soil samples on base map showing the lithology of the study area, with names of places written on it.

4.2. Laboratory analysis

Different laboratory tests were conducted on the disturbed soil samples that were collected from different localities of the study area. Sample preparation and testing followed the requirements of different standard procedures and specifications. Among the laboratory tests are index tests

(Atterberg limits) and free swell tests on all the eighty soil samples; and cation exchange capacity (CEC) tests on seventy-one soil samples obtained from the top 0-30 cm surface soil.

Apart from conducting the engineering tests, soil reflectance spectra were acquired using the ASD fieldspec (350 nm to 2500 nm) and the PIMA (1300 nm to 2500 nm) spectrometers.

Some of the laboratory tests (Atterberg limits and free swell tests) were done in Addis Ababa at the Ethiopian Roads Authority (ERA) and SUR construction share company laboratories; some at the Delft University of Technology, TU Delft (Cation exchange capacity determination) & soil reflectance spectra acquisition at the ITC remote sensing laboratory.

4.2.1. Atterberg limits (liquid limit, plastic limit and plasticity index) tests

Atterberg limits (after a Swedish soil scientist A. Atterberg) are ranges of consistency (the ease with which a soil can be deformed) of cohesive soils as a function of changes in moisture content (Perloff and Baron, 1976). They represent empirical boundaries which divide the various states that cohesive soils exhibit with varying amount of moisture content namely; solid, semisolid, plastic and semi-liquid states.

Since water has a significant effect on the engineering behaviour of clayey soils in such a way that clayey soils with higher moisture content are weaker & easily deformable than their same varieties with lower moisture content (Lambe and Whitman, 1979; Perloff and Baron, 1976), determination of the Atterberg limits of such soils has proved to be useful in engineering applications.

Atterberg limits can give a good indication about soils expansive potential and shrinking properties. They are also directly used in construction specifications. Figure 4.2 shows the four Atterberg limits namely; shrinkage limits, plastic limits, liquid limits and plasticity indices; and the various states that clayey soils exhibit with varying amount of moisture content. Among the four Atterberg limits, shrinkage limit was not used in this thesis research for it is a lot more time consuming and expensive than the other three limits.

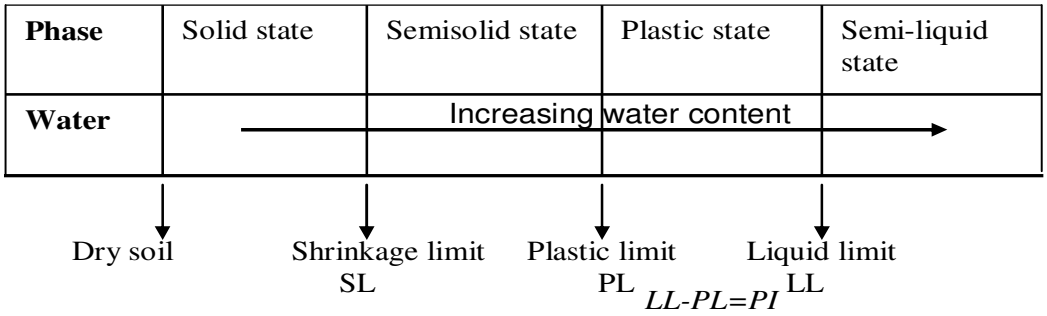

Figure 4-2: Definition of Atterberg limits with respect to the various states at which clayey soils exist with varying amount of moisture content.

Atterberg limits tests were conducted following the standard test procedures of AASTHO specifications (AASHTO, 2002). These specifications are comparable to ASTM D4318-00 standard test methods for liquid limit, plastic limit and plasticity index of soils (ASTM, 1989).

- AASHTO T89 Determining the Liquid Limit of Soils
- AASHTO T90 Determining the Plastic Limit and Plasticity Index of Soils

Soil samples were air dried except for the six soil samples obtained from the Bole area which were oven dried due to their very high moisture contents. After drying them the soils were sieved by no. 40 sieve (of sieve aperture 425μm). The liquid limit and plastic limit tests were performed on the portions of materials passing through the no.40 sieve openings.

The liquid limit i.e. the moisture content above which soil will turn to a semi liquid state or the lower limit of viscous flow (Perloff and Baron, 1976) was determined using the hand operated Casagrande apparatus. As indicated on figure 4.2 liquid limit defines the boundary between a soil plastic state and liquid state.

The fine fraction of each soil sample (approximately 200 g) that passed through the no. 40 sieve openings was mixed with distilled water to make a uniformly mixed paste. Prior to conducting the liquid limit test, the prepared soil samples were soaked overnight to ensure that the soil grains had absorbed water and softened thoroughly (AASHTO, 2002; Kezdi, 1980). The paste was then placed on the Casagrande cup and grooved by a standard grooving tool. The number of blows required to close an opening of the standard groove over a distance of $1\frac{1}{2}$ inch was recorded together with the determination of the moisture content of the respective specimen. The number of blows and the moisture content of three specimens from each soil samples were then plotted on a graph paper prepared for this purpose. After plotting three successive numbers of blows to a logarithmic scale (abscissa) against the respective moisture contents (ordinate) found, a straight line (flow curve) was drawn to connect the three points. The moisture content at the 25th number of blows was reported as the liquid limit of that soil sample.

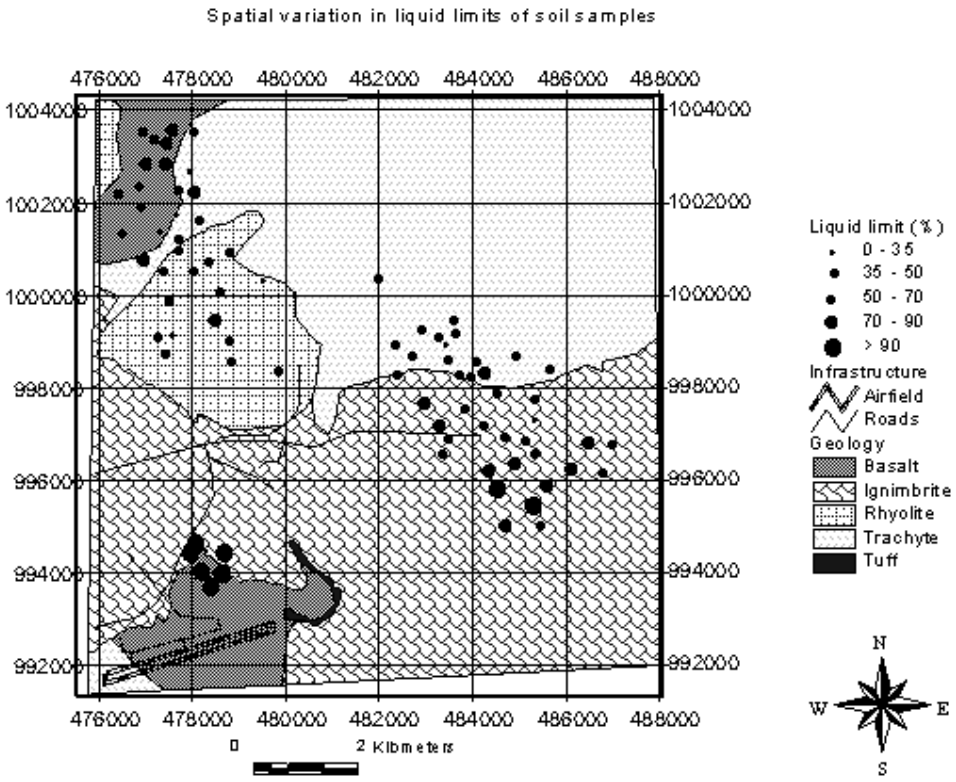

Figure 4-3: Variation in liquid limits of the different soil samples.

The Plastic limit of the soil samples i.e. the moisture content between the plastic and semisolid states was determined on a portion of the soil samples passing through the same sieve size. Approximately 100 g of soil was mixed with water to make a thick paste that won't adhere to hands and can be readily rolled (AASHTO, 2002). Then the paste was remoulded and rolled into threads on a glass plate until the threads started to crack at a diameter of about 3-4 mm. The moisture content at which the threads of soils started to crumble, at the specified diameter, was recorded as the plastic limit (PL) of that soil sample. Two of these tests were conducted per sample for reproducibility and the average results were reported.

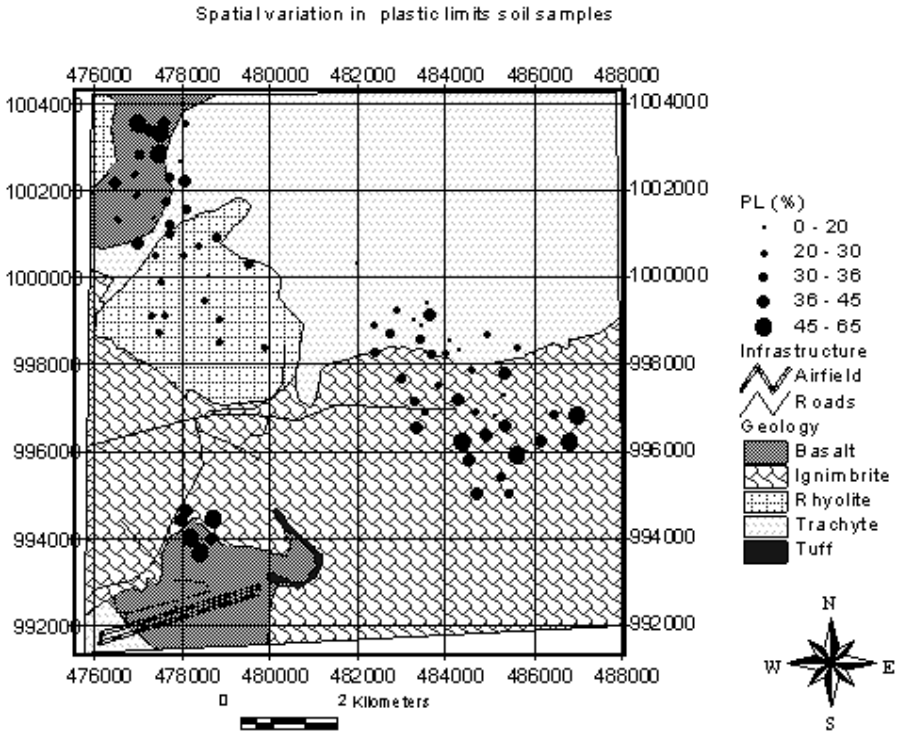

Figure 4-4: Variation in plastic limits of the different soil samples.

Plasticity indices of soils were calculated by subtracting the results of plastic limit from the liquid limits of every soil samples (*PI= LL –PL).* Ion free distilled water was used for all the tests to avoid influence from the composition of the water.

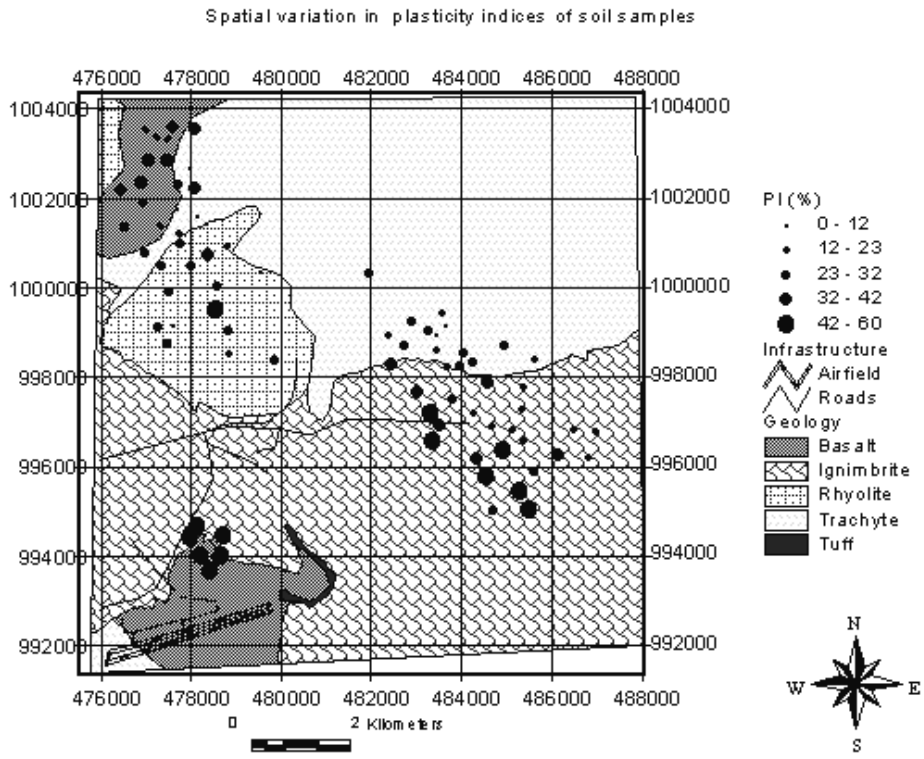

Figure 4-5: Variation in plasticity indices of the different soil samples.

Corrections on their respective liquid limits were done for the six samples that were subjected to oven drying which was a 10 % increase (Bowles, 1984). But care was taken not to dry them until the drying causes irreversible changes in their adsorbed water by controlling the oven temperature and the maximum drying time.

All the necessary precautions and measures were taken to eliminate possible sources of errors that could affect the results of LL, PL and hence PI during the laboratory measurements to get reproducible and reliable results. Among the precautions are for example; sticking to the standard methods of testing (AASHTO, 2002; ASTM, 1989) like using standard instruments, controlling the dropping height of the Casagrande cup to the specified standard requirement (1cm) by careful calibration, controlling the blow frequency, preparing a homogenous soil water mixture, and keeping the laboratory room temperature constant etc. Some examples of the Atterberg limit tests as determined by the laboratory experiments are attached (Appendix B). And appendix A gives summary of all the laboratory results for the 80 soil samples for which the reflectance spectra is also available.

4.2.2. Free swell tests

Free swell tests are known to indicate the presence of swelling clays in soils (Head, 1980); the tests are relatively simpler and less time consuming. Free swell test results indicate the potential expansiveness of soil samples without being loaded.

The free swell tests were conducted on the fraction of soil samples passing through the no.40 sieve openings. The sample preparation has followed the methods and procedures discussed by Head (1980).

A carefully measured 10 cm^3 loose oven dried soil sample were poured into a 50 ml of distilled water that is placed in a graduated cylinder. Changes from the original volume were then observed and readings of final volume were taken after the soil particles had settled.

The percent free swell was calculated as; $\%FS = \left[\frac{vf - 10}{10} * 100\right]$ (Head, 1980)

Where; %FS= percentage free swell

V_f = final volume recorded (cm^3)

Free swell results range from a minimum of 4 % for a non-plastic soil (sandy silt) that was obtained from a river bed, up to a maximum of 185 % for a highly plastic soil obtained from the low land flood plains of Addis Ababa, namely CMC and Bole areas.

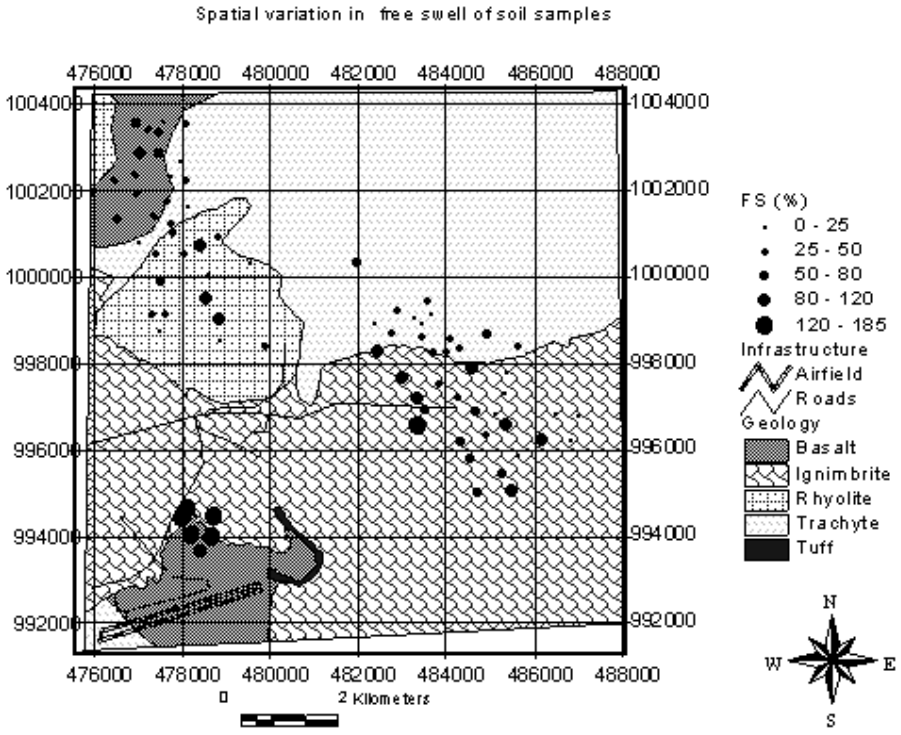

Figure 4-6: Variation in free swell results of the different soil samples.

4.2.3. Cation exchange capacity determination

Cation exchange capacity of soils is a measure of easily exchangeable cations in the soil; and is greatly influenced by the mineralogical content & specific surface area of soil grains (Chen, 1988). While this test is used to obtain information about soil fertility in agricultural applications, it indicates the potential expansive properties of soils in engineering applications.

Methylene blue adsorption test was conducted for the determination of the cation exchange capacity of the soil samples. The method employed was the "spot" method (Verhoef, 1992).

The sample preparation was done following the requirements and procedures of Verhoef (1992). The soil samples were sieved with a sieve of 63 µm openings and 2 g of the fraction passing this sieve was taken for the analysis. One sample (sample number 13) which was composed of sand & fine silt was ground into powder because it was impossible to get portion of materials passing the mentioned sieve size. The methylene blue adsorption value was calculated in grams of methylene blue adsorbed by 100 g of the sample as follows:

$$MBA = (C*P)/(A/100)\ (g/100g)$$

Where; MBA= Methylene blue adsorption value
C= Concentration of the methylene blue solution (g/ml)
P= Amount of MB adsorbed (ml)
A= Weight of soil (g)

The adsorption was then calculated in milliequivalents per 100 g of the soil samples as follows:

$$M_f = (100*N*P)/A\ (meq/100g)$$

Where; N= Normality of the MB solution (meq/l), &
M_f is regarded as equivalent to the cation exchange capacity of the soil samples.

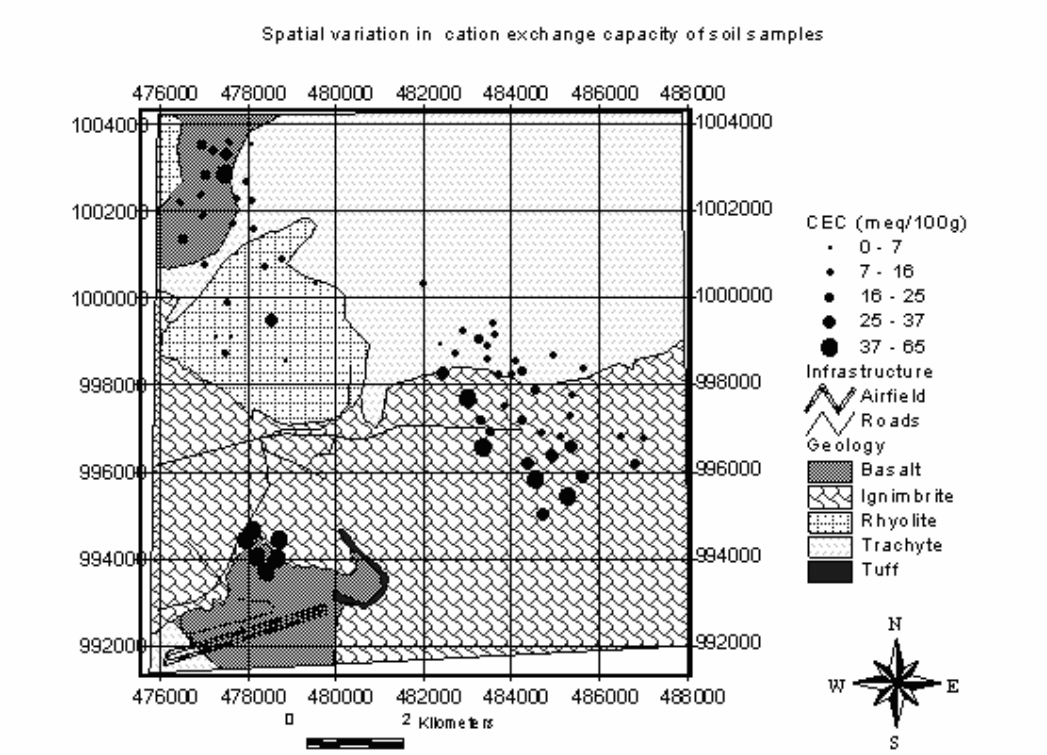

Figure 4-7: Variation in cation exchange capacity results of the different soil samples.

4.2.4. Spectral measurements

Soil reflectance spectra were acquired using the ASD fieldspec and the PIMA spectrometers which cover the 350 nm -2500 nm & the 1300 nm - 2500 nm wavelength region of the electromagnetic spectrum respectively.

4.2.4.1. The ASD fieldspec spectrometer

The ASD (Analytical Spectral Devices, Inc) fieldspec spectrometer is a field portable spectrometer that covers the visible, near infrared and short wave infrared spectral region (350 nm -2500 nm) of the electromagnetic spectrum. The spectrometer has got a wide range of application in various disciplines of which identification of minerals and assessment of soil potential are also some of the renowned ones.

The spectral resolution of the ASD fieldspec spectrometer is 3 nm for the 350 nm - 1000 nm region and 10 nm for the 1000 nm - 2500 nm region; whereas its spectral sampling interval is 1 nm (Analytical Spectral Devices, 1999). The spectrometer has three separate detectors, one in the visible & near infrared regions (VNIR) and the two are in the short wave infrared (SWIR) region.

Measurements can be done either in contact mode or from a distance as needed. Little or no sample preparation is required and measurements will cost only a few seconds or minutes per sample.

Since the major absorption features associated with clay minerals are found in the SWIR regions of the electromagnetic spectrum, clay minerals are among the mineral groups that are suitable for ASD analysis. Besides, the ASD fieldspec spectrometer can give additional spectral information from the VNIR regions.

4.2.4.2. The PIMA spectrometer

The PIMA (Portable Infrared Mineral Analyzer) spectrometer is a field portable, infrared spectrometer that operates in the shortwave infrared (1300 nm – 2500 nm) wavelength region of the electromagnetic spectrum (Spectral International INC SII, 2005). Among the applications of the PIMA spectrometer are mineral identification, soil regolith mapping, alteration mapping & core logging etc. The spectral resolution of the PIMA spectrometer is ~7 nm, with a spectral sampling interval of 2 nm. Among some of the characteristic features of the PIMA spectrometer are use of an internal light source for reproducibility & stability, automatic wave length calibration, radiometric calibration during each spectral scan etc (Spectral International INC SII, 2005).

Measurements can be done either in contact mode or from distance as needed. Little or no sample preparation is required and taking measurements will cost only a few seconds or minutes per sample.

Due to the presence of OH, H_2O, AlOH, FeOH & MgOH molecules in clay minerals, the major absorption features associated with clay minerals are found in the SWIR region of the electromagnetic spectrum. Hence, clay minerals are among the mineral groups that are suitable for PIMA analysis.

4.2.4.3. Measurement of soil reflectance

A small portion of air dried soil samples were used for the spectral measurements. We prepared the soil samples for the spectral measurements in their natural state without standardizing them. For example, their grading except for the removal of the cobble and above size rock fragments during the sampling. However, a large portion of the soil samples were naturally finer; i.e. passing the no.4 (of sieve aperture 4.75 mm) openings. The coarser texture in some soil samples arose due to clay particles lamped together instead of separate larger grains of soil. The later was apparent especially in black cotton soils which are renowned for exhibiting a popcorn texture when dry (Gourley et al., 1993). The spectral measurements were done using the ASD fieldspec and PIMA spectrometers in contact mode.

The time spent for acquiring the reflectance spectra of the soil samples was on the order of hours which saves a great deal of time in comparison with the conventional engineering tests that took weeks time.

However, due to problems related to the instruments, the measured spectra (especially of the ASD spectra) had some noise at the beginning (up to the ~400 nm wavelength region) and towards the longer wave length regions (getting worse especially after the ~2300 nm). Figure 4.8 shows some of the laboratory measured soil spectra as measured by the ASD fieldspec spectrometer.

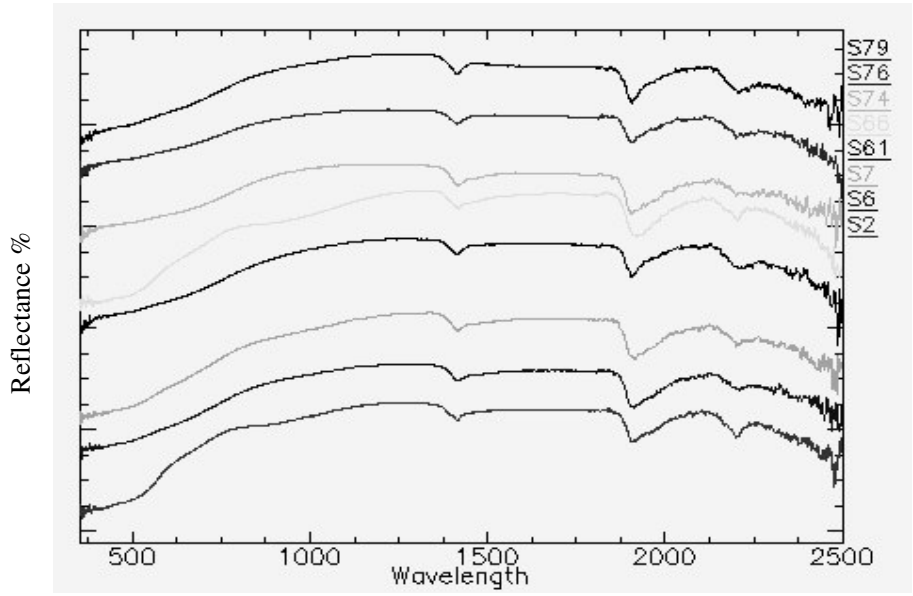

Figure 4-8: Laboratory measured reflectance spectra of some soil samples (from the ASD fieldspec spectrometer measurement), noisy at the beginning (up to ~400 nm) and towards the longer wavelength (~2300 nm to 2500 nm) regions (spectra is offset).

The spectra of the soil samples measured in the laboratory were imported to The Spectral Geologist (TSG Professional, 2005) software for further analysis. Absorption feature parameters (relative absorption depth, relative absorption width, relative absorption area etc) were calculated from the soil reflectance spectra (for all the 80 soil samples) using TSG. No smoothing techniques were applied on the soil spectra during the calculation of the absorption feature parameters in order to avoid the risk of losing subtle spectral differences that might be useful in the analysis and discrimination of various types of clay minerals.

The reflectance spectra of the soil samples under investigation show variability in reflectance and other diagnostic absorption features. In the visible and near infrared portion of the spectra changes in slopes were the prominent features that were recognized coupled with changes in reflectance intensities. The absorption features that are apparent on the VNIR region are relatively few, broad, wider and less intense. Whereas, in the SWIR region the main absorption features of clay minerals were observed with variable intensity.

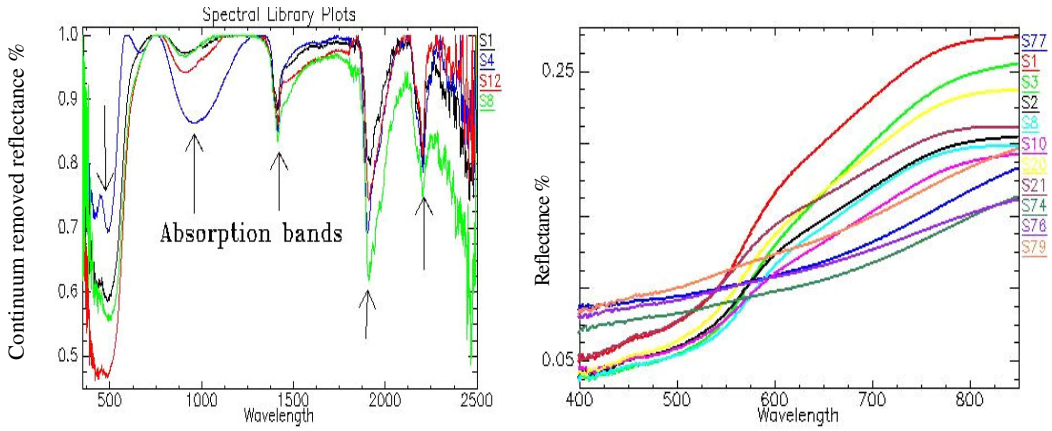

Figure 4-9 a & b: Absorption features of variable intensity and shapes on a continuum removed spectra; and differences in slopes of different soil spectra (~400 nm to ~800 nm) respectively.

4.3. Analysis of laboratory results

We analysed the different parameters obtained from the laboratory measurements (engineering as well as absorption feature parameters) independently before integrating them for further analysis.

4.3.1. Engineering parameters

We plotted the results of liquid limits and plasticity indices of the soil samples on the famous plasticity chart of Casagrande to see their respective plasticity characteristics and classes with respect to the "A-line". Figure 4.10 shows this diagram and the ranges of plasticity of the soil samples. The "A-line" is an empirical division between soil types. Soils that fall above the "A line" are clayey and those that fall below it are silty in nature (the terms clayey and silty being used to refer to particle sizes). According to the British standard (1981), Fat or plastic clays plot above the "A line" whereas organic soils, silty and clayey soils containing a large portion of rock flour (finely ground non-clay minerals) plot below it. The formula of the "A line" is given as;

$PI = 0.73(LL - 20)$ Where; PI= plasticity index & LL=liquid limit (Perloff and Baron, 1976).

The grey and black cotton soils obtained from the Bole area (located near the Bole international airport) and similar soil samples obtained from the CMC area fall on the extremely higher plasticity portion of the chart. Whereas soils found from the hilly areas of Kotebe fall on low and intermediate plasticity portions of the chart.

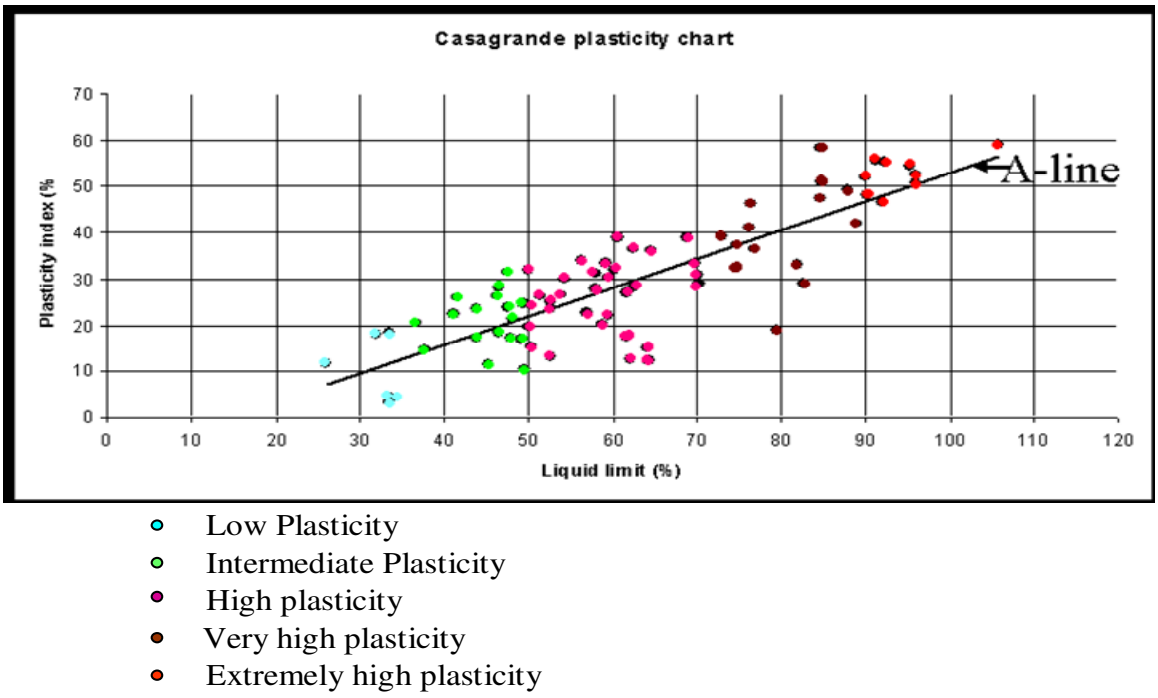

Figure 4-10: Casagrande plasticity chart with "A" line showing the empirical division between clayey and silty soils (clay and silt referring to particle sizes).

According to the classification of Casagrande soil plasticity chart, soils having a LL < 35 % fall within the low plasticity class, 35 % < LL < 50 % within the intermediate plasticity class, 50 % < LL < 70 % within the high plasticity class, 70 % < LL < 90 % within the very high plasticity class and LL > 90 % within the extremely high plasticity class. NB! LL = 0 to 20 % is Non plastic (one sample was found to be non plastic with LL impossible to determine i.e. the sample has little to pass the no. 40 sieve openings and the fraction that passed was mainly fine sand & silt). Zero liquid limit represent that it is impossible to determine the liquid limit of the given soil sample and is reported as NP (non plastic).

The distribution of the soil samples on the Casagrande plasticity chart depicted that the observed values of plasticity of the soil samples cover a wide range of variability in plasticity characteristics of the soil samples. Thus as for the spatial variability of soils, we were also able to represent the required range of variability in their plasticity character. Hence our objective of obtaining soil samples of variable expansive potential (from low to high) was fulfilled.

After classifying the soil samples into different classes of plasticity using the Casagrande plasticity chart, the sampling points were overlaid on top of the geological map of the study area to see if there is a relationship between soil plasticity nature and the lithology of the study area. Figure 4.11 shows sampling points classified by the plasticity classes of the soils overlaid on top of the geological map area.

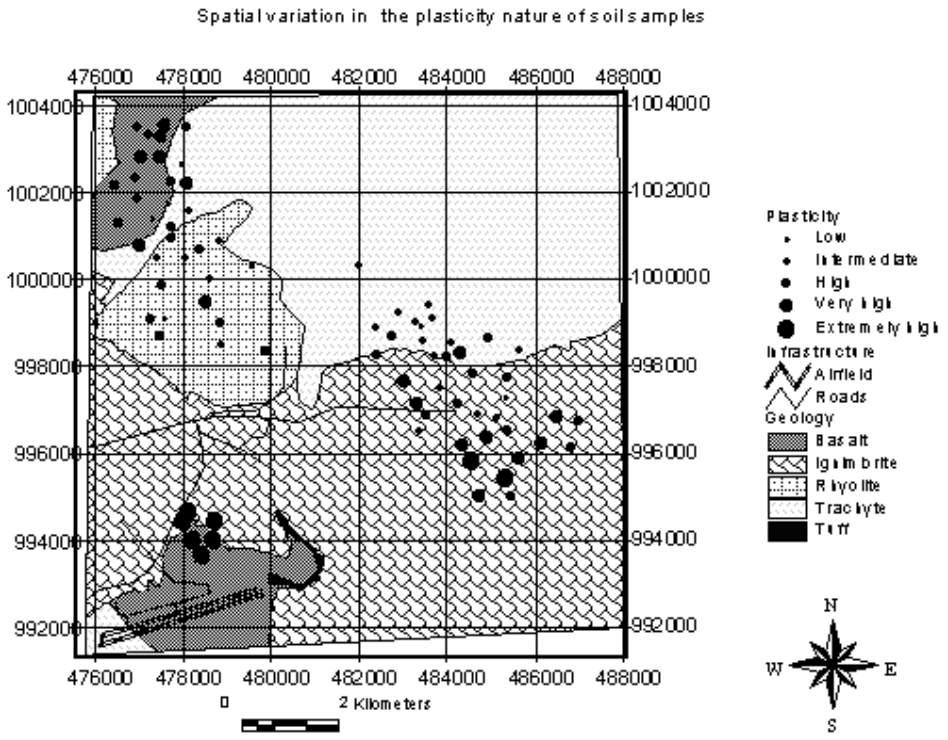

Figure 4-11: Sampling points classified by the plasticity classes of soil samples showing the spatial variations in their plasticity nature overlaid on the geological map of the study area.

Samples obtained from the northern rim of the study area on the basaltic lithology fall mostly on the very high plasticity class with few samples falling in the high plasticity class. GSE (1990) classified these soils as residual soils developed as a result of in situ decomposition and weathering of the basaltic rocks on which they overlie. During the collection of soil samples it was noted that soils in many parts of this area were saprolites i.e. soils that show the original rock fabric and structure somehow retained or not fully destroyed for example discontinuity or joint relicts (Appendix C soil description). Since basalt is a mafic rock that is rich in magnesium and iron it has high Base Exchange capacity and thus it is expected that soils derived from basaltic rocks exhibit higher plasticity.

The rhyolite and trachyte parts are dominated by low and intermediate plasticity soil classes with few high plasticity classes in between. Since rhyolite and trachyte rocks are silica rich it is expected that soils derived from these rocks will exhibit lower plasticity. According to GSE (1990) soils in these areas are residual and colluvial soils (but their map does not cover the whole study area).

Soils on the ignimbrite parts fall on all the classes of plasticity from low to extremely high; being the dominant class extremely high plastic soils which has no relation with the lithology. Since ignimbrite is an intermediate type of rock with fairly high amount of silica content, it is unlikely that soils derived from such a parent rock are of an extremely high plastic nature. GSE (1990) mapped this part of the study area as covered by soils of lacustrine origin. The area is flat towards the south

and southwest with an elevation of about 2300 m above sea level which is the relatively low elevation as compared to the other parts of the city. It is also a poorly drained ground where swamps are common during rainy seasons. According to GSE (1990) the area was covered by a water body that was fed by sediments from streams coming from higher altitudes.

As far as cation exchange capacity is concerned, soil samples that showed high and extremely high plasticity also showed higher values in methylene blue absorption values. These soils fall on the montmorillonite clay groups which are also in agreement with the mineralogical composition identification from the soil spectra. For example the extremely high plastic grey and black cotton soil samples of the Bole area are identified as montmorillonite and the methylene blue adsorption value also fell on the montmorillonite mineral groups of Verhoef (1992). Verhoef (1992) reported CEC value of montmorillonite clays in the range of 50 - 96 meq/100 g.

On the other hand, free swell values of the different soil samples were also observed to increase with an increase in liquid limit, plasticity indices and cation exchange capacity of the soil samples. The free swell values show greater variability which is an indication of the variability in the expansive property of the soil samples. While soil samples classified as of low & intermediate plasticity nature on the Casagrande plasticity chart exhibit lower free swell values. Those that are classified as very high and extremely high plasticity exhibit larger free swell values, and most of which have free swell values of 100 % and above.

4.3.2. Soil reflectance spectra

The soil spectra were pre-processed (in case of ASD acquired spectra splice correction and conversion to text files) and imported to The Spectral Geologist software for spectral interpretation and subsequent analysis of absorption features.

Differences in spectral characteristic among the spectra of the different soil samples were noted and used in differentiating the various clay mineral types that might be present in the soil samples. Position of the absorption features, their shapes, types & number, depth intensity and symmetry; shape of the spectral curves, the differences in slopes of the spectral curves and the variation in reflectance intensity of the different spectra were some of the important qualitative parameters that helped in the identification of spectrally dominant clay minerals from the soil reflectance spectra. Hence, we were able to spectrally discriminate and identify different clay minerals. This was by carefully studying the soil reflectance spectral curves and comparing & matching them with available mineral spectral libraries. Spectra of clay minerals from The Spectral Geologist (TSG Professional, 2005) and ENVI software libraries (ENVI, 2005) as well as from the USGS digital spectral library (USGS, 2003) were used together with manuals that are prepared to help spectral interpretation of minerals for example the G-MEX field manuals of AusSpec International (Pontual et al., 1997).

Some spectra show lower reflectance intensity throughout the whole wavelength range of the electromagnetic spectrum and were on overall dark. They also exhibited monotonously rising convex slopes in the VNIR wavelength region and less variable reflectance intensity in the SWIR.

Other spectra show a sharp rise in slopes and variable reflectance intensity throughout the whole wavelength regions. Some show moderate rise in slopes and also moderate increase in reflectance intensity from the VNIR to the SWIR wavelength regions. These differences in spectral characteristics are shown on figure 4.12.

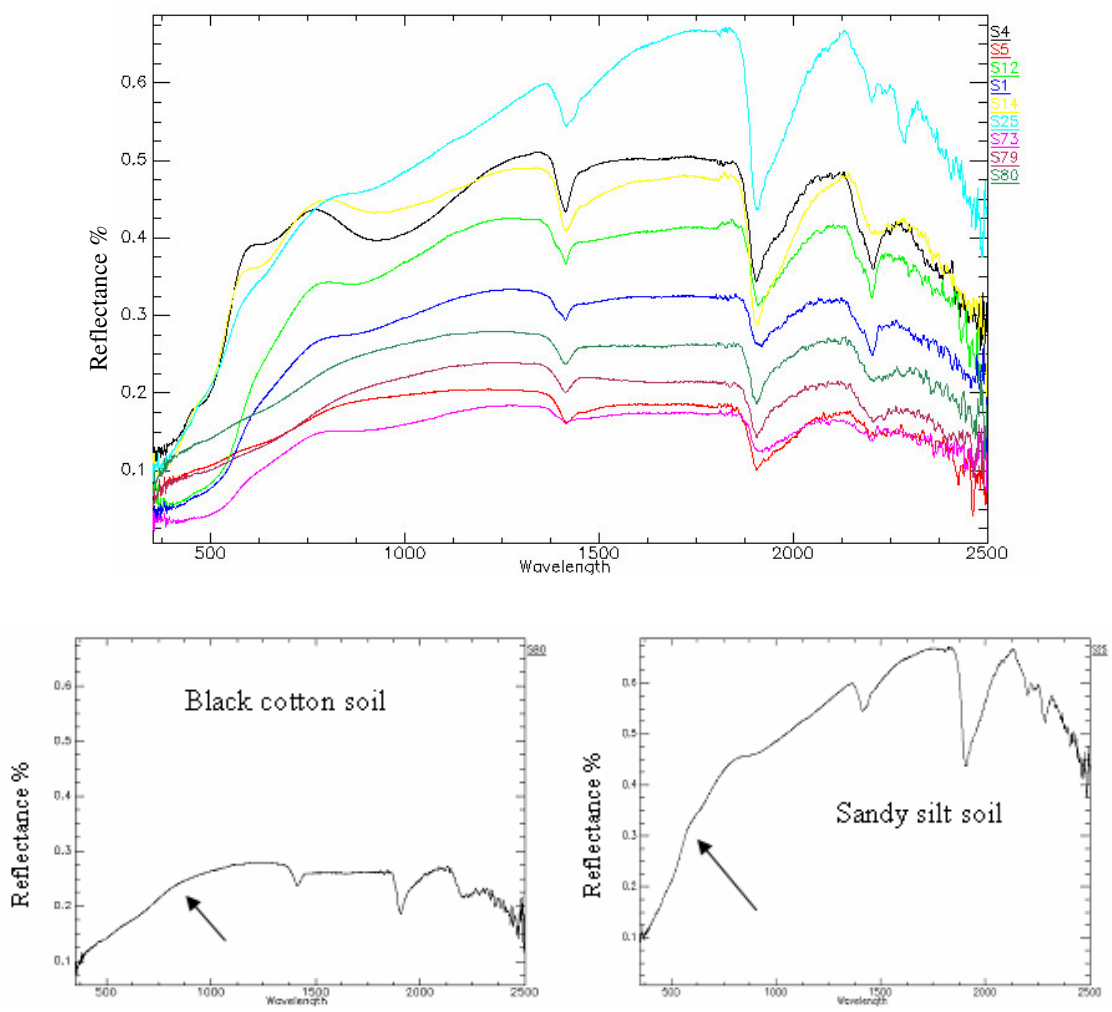

Figure 4-12: Variability in spectral characteristics of different soil samples (no offset). Note the differences in shapes of spectral curves; slopes; overall reflectance intensity; shape, position & number of absorption bands.

After the spectral interpretation of the spectra of each soil sample, we grouped the soil samples into three major classes of mineralogical composition namely; Kaolinite, Mixtures and Smectite classes. Among the smectites are montmorillonite and nontronite; and of the kaolinite groups are halloysite and kaolinites. Spectra of montmorillonite, nontronite, halloysite, kaolinite and mixtures are shown in figure 4.13.

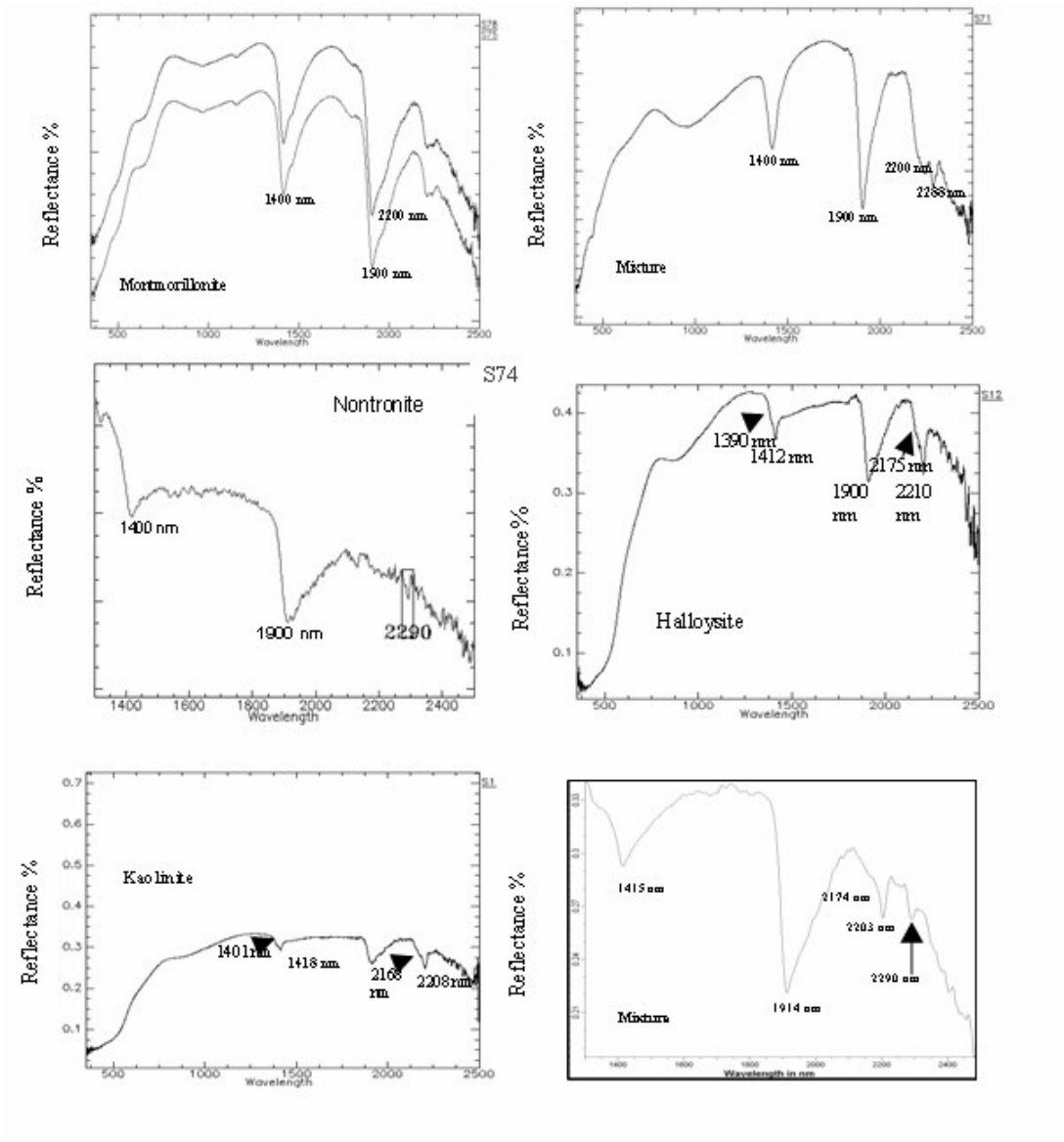

Figure 4-13: Reflectance spectra of Montmorillonite, Nontronite, Halloysite, kaolinite and mixtures with characteristic absorption feature positions.

Montmorillonite show strong absorption features at ~1410 nm, ~1910 nm and additional one at ~2208 nm. The depth of the features being intense at ~1910 nm & ~1410 nm coupled with sharp minima and asymmetric shape. Montmorillonite, $(Ca, Na)_{0.67}Al_4(Si, Al)_8O_{20}(OH)_4 \cdot nH_2O$, is a product of weathering of Fe and Mg rich parent materials and is one of the most common smectite minerals (AusSpec International, 2005) found in soils. Since the study area is located within the central plateau of Ethiopia which is covered by rocks of volcanic origin where mafic rocks like basalt are common and abundant, the occurrence of montmorillonite in the study area can be favoured by the environment.

Nontronite was identified by the presence of a diagnostic absorption feature at ~2270 nm to 2296 nm in addition to the strong water absorption features at ~1410 nm and ~ 1910 nm which show similar depth intensity and asymmetric shape as montmorillonite. The absorption feature at ~2208

nm that is apparent on the spectra of montmorillonite is missing or less resolved on the spectra of nontronite. Nontronite, $(Ca, Na)_{0.66} Fe_3^{+4}(Si, Al)_8O_{20}(OH)_4 \cdot nH_2O$, is also a common smectite mineral found in soils and weathered bedrock. Its formation is favoured by alkaline to neutral pH environments, as well as by the availability of Fe and Ca minerals (AusSpec International, 2005).

Halloysite was identified by the presence of diagnostic doublet features at ~1390 nm & ~1412 nm, and ~2175 nm & ~2210 nm respectively coupled with the water absorption feature at ~ 1910 nm. Halloysite, $Al_2Si_2O_5(OH)_4 \cdot 4H_2O$, occurs in soils and the uppermost weathered part of bedrock (AusSpec International, 2005). It is a kaolinite group clay mineral formed as a result of weathering of Al rich minerals that are also abundant in the study area and its surroundings.

Kaolinite show diagnostic doublet features at ~1400 nm & ~ 1450 nm, and ~2166 nm & ~2206 nm respectively (AusSpec International, 2005). Since there is no adsorbed water in the internal structure of kaolinite clays, the ~1900 nm absorption band is either missing or less resolved. Kaolinite, $Al_2Si_2O_5(OH)_4$ is another commonly occurring clay mineral in soils. It can be derived from almost all silicate minerals (AusSpec International, 2005; McSweeney, 1999), hence its formation in the study area can be favored by the environmental conditions.

Soil spectra showing signatures of different minerals rather than one particular dominant spectral signature of a single mineral are assigned as mixtures. For instance, the spectra of the mixtures that are shown in figure 4.13 appear to be a mixture of nontronite & montmorillonite and nontronite & halloysite respectively.

The analysis of the soil spectra has revealed some interesting results. For example the spectra of a sample number 13 shows probable presence of montmorillonite in the soil sample. This particular sample was obtained from a riverbed where local people used to take sand for small construction purposes. The sample was visually identified as sand, and the Atterberg limits tests conducted on it indicated that it is a non plastic material. The free swell was also very low which agreed with the Atterberg limit results. On the contrary, the cation exchange capacity test gave a higher result which indicated the presence of potentially expansive mineral within the soil sample. Sand is known to exhibit none or very low cation exchange capacity unless it contained significant amount of organic matter or iron. The lowest CEC for sand was reported to range from 0 to 3 meq/100g for dune sands (NSW, 2004), whereas this particular sample exhibited a CEC of 9 meq/100 g. Spectroscopy on the other hand indicated the presence of montmorillonite which is known to be a highly expansive or active clay mineral species. Figure 4.14 shows reflectance spectra of sample number 13. This gives an indication of spectroscopy's potential to support conventional testing methods in avoiding such inaccuracies which can sometimes lead to a big problem (Gourley et al., 1993) and also under-sampling of sites. Gourley et al (1993) discussed some common measurement inaccuracies that are associated with index tests (e.g. LL, PL & PI), of which deceiving results due to lack of material passing the required sieve openings is one. In case of sample number 13 almost nothing have passed through the no. 40 sieve (of sieve aperture 425µm) openings and the portion of the material that passed through was very silty. Hence it was not possible to determine the LL and PL of the sample. The cation exchange capacity test that gave higher value was done after grinding the soil sample.

Another sample, sample number 25 which is a sandy silt soil that was found to be of low plasticity character in the Atterberg limits tests, exhibiting low free swell values and cation exchange capacity showed the features of montmorillonite & nontronite on its reflectance spectra. Reflectance spectra of sample number 25 are shown in figure 4.14 and also figure 4.12.

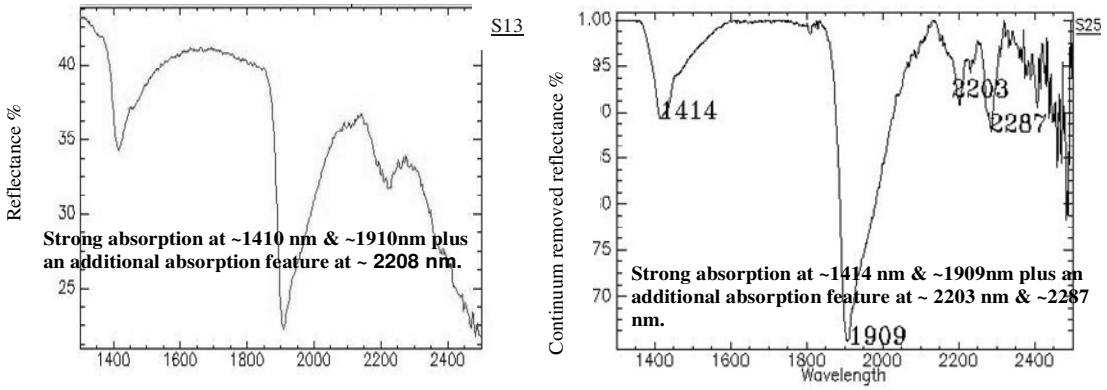

Figure 4-14: Spectra of sample number 13 (reflectance) and 25 (continuum removed) respectively, showing the presence of active clay minerals in the soil samples.

Some spectra show presence of iron oxides in the soil samples. Different kinds of iron oxides, for example, goethite ($\alpha FeO^{+3}(OH)$) might be present in the soil samples as a result of a weathering product of Fe-bearing minerals (McSweeney, 1999). Since volcanic rocks that are rich in Fe minerals are abundant in the study area; which is coupled with the action of chemical weathering in the humid atmosphere of the local tropical climatic conditions; presence of goethite in the soil samples can be favoured by the environmental conditions. Spectra of some soil samples showing diagnostic features of iron oxides similar to the spectral characteristics of goethite (Crowley et al., 2003) are shown in figure 6.13 (e.g. spectra of soil sample number 4 & 14).

5. Analysing relations of engineering parameters versus spectral parameters

5.1. Statistical analysis

We explored the data and examined the relationships between the different soil engineering parameters that were determined by the laboratory experiment using different statistical analysis techniques. The relations between the engineering parameters and the absorption feature parameters were also explored in the same way.

5.1.1. Preliminary data exploration

We used graphical as well as numerical univariate statistical analysis techniques to examine the structure and distribution of all the variables in the dataset. This enabled us to get meaningful information for better understanding of the dataset as well as to see whether the dataset is suitable for the intended analysis. Descriptive statistics (minimum, maximum, mean etc) were calculated. Histograms, box plots and plots for testing the normality of variables like Q-Q plots, P-P plots together with numerical methods (Kolomogrov Smirnov & Shapiro wilk tests) were used. Variables that show departure from a normal distribution were transformed using appropriate transformation methods (mostly logarithmic transformations) to fulfil the linear model assumptions. Table 5.1 shows descriptive statistics for the five engineering parameters (liquid limit, plastic limit, plasticity index, free swell and cation exchange capacity). Box plots of these engineering parameters are also shown in figure 5.1.

	Minimum	Maximum	Mean	Median	Std.dev	Variance
LL	0.0	96.5	60.2	58.8	18.3	355.1
PL	0.0	60.0	32.0	30.4	10.5	111.0
PI	0.0	57.7	28.2	28.2	13.1	171.1
FS	4.0	185.0	56.4	40.0	42.3	1793.0
CEC	4.7	64.1	21.1	15.4	15.4	238.2

Table 5-1: Descriptive statistics for the five engineering parameters.

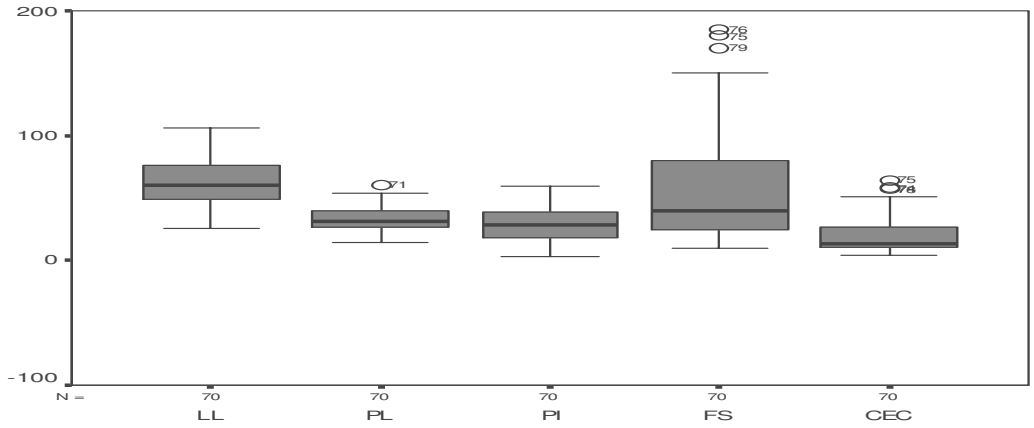

Figure 5-1: Box plots of the five engineering parameters, Liquid limits (LL), Plastic limits (PL), Plasticity index (PI), Free swell (FS) and Cation exchange capacity (CEC).

Visual inspection of the box plots of the engineering parameters indicated that the soil samples show greater variability in free swell results (ranges from 4% to 185 % see also table 5.1) than the other results. However, the variability in liquid limits (ranges from 0% to 96.5%), plastic limits (ranges from 0% to 60 %), plasticity indices (ranges from 0% to 57.7 %) and cation exchange capacity (ranges from 4.7 meq/100 g to 64.1 meq/100g) results are also high.

The box plot outliers that are seen sticking out from the box plot of free swell (FS) are extreme values from the Bole soil samples that were obtained near to the Bole international airport. The same samples are also seen as extreme values on the box plot of the cation exchange capacity (CEC) results. However, the box plot outlier that is apparent on the box plot of plastic limit is a soil sample obtained from the Ferensay area. It is a less decomposed and sandy silt residual soil. The fact that this sample (S71) has exhibited a high liquid limit value (79.6 %) indicates the presence of active clay mineral in its composition. Its high cation exchange capacity (36 meq/100g) and fairly high free swell (60 %) values also confirm the presence of active clay mineral in the sample. But, its high plastic limit (60.5 %) which in turn resulted in lower plasticity index (19.1 %) is due to the sandy silt nature of the soil sample. Soils that are largely composed of fine sand and silt fractions are difficult to mould and need a large amount of water to be rolled into threads of a diameter specified for plasticity limit tests. Kezdi (1980) attributed higher plasticity limits exhibited by such type of soils which sometimes resulted even in a negative plasticity index values with the need of much water to easily mould them.

As far as the distributions of the engineering parameters are concerned, the box plots show that the distribution of free swell and cation exchange capacity is skewed. The distribution of plastic limit & plasticity index is approximately normal and the distribution of liquid limit is more or less symmetrical. The distribution of plastic limit and free swell are shown using histograms, Q-Q plots and numerical normality tests in figure 5.2 and 5.3.

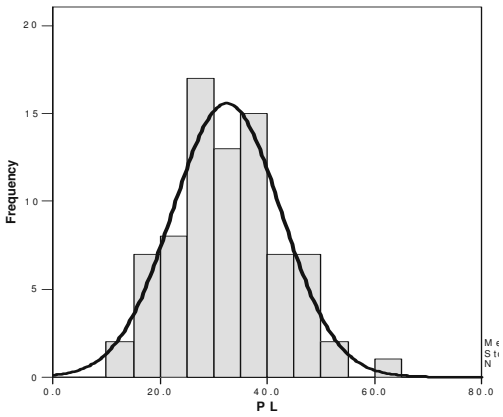

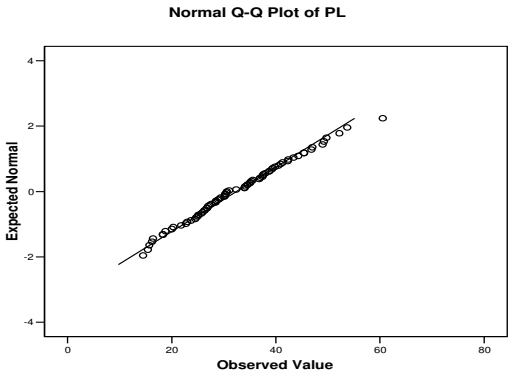

Tests of Normality

	Kolmogorov-Smirnov(a)			Shapiro-Wilk		
	Statistic	df	Sig.	Statistic	df	Sig.
PL	.078	79	.200(*)	.985	79	.481

* This is a lower bound of the true significance.

a Lilliefors Significance Correction

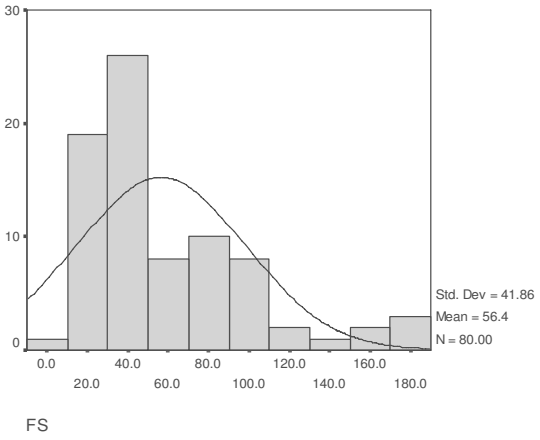

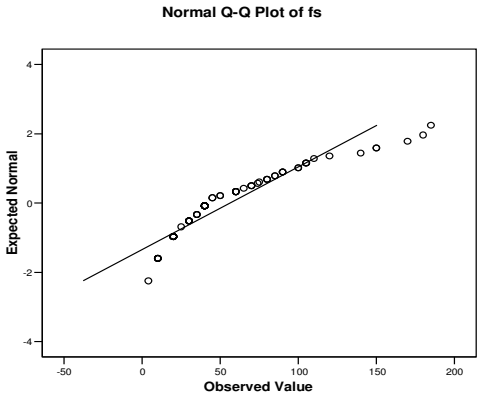

Tests of Normality

	Kolmogorov-Smirnov(a)			Shapiro-Wilk		
	Statistic	df	Sig.	Statistic	df	Sig.
FS	.202	80	.000	.872	80	.000

* This is a lower bound of the true significance

a Lilliefors Significance Correction

Figure 5-2: Histograms and QQ plots of some variables (plastic limit and free swell respectively) with their respective normality test results.

The histogram of free swell is right skewed and the Q-Q plot shows deviation from normality. The K-S (Kolomogorov – Smirnov) statistics is significant implying rejection of the assumption that the data distribution is approximately normal. Thus appropriate transformation method was applied to transform the data so that it fulfils the assumption of normality.

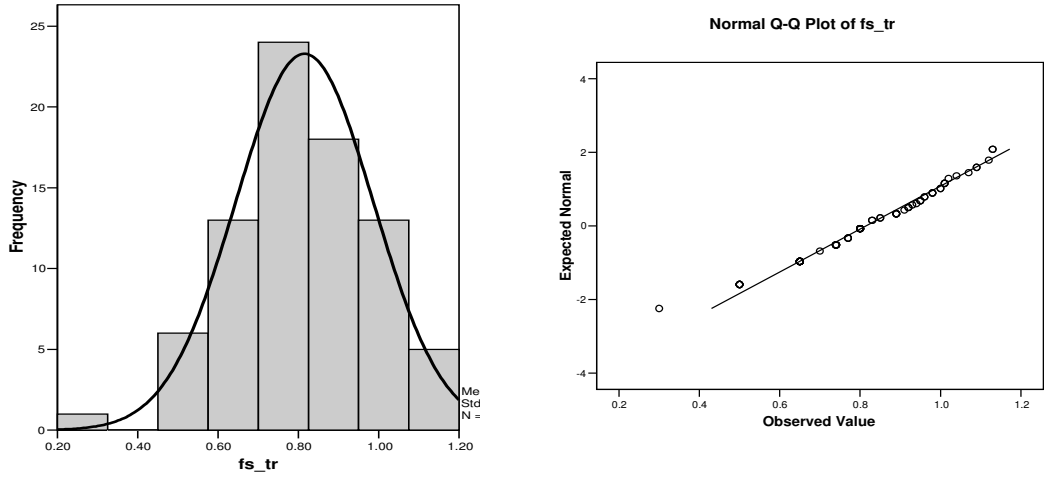

Tests of Normality

	Kolmogorov-Smirnov(a)			Shapiro-Wilk		
	Statistic	df	Sig.	Statistic	df	Sig.
FS_TR	.085	80	.200(*)	.971	80	.070

* This is a lower bound of the true significance.
a Lilliefors Significance Correction

Figure 5-3: Histogram, Q-Q plot and normality test results of free swell after applying an appropriate transformation method.

Now, the histogram is approximately normal and the Q-Q plots show not much deviation from normality (the points are aligned following the reference line). The K-S (Kolomogorov – Smirnov) statistics is not significant implying the assumption that the data distribution is approximately normal is acceptable. Thus, the transformation that was applied (logarithmic transformation) has fulfilled its purpose. We also did the same kind of data exploration analysis on the absorption feature parameters that were calculated from absorption bands at ~1400 nm, ~1900 nm and ~2200 nm.

The proportion of samples that belong to different mineralogical and soil plasticity classes were visualised by plotting frequency plots using bar and pie charts together with frequency tables that provided with a summary of the frequency and cumulative percentages of each classes. Figure 5.4 shows bar charts presenting the relative frequencies of each class from the mineralogical groups and soil plasticity classes.

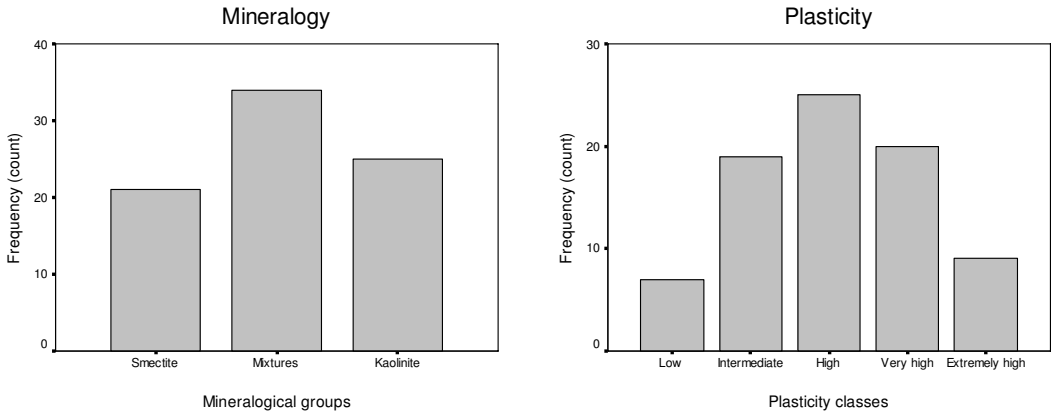

Figure 5-4: Bar charts showing the relative proportion of samples within each mineralogical groups and plasticity classes.

5.1.2. Correlation analysis of engineering parameters & absorption feature parameters

The strength and trends of relationships between the different engineering parameters as well as that of the absorption feature parameters were computed by conducting correlation analysis. Quantitative measures of the linear associations between the different parameters were obtained from the correlation coefficients of pairs of parameters. Table 5.2 shows the summary of correlations among the five engineering parameters: liquid limit, plastic limit, plasticity index, free swell and cation exchange capacity.

	LL	**PL**	**PI**	**FS**	**CEC**
LL	1.00				
PL	0.696	1.00			
PI	0.845	0.203	1.00		
FS	0.677	0.295	0.703	1.00	
CEC	0.846	0.514	0.758	0.816	1.00

Table 5-2: Summary of correlation coefficients among the engineering parameters of the soil samples showing the magnitude and trends of the relationships.

In general the results show fairly high correlations among the engineering parameters, but lower than one might ideally expect. The measured engineering parameters are governed by the mineralogy and amount of clay fractions (e.g. Chen, 1988; Perloff and Baron, 1976) that can be present within the soil samples. However, the soil samples are not constituted by a pure clay material. They are rather natural inhomogeneous mixtures of different amounts of sand, silt and organic matter etc. This has an influence on the overall relationships between the soil engineering parameters. Besides, the fine sand and silty fractions can be and mostly composed of quartz which

do not exhibit expansion and shrinking character at all but can have a diluting effect on the test results.

Since soil expansion potential is an intrinsic characteristic of clay minerals, it manifests only the character of the clay fractions in the soil samples. As far as Atterberg limits are concerned, Lambe and Whitman (1979) indicated that because of the great increase in surface area per mass with decreasing particle size, the amount of water attracted will be influenced by the amount clay in a soil sample. On the other hand, Perloff and Baron (1976) discussed differences in specific surface area and nature of exchangeable cations among different types of clay minerals and thereby their water affinity. They mentioned that smectites have larger specific surface area and net negative charge. Thus, smectites have a higher water affinity than the illite and kaolinite clay varieties. As for the cation exchange capacity of soils, the same principle holds true. Only the clay minerals can absorb the methylene blue solution. The absorption is higher for the smectite clays than the illite and kaolinite varieties (Verhoef, 1992). Hence, the relative proportion of the fine sand and silt fractions that has passed through the specified sieve apertures (425 µm in the case of Atterberg limits & free swell tests, and 63 µm in the case of cation exchange capacity test) can be attributed to be responsible for diluting the overall relationship that is exhibited among the engineering parameters.

All the engineering parameters show relatively comparable magnitude of relationships among themselves. However, plastic limit shows lower correlation with other engineering parameters for example plasticity index and free swell, and fairly high correlation with liquid limit and cation exchange capacity. As mentioned in the previous chapters (chapter 2 & 4), plastic limit indicates the moisture content at which a certain soil specimen will change from plastic to semisolid state. Plastic limit do not alone indicate soil expansion potential but is mainly used to obtain another important parameter named plasticity index. There is a general perception that as plastic limits of soils becomes larger so does their expansion potential. Though, no specific conclusions are given except for a wide range of values that often overlap with other classes. This is partly because of the fact that the diluting effect from fine sand and silty fractions is higher on plastic limit determination tests (Kezdi, 1980). For example soils with low plasticity can sometimes exhibit higher plastic limits due to the difficulty to mould such soils at lower moisture contents.

Correlation coefficients between the engineering parameters and absorption feature parameters were also calculated. Table 5.3 shows the summary of results of correlation coefficients between absorption feature parameters (calculated from the soil reflectance spectra acquired by the PIMA spectrometer) and the five engineering parameters for all the 80 soil samples.

~1400 nm wavelength	Position	Depth	Area	Width
LL	0.28	0.72	0.65	0.16
PL	0.15	0.51	0.47	0.20
PI	0.27	0.60	0.53	0.14
FS	0.17	0.60	0.53	-0.13
CEC	0.27	0.74	0.72	-0.25
~1900nm wavelength	**Position**	**Depth**	**Area**	**Width**
LL	-0.45	0.72	0.68	0.25
PL	-0.31	0.47	0.41	0.32
PI	-0.38	0.63	0.62	0.30
FS	-0.46	0.59	0.53	0.07
CEC	-0.62	0.75	0.67	0.08
~2200 nm wavelength	**Position**	**Depth**	**Area**	**Width**
LL	0.52	-0.46	0.36	0.37
PL	0.35	-0.29	0.19	0.14
PI	0.45	-0.41	0.35	0.41
FS	0.43	-0.30	0.30	0.45
CEC	0.67	-0.27	0.31	0.52

Table 5-3: Summary of correlation coefficients between engineering parameters and absorption feature parameters (of all the 80 soil samples) at ~1400 nm, ~1900 nm and ~2200 nm wavelengths respectively; showing the magnitude and trends of the relationships.

Depth gave higher correlation at ~1400 nm and ~1900 nm. As mentioned earlier (table 2.3 on page 17), the absorption features at ~1400 nm and ~1900 nm are due to the presence of OH & H_2O, and H_2O respectively at the two absorption bands; and those are present within clay minerals. All clay minerals are OH bearing. Most clays contain large percentages of water trapped in their internal structures between the silicate sheets i.e. they are characterized by strongly adsorbed water (e.g. Bowles, 1984; Perloff and Baron, 1976). The amount of this bound water is different for different clay types (Gillott, 1968). While the smectite clay groups (Montmorillonite, Nontronite, Saponite and Hectorite) are characterized by large amount bound water, the illite groups with lesser amounts and the kaolinite groups with little to no adsorbed water. Among the kaolinite group clay minerals, halloysite has adsorbed water in its internal structure.

"*Absorption depth is an indicator for the amount of the material causing the absorption present in a sample*" (Van der Meer, 2004a).

As a result the soil spectra exhibited these differences in adsorbed water and hence the absorption depth of different clay minerals differs in accordance with their composition. Figure 5.5 shows variation in absorption depth of compositionally different clay soils in the data set. The absorption depth exhibited by the different clay minerals at different absorption bands shows differences. Especially at the ~1900 nm absorption band the differences are clearly manifested for the three clays mineral groups in the data set.

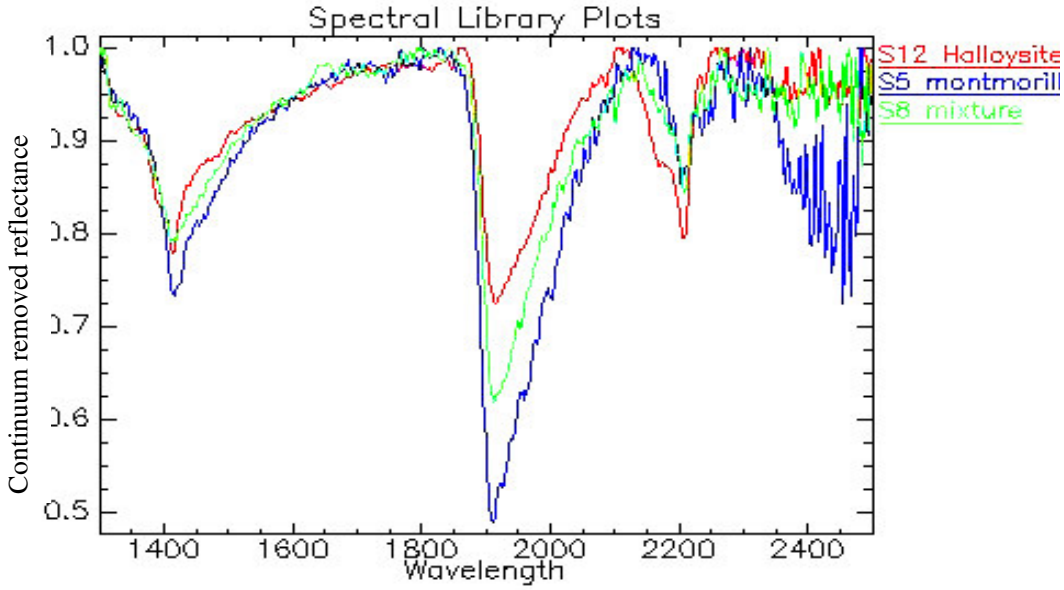

Figure 5-5: Differences in absorption depth, position, width and area of different clay types at different absorption bands.

Absorption area which is a function of depth and width is also influenced in the same manner. Hence absorption area at ~1400 nm and ~1900 nm gave higher correlation coefficients with the engineering parameters.

However, absorption feature parameters can be influenced by variations in grain size and other impurities (e.g. van der Meer, 1995, 2004) like organic matter and quartz which are common in soils (Fitzpatrick, 1980); and iron oxides that might be present in soils either as a primary mineral or as a result of weathering of parent materials (McSweeney, 1999).

Van der Meer (1995) demonstrated the effect of grain size on reflectance spectra of minerals & found that it influences the overall brightness and depth of the absorption bands. While he observed the fine grained samples to appear relatively bright and show weaker absorption features; the coarser samples were recognised to be darker and show deeper and more prominent absorption features. Such effect of grain size on the spectral response of montmorillonite clays was also presented by Christopher and Mustard (1999). On the other hand, Porosity is also found (Jeffrey et al., 1998) to

be another factor that can have an influence on soil spectral responses and subsequently on absorption feature parameters.

In general the information contained in the soil spectra is a multiple response of the different materials that can be present in the soil samples (e.g. quartz, organic matter etc). It can also be influenced by some physical properties of the soil samples (e.g. texture which includes grain size and porosity). Hence not all the information carried by the spectral data is relevant to the soil's expansion potential related properties. The same holds true as for the engineering parameters. While presence of quartz can have a diluting effect on the engineering parameters, presence of organic matter and iron oxides (if amorphous) can enhance the values of the engineering parameters. This contribution of other non clay minerals to the soil reflectance spectral response as well as to that of the engineering parameters is responsible for the overall lower relationships obtained between the engineering parameters and absorption feature parameters.

Absorption feature positions at ~1400 nm and ~2200 nm show positive relations with the engineering parameters. On the contrary, negative relation is apparent between position at ~1900 nm & the engineering parameters. As the soils expansion potential increases, the wave length position at ~1900 nm tends to shift towards the shorter wave length even if the magnitudes of relations are just fairly strong. On the other hand, absorption feature depth which shows a positive relationship with the engineering parameters at other absorption bands show a negative relation for the absorption band at ~2200 nm. Figure 5.5 shows the absorption depth exhibited by the three different clay mineral groups.

5.1.3. Simple linear regression models to predict engineering parameters from soil reflectance spectra

Box plots are important and strong graphical statistical tools to explore the structure of data and visualize the spread and variability, possible relationship between variables etc (Hocking, 2003).

We used box plots to explore the relationships between different variables from the engineering parameters versus the absorption feature parameters. The relationships are found to be clearer when using category variables to group the soil samples in to classes of more or less similar nature. We used mineralogical composition classes resulted from the spectral interpretations and plasticity classes from the classification results of soil plasticity classes using the Casagrande plasticity chart as category variables.

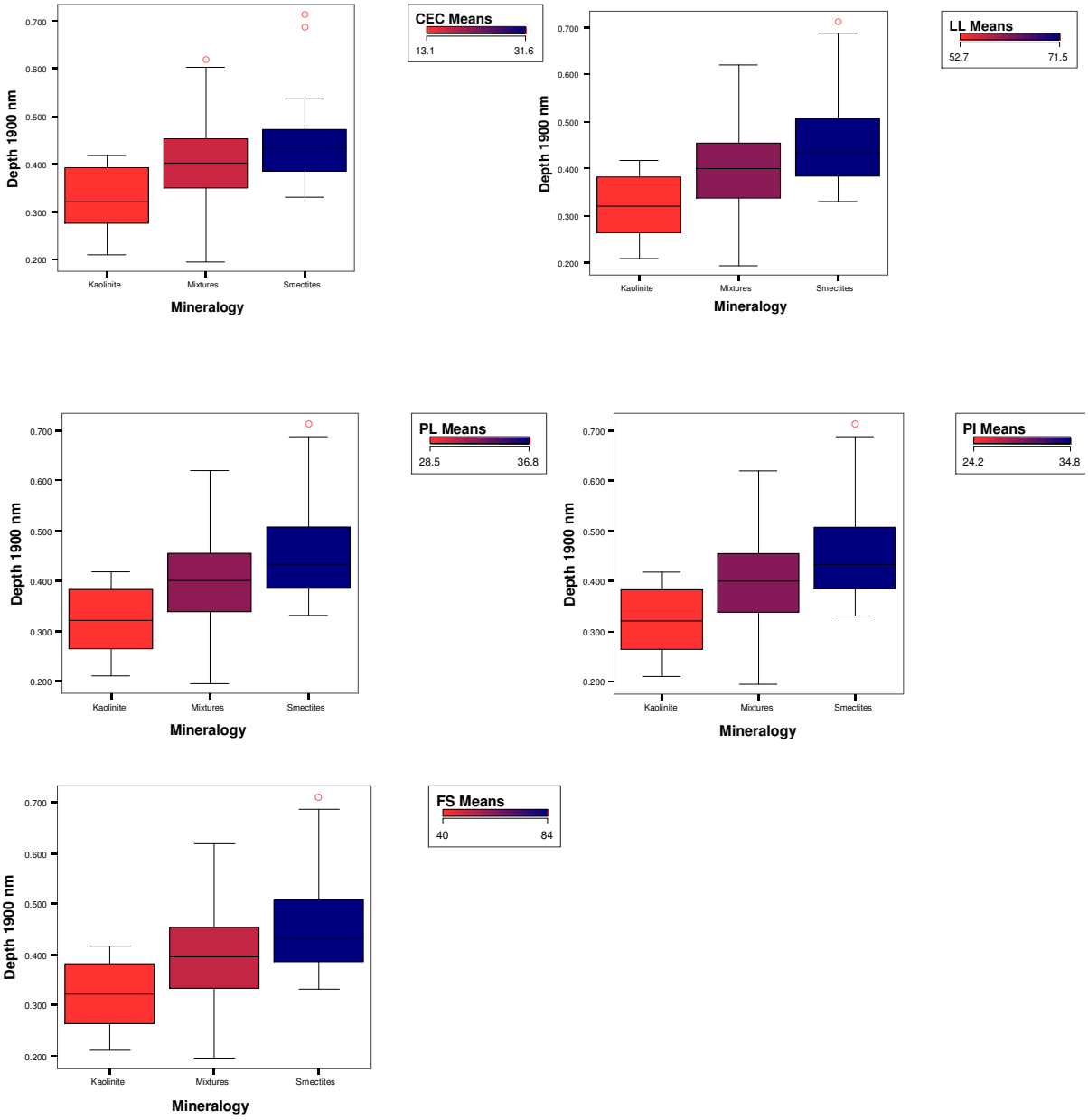

Figure 5-6: Box plots of depth at ~1900 nm versus cation exchange capacity, liquid limit, plastic limit, plasticity index and free swell as a function of mineralogy; suggesting a near linear relationships between the parameters and showing the influence of mineralogical composition of the samples on the absorption depth parameter as well as on the engineering parameters.

The above box plots suggest a near linear relationship between depth at ~1900 nm and Cation exchange capacity, liquid limit, plastic limit, plasticity index and free swell results of the soil samples. The means of each category is increasing positively with an increase in soil expansive potential. They also reveal an interesting characteristic in the data, an influence from mineralogical composition of the soil samples on absorption feature parameter depth. This is in agreement with previous works done in this respect (e.g. Kariuki, 2003; Pontual et al.). Smectites show higher depths due to the presence of strongly adsorbed water in their structure followed by the mixtures,

and the kaolinite groups which do have little (e.g. halloysite) or no (e.g. kaolinite) bound water in their internal structure. The mixtures group show larger variability (note the extended whiskers of their box plots) as it might be expected.

Simple scatter plots were used to examine the magnitude of relationships that soil samples in each category of mineralogical groups can exhibit with respect to the engineering parameters and the absorption feature parameter depth. The scatter plots in figure 5.7 show an overview of the strength of relations between depth at ~1900 nm and, CEC and liquid limit respectively of the different clay mineral categories (kaolinite, mixtures and smectite groups).

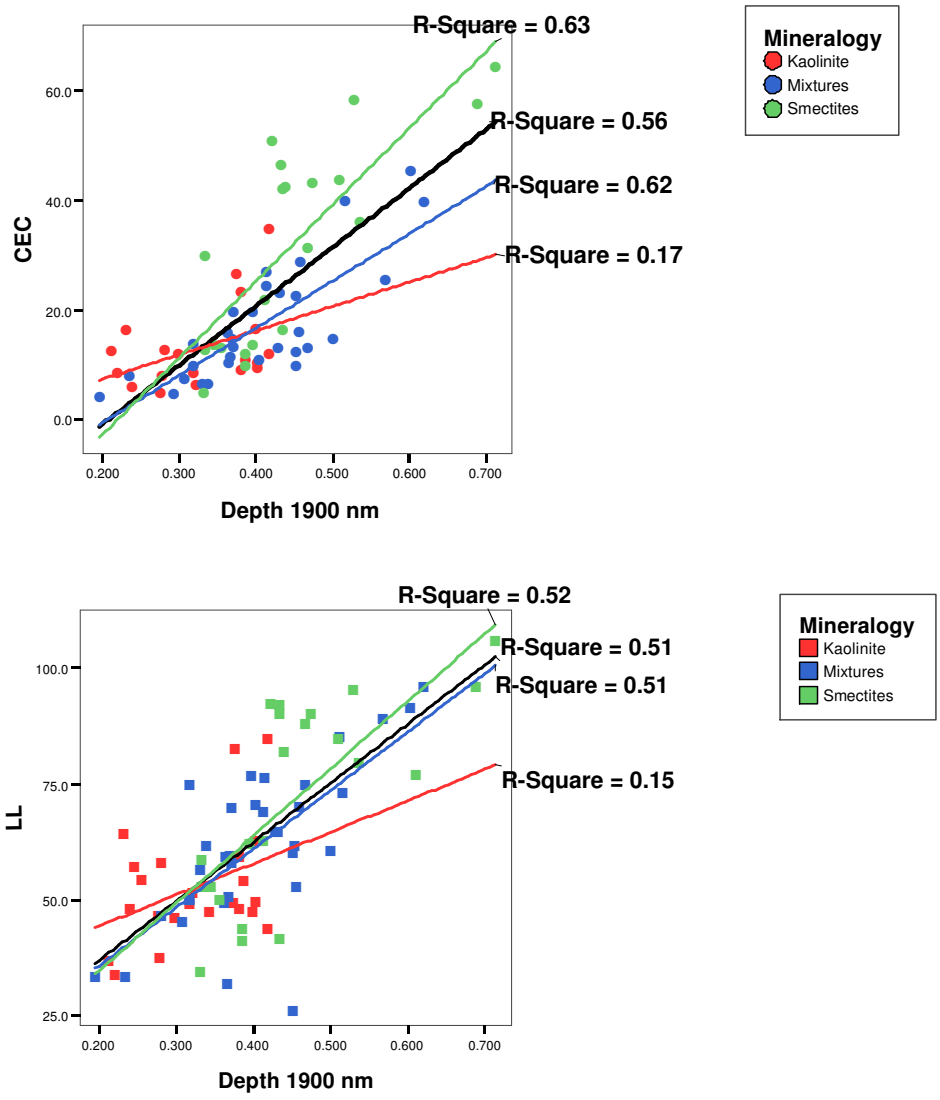

Figure 5-7: Scatter plots showing the relationship between depth at ~1900 nm and, CEC and liquid limit respectively of different clay mineral categories; showing the magnitude of the linear association per mineralogical group. The total regression line is shown in black line.

As it is apparent in the scatter plots, the magnitude of relationship between depth and the two engineering parameters is highest for smectites followed by the mixtures. Kaolinites show the lowest correlation.

As far as the absorption feature position is concerned, researchers have found out that OH and H_2O molecules bond with cations (Al, Fe, Mg etc) have different bond lengths. Hence different wave length positions that will help in discriminating different mineral types (Clark, 1999; Van der Meer, 1995). The box plots in figure 5.8 reveal the effect of mineralogical composition on absorption feature position. They also suggest a near linear relationship (negative as also indicated in table 5.3) between position at ~1900 nm and CEC, LL, PL, PI and FS. This is in agreement with previous work done in this respect for example Kariuki's (2003) observations. Kariuki (2003) observed the tendency of the absorption feature position at the ~1900 nm of kaolinite rich clay mineral mixtures to shift to the longer wavelengths. He also noticed that it tends to shift to the shorter wavelengths with an increase in smectite content.

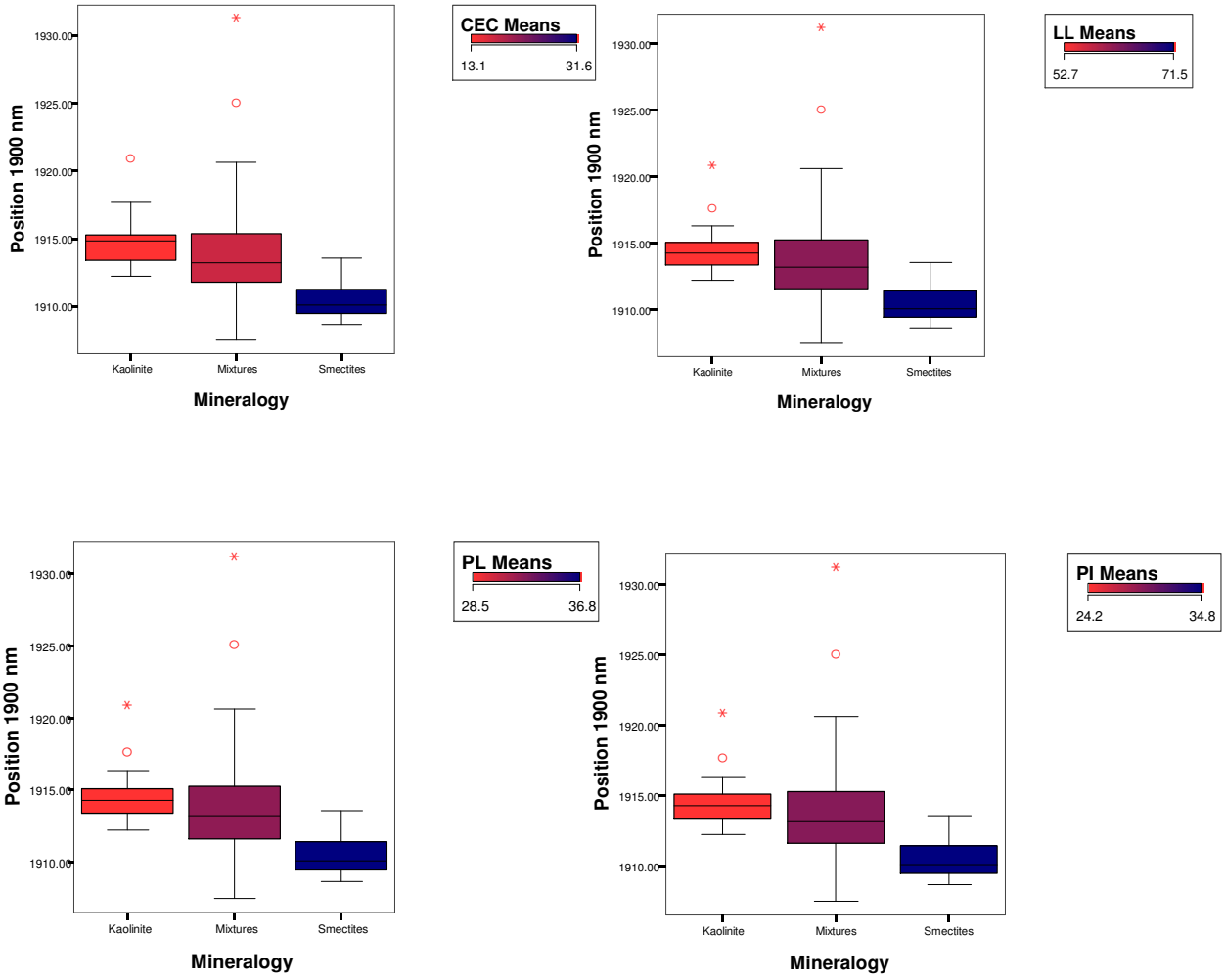

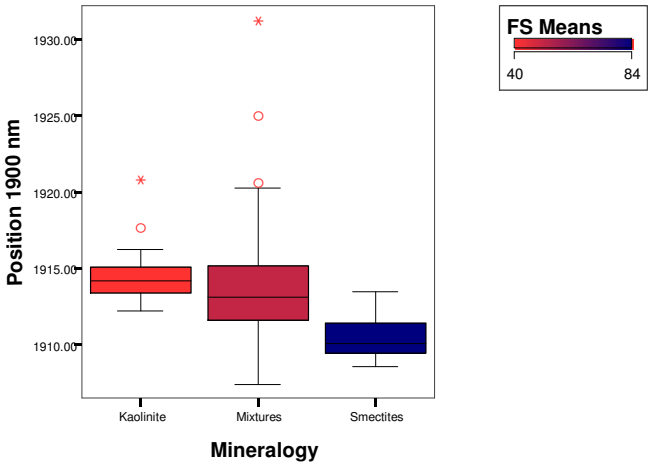

Figure 5-8: Box plots of position at ~1900 nm versus cation exchange capacity, liquid limit, Plastic limit, Plasticity index and free swell as a function of mineralogy; suggesting a near linear relationships between the parameters & showing the influence of mineralogical composition on the position of the absorption band as well as on the engineering parameters.

After having seen the possible relationships between individual engineering parameters and absorption feature parameters, we established simple linear regression models linking the engineering parameters with the absorption feature parameters. Figure 5.9 shows relations between the five engineering parameters with depth at the ~1900 nm absorption feature.

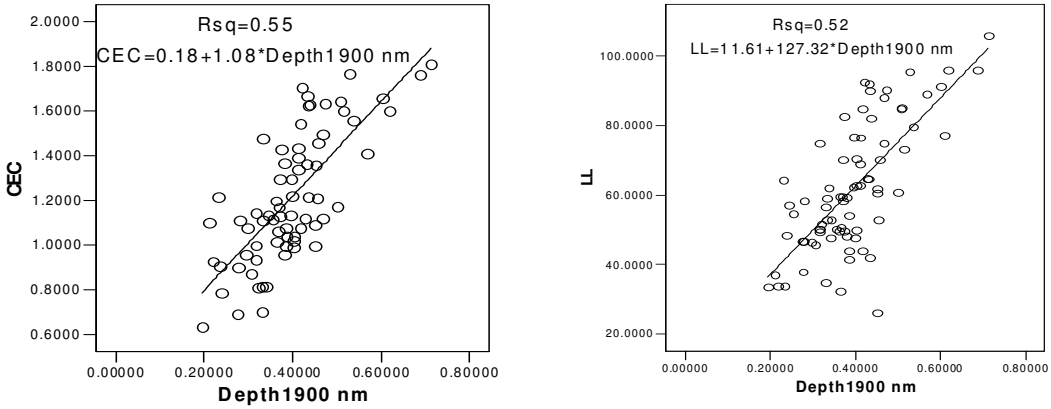

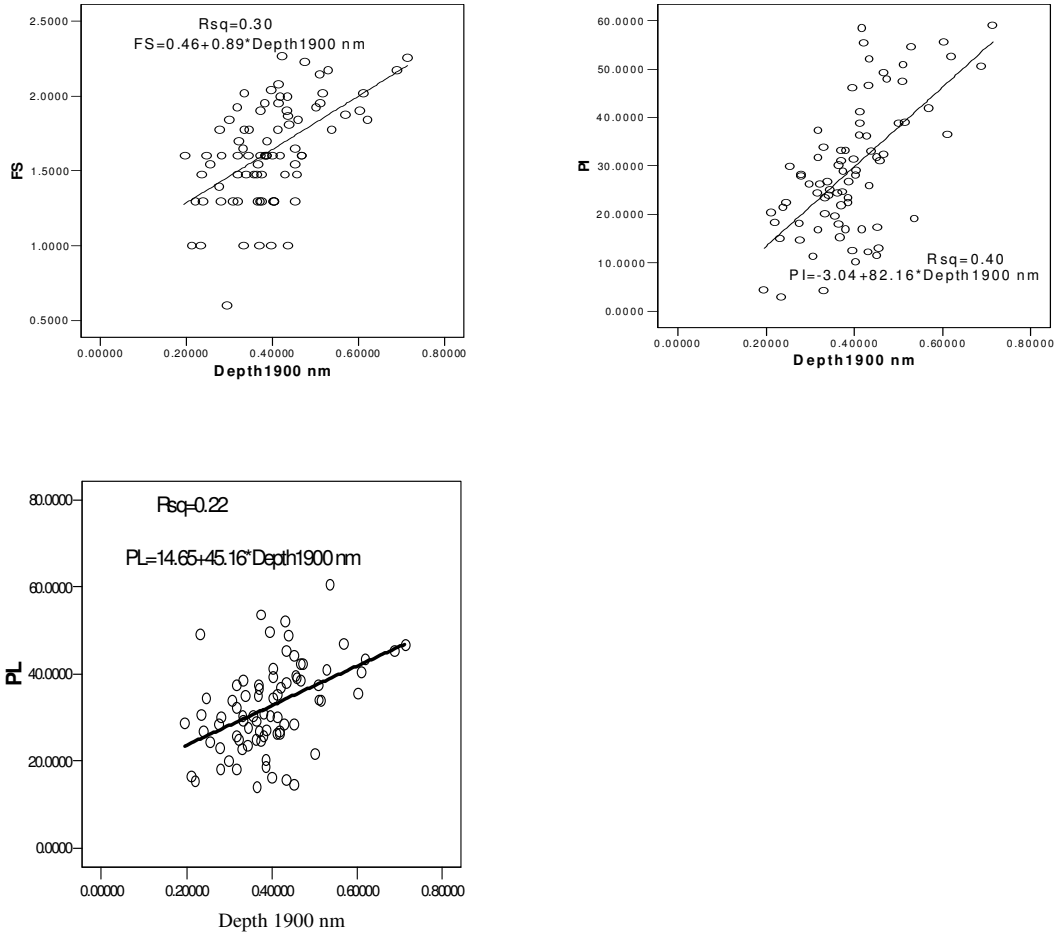

Figure 5-9: Relations between CEC, LL, FS, PI and PL with absorption feature depth at ~1900 nm.

The regression models were tested for statistical significance and the residual plots were examined. The standard error of estimate was found to be 0.1 for CEC, 13 for LL, 0.14 for FS, 1.06 for PI and 9 for PL respectively.

The results that we obtained are different from the results demonstrated by others (e.g. Kariuki, 2003). Apart from the similarities in overall trends and relative magnitudes, our results in terms of models equations and coefficients of determination are different. This gives an indication of the influence of environmental specific factors responsible for soil formation; which in turn result in differences in soil properties of different environments. Kariuki (2003) demonstrated correlation coefficients and regression results of higher magnitude for clay mineral mixtures and soil samples that he obtained from Spain and Kenya.

The different soil forming factors; parent materials, climate, topography, vegetation and organic matter, human activity and time (Gray and Murphy, 2002) differ from environment to environment. For example climate which controls weathering of the parent material, leaching of soluble bases, down slope movement and deposition of clays, soil biotic activity and organic matter production etc (Gray and Murphy, 2002) is different in different geographic locations. Gray and Murphy (2002)

have demonstrated the strong control from topography, organic activity and time on soil properties. They discussed the influences of topography on soil properties in relation with its significance on drainage and hence leaching and oxidation. They also presented the control from organic activity on properties like the contents of organic matter in soils. In addition they mentioned that chemical composition of soils might diverge from that of the original parent material and hence soils derived even from the same parent material might exhibit different pedologic characteristics due to age differences. Hence, models developed for soils of a particular environment might not be applicable for another different environment of different geographical setting. This is also reflected by the results we obtained here.

6. Predicting engineering parameters from spectral data using PLSR

We used a multivariate calibration method, partial least squares regression (PLSR) analysis (Martens and Naes, 1989; Wold et al., 2001), to construct empirical prediction models that enable the quantitative estimation of engineering parameters of expansive soils from their respective reflectance spectra.

Absorption feature parameters (Kariuki, 2003; Van der Meer, 1995, 2004a) and simple wavelength approaches (Kooistra, 2004; Scholte, 2005) were employed in establishing the empirical relations.

6.1. Partial least squares regression (PLSR)

PLSR is defined by Herman Wold (2001), who originally invented the method, as regression by means of projections to latent variables. The method was first proposed in the 1970's, and is currently very popular in various disciplines, among which is spectroscopy. In VNIR spectroscopy, PLSR has become a widely spread technology for qualitative and quantitative analysis. This includes routine quality control activities; in chemical, pharmaceutical and agro-industries, for it is found to be a fast, cheap, simple and non-destructive technique with little or no sample preparation requirements (Herve, 2003).

The Multivariate calibration method PLSR is found to be particularly important (Martens and Naes, 1989) when dealing with a large number of variables that express common information to avoid collinearity problems. It has also been mentioned that it reduces the impact of irrelevant X variation in the calibration modeling by balancing the information in the X and Y spaces. This is especially the case when one acquires a large data set using modern instrumentation like spectrometers, where, apart from having numerous X-variables, there is also a tendency of these variables for being correlated, sometimes noisy and incomplete (Wold et al., 2001).

On the other hand, the need to use PLSR analysis method can arise from the difficulty to obtain measurements only of the specific parameters that one is interested in. Martens and Naes (1989) discussed problem of selectivity while trying to take measurements of specific properties from inhomogeneous materials and presented a multivariate calibration method, PLSR as a solution.

Partial least squares (PLS) deals with prediction of a set of dependent (response) variables from a set of independent variables (predictors). It combines features from principal components and multiple regression (Herve, 2003). As in multiple linear regression it builds a linear model Y=XB+E, where Y is an n cases by m variables response matrix, X is an n cases by p variable predictor matrix, B is a q by m regression coefficient matrix, and E is a noise term for the model which has the same dimensions as Y (Wold et al., 2001).The purpose is to predict Y from X & describe their common structure (Martens and Naes, 1989). Unlike PCA which decomposes the X variables to eliminate

multi-collinearity problems & extract components that explain X, PLS finds components from X that are also relevant to Y. Since PLS considers the variation in Y when calibrating the model, the covariance structure between the predictor and response variables is reflected (Martens and Naes, 1989; Wold et al., 2001). This is achieved by projecting the X and Y-spaces into new coordinates T and U-scores respectively that summarize the common structure in the two.

Scaling of input data was found to influence the results of projection methods such as PLSR. Wold et al. (2001) mentioned and demonstrated that with an appropriate scaling, one can focus the model on the more important Y-variables, and use experience to increase the weights of more informative X-variables. They also discussed that in the absence of knowledge about the relative importance of the variables, the standard multivariate approach is to (i) scale each variable to unit variance by dividing them by their standard deviations, and (ii) center them by subtracting their averages, so-called auto-scaling. This corresponds to giving each variable (column) the same weight, and hence the same prior importance in the analysis.

Variable selection is based on significance tests. Marten's uncertainty tests show which variable contributes significantly to the model. Stability plots can be used to identify which variable causes perturbation to the models.

The models performance can be evaluated using different tests, for example measures of the error terms. Martens and Naes (1989) discussed two types of prediction errors that have opposite trends. One is the estimation error that can be caused by random measurement noise of various kinds. Root mean square error of calibration and prediction are measures of the average difference between the predicted and measured response values at the calibration and validation stages. Another is the interference error (underlying bias) which is the systematic error due to the un-modelled interference in the spectral data. Minimal prediction error is obtained when the remaining interference error and the uncertainty error balance each other.

In PLSR, the focus is on prediction rather than in trying to understand the underlying relationships between the variables (Scholte, 2005). Hence PLSR is rather a hypothesis generating tool for which the interpretation would lead to the requirement of more experimental and analytical work for verification (Martens and Naes, 1989).

6.2. PLSR models to predict engineering parameters from soil reflectance spectra

Different approaches were employed to predict the engineering parameters of the soil samples from their reflectance spectra.

The first approach was a knowledge driven approach as demonstrated by Van der Meer (1995 and 2004a) and Kariuki (2003). This involves the use of absorption feature parameters that were previously calculated from the known wavelength regions (table 2.3 on page17) for clay minerals related spectral characteristic indications in establishing a link to the engineering parameters. We run the PLSR analysis on all the reflectance spectra of the eighty soil samples.

The second approach was a data driven approach. Scholte (2005) and Kooistra (2004) have demonstrated this approach in which they used all the wavelengths of the spectrometers to predict the desired response variables. This type of data driven PLSR approach has also been presented in Wold et al. (2004), where it was found to be an appropriate method in facilitating the understanding of complex data structures and thereby complementing the knowledge driven research approaches.

6.2.1. Knowledge driven PLSR to predict engineering parameters from spectral data

The absorption feature parameters that were calculated from the absorption bands at ~1400 nm, ~1900 nm and ~2200 nm were used for predicting the five engineering parameters.

The PLS1 analysis (predicting a single engineering parameter at a time) method implemented in The Unscrambler software (CAMO, 1986-2005) was used for the multivariate calibration and validation.

We performed outlier detection, since their presence in the input dataset can deteriorate the models prediction ability and also their reliability. Outliers are abnormal observations that show significant deviation from the rest of the dataset in the population (Martens and Naes, 1989). They might arise either due to error in the experiment or instrument. They might also represent different information other than the material of interest and hence irrelevant. Presence of outliers in the data set is known to influence both the calibration and validation of PLSR models. To avoid erroneous calibration and deterioration of a model's prediction ability, it is important to detect outliers and remove or replace them by accurate values (Hocking, 2003; Martens and Naes, 1989). Outliers were mainly identified manually instead of using the automatic outlier detection method. The automatic detection tends to include many of the extreme values (either from the lower or higher extremes) in the outliers list.

Different methods are developed to detect sample outliers in PLSR modeling. Martens and Naes (1989) presented outlier detection criteria based on the analysis of residuals and leverages. In PLSR modelling, residuals are of diagnostic interest. It is possible to examine the residual variances (the variation that is left unexplained) in the X as well as the Y-spaces. Wold et al. (2004) demonstrated that large Y-residuals indicate that the model is poor. Normal probability plots of the residuals of a single Y-variable are also useful for identifying outliers in the relationship between T and Y. The X-residuals (part of X that is not used in modelling Y) are also useful for identifying outliers in the X-space, i.e., observations that do not fit the model. In addition, uncertainty tests e.g. Martens uncertainty limit tests (CAMO, 1986-2005; Martens and Naes, 1989) can be used for testing which variables are causing perturbations in the model. We used Martens uncertainty limit tests to test the stability of all variables in the model. The stability of each predictor with respect to the samples was examined by using stability plots. In general outlier detection was done based on using a combination of different tests rather any single method. A total of five sample outliers from CEC, ten from Atterberg limits and twelve from FS were detected, and removed from the dataset. Soil samples having sandy and silty nature (mainly less decomposed) and samples obtained from forested areas were those in the outliers list.

A sufficient number of PLS factors were used in predicting various engineering parameters from the soil spectral data in order to explain as much of their variance as possible. However, including too many PLS factors was observed to often lead to over fitting problems (Kooistra, 2004; Scholte, 2005) for it incorporates irrelevant information or noise. Hence, the number of PLS factors used in the models were based on different tests intended for testing the significance of the PLS factors in the prediction. The tests are implemented in The Unscrambler software, and among them are simultaneous examinations of the residual variances and the root mean square errors (RMSE) of each factor coupled with significance tests through cross validation. Cross validation is mentioned to be a practical and reliable way of testing the predictive significance of PLS factors (Davies, 2001; Wold et al., 2001) that has become a standard in PLS analysis (Martens and Naes, 1989). Davies (2001) demonstrated the application of cross validation methods for determining the number of PLS factors that should be included in a model for the proper explanation of the phenomena of interest that one would like to model.

In deciding which variables, among the predictors, should be retained in the model, we used Martens uncertainty limit test. Martens uncertainty limit test is significance test in PLS analysis. It is useful in testing whether the regression coefficients used in a model are significantly contributing to the model. Regression coefficients that are significant were then identified and those that have got an uncertainty limits passing the origin were left out.

Another uncertainty test that was applied on the score and loading plots was stability calculation which can be visualized in The Unscrambler as *stability plots.* It shows the influence of each variable and hence its significance (CAMO, 1986-2005) in the model. Samples far from the center have more influence on the model than those that are near, and the uncertainty is larger on those with larger spread implying that these variables are not significant (CAMO, 1986-2005; Davies, 2001).

Prior to considering the calibrated models for practical applications, i.e. the prediction and subsequent understanding of new data set or samples, the model should be validated (Wold et al., 2001). This is a crucial step in PLSR modeling, for it gives an indication on how well the models will perform in the future and the degree of certainty that one might expect while using the models to solve practical problems. Different types of validation methods were discussed and presented in various literature (Kooistra, 2004; Martens and Naes, 1989; Scholte, 2005; Wold et al., 2001). Of which, cross validation method has found its application in cases where the data set that one is working on is small and hence a separate or independent and representative validation data set is unavailable (Martens and Naes, 1989; Wold et al., 2004). Kooistra (2005) used a full cross validation method, which is based on a leave one out principle where one sample will be left out at a time and the model is calibrated on the remaining samples (CAMO, 1986-2005). This will be repeated N times until every sample is left out once and the model is computed on the remaining samples and the left out sample is predicted. The results of the PLSR modeling for the five engineering parameters are shown in figures 6.1 to 6.5 for CEC, LL, PL, PI and FS respectively.

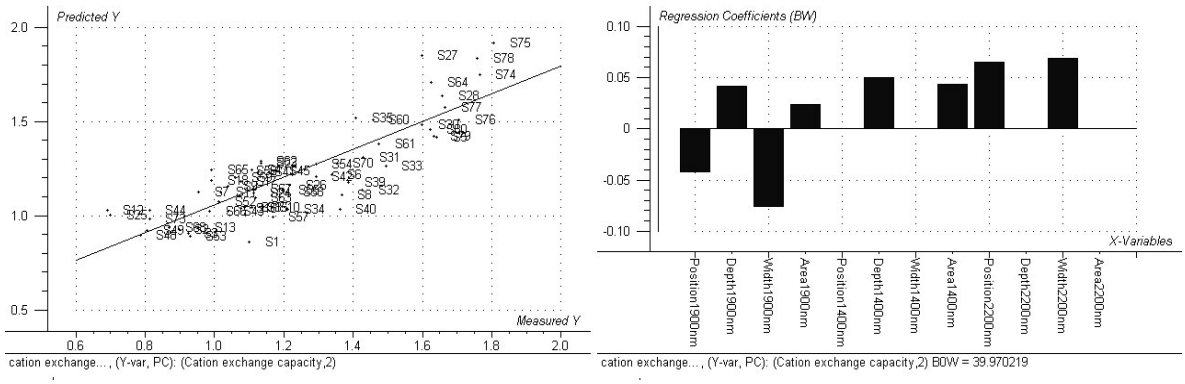

Figure 6-1: Results of knowledge driven PLSR modeling for CEC; regression overview of prediction showing the predicted versus measured CEC and significant regression coefficients respectively.

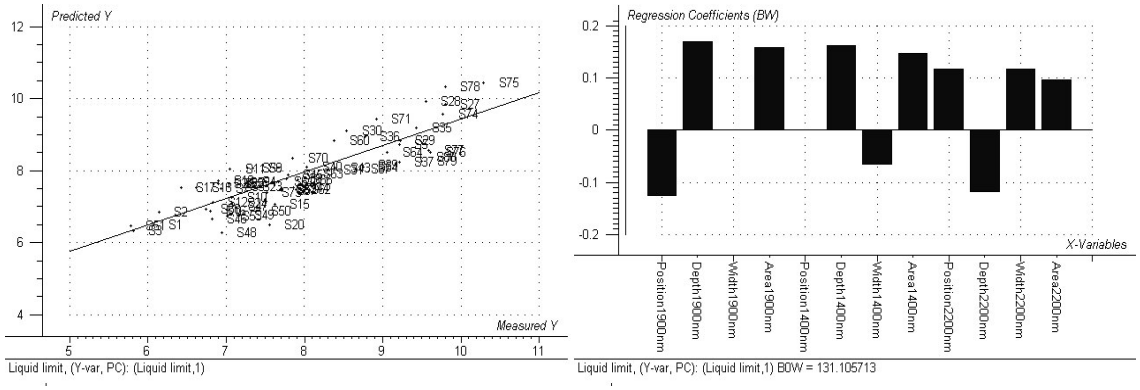

Figure 6-2: Results of knowledge driven PLSR modeling for LL; regression overview of prediction showing the predicted versus measured LL and significant regression coefficients.

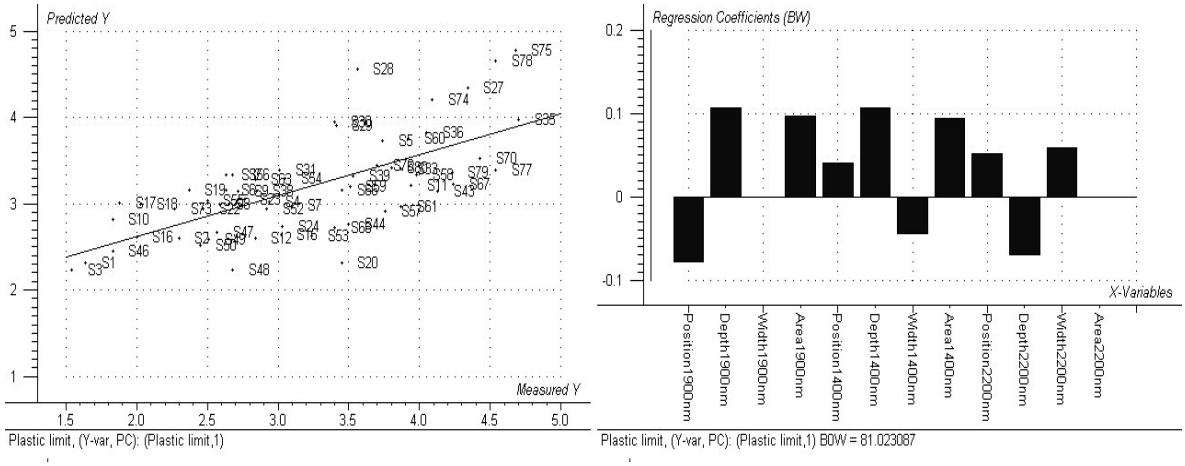

Figure 6-3: Results of knowledge driven PLSR modeling for PL; regression overview of prediction showing the predicted versus measured PL and significant regression coefficients.

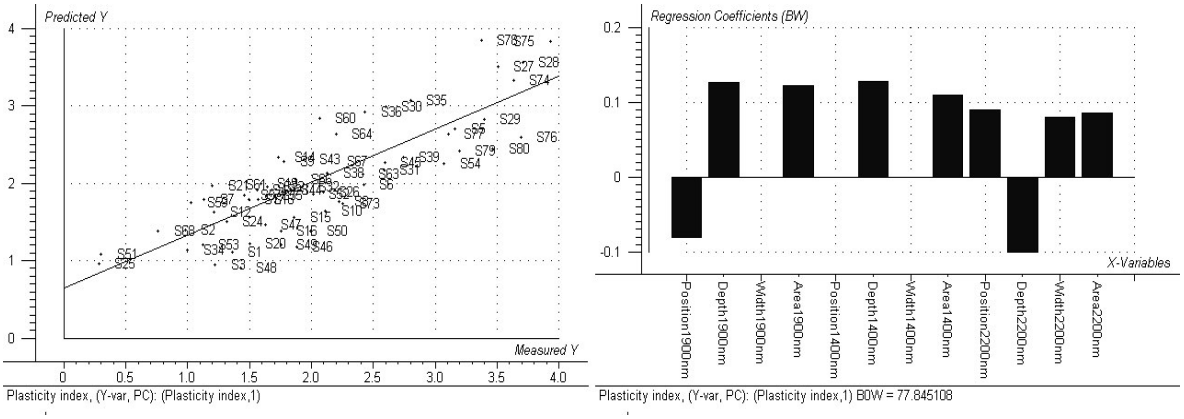

Figure 6-4: Results of knowledge driven PLSR modeling for PI; regression overview of prediction showing the predicted versus measured PI and significant regression coefficients.

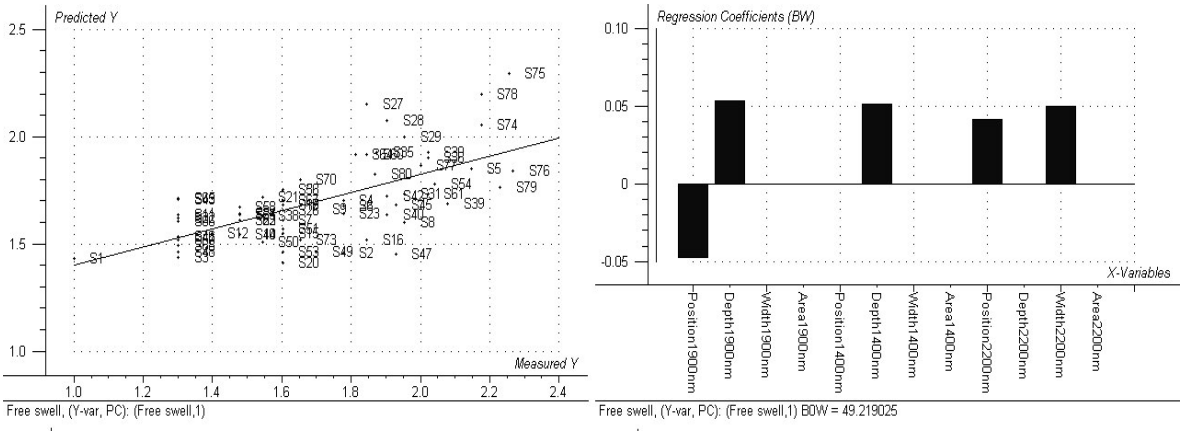

Figure 6-5: Results of knowledge driven PLSR modeling for FS; regression overview of prediction showing the predicted versus measured FS and significant regression coefficients.

In all the five models the estimation error, both RMSEC and RMSEP are small (see table 6.2 on page 72 for summary of the results of PLSR modeling). This indicates that if we made prediction on new samples using these models the expected error will be within the acceptable limits.

The smallest CEC is zero for a soil sample composed of pure sandy material. However, small intercalation of active clays can raise the CEC of sandy soils up to a minimum of 3 meq/100 g of clay (NSW, 2004). The smallest liquid limit is undefined for a soil sample composed of pure sand and silty material, for it is not possible to determine liquid limit of such soils. However a small intercalation of active clays can raise the liquid limit of such soils up to a minimum of 20 % (Mitchell, 1993; Perloff and Baron, 1976). The smallest Plastic limit and plasticity index for a soil sample is also undefined for it is not possible to determine it. As far as free swell is concerned, a soil sample without an active clay minerals or organic matter doesn't exhibit any swell at all.

The standard error of calibration and prediction, SEC and SEP which indicate the precision of the predication over the whole samples (CAMO, 1986-2005) are also small. The bias, which is the

average value of the difference between the predicted and measured values, is also small (both in the calibration and prediction stages) for the given number of PLS factors indicating that the effect of bias is negligible (Martens and Naes, 1989).

6.2.2. Data driven PLSR to predict engineering parameters from spectral data

In this approach, we simply used all the wavelengths of the ASD fieldspec acquired soil spectra that also fall within the nine ASTER band sets in the VNIR and SWIR wavelength regions. A total of six hundred and twelve variables were resulted while limiting the spectral regions in to ASTER band sets. The absorption features at ~1400 nm and ~1900 nm are not available in this case. The minor water absorption feature around the 900 nm spectral region, which is also related to Fe- bearing minerals spectral characteristic is also not available. Since these are situated in atmospheric attenuation windows due to atmospheric water, there are no ASTER bands situated in these particular wavelength regions of the electromagnetic spectrum.

The distribution of spectral variables was examined. Appropriate transformations (in most cases a logarithmic transformation) were carried out on variables that showed skewed distributions to make their distribution fairly symmetrical (Wold et al., 2001). We applied different spectral data preprocessing techniques on the soil spectra prior to performing the PLSR analysis. Scholte (2005) discussed the importance of spectral preprocessing as a crucial step in PLSR modeling for this help in enhancing spectral features so as to obtain accurate input data for the PLSR analysis. He also mentioned some useful techniques in this respect. On the other hand, Martens and Naes (1989) discussed spectral data preprocessing in relation to improving models prediction ability and reduction of prediction errors. They discussed the importance of avoiding or reducing irrelevant variation in the X-space that can arise from interferences due to instrument noise or some other physical properties unrelated to the phenomena of interest that one would like to model.

Spectral data normalization was done by dividing each variable by the maximum value for better account of spectral range (Scholte, 2005). Martens and Naes (1989) mentioned the need to normalize spectral input data in order to remove uncontrollable scale variations which they also illustrated mathematically. Normalization will not induce any change into the data set except for simply scaling the spectral parameters.

Multiplicative scatter correction, MSC (in this case common amplification) was done to avoid scatter effects from the soils texture, grain size and porosity. In MSC correction, the scatter for each sample will be estimated relative to that of the reference sample (in this case the mean spectrum that is calculated from all spectra).

To achieve this, the average or mean spectrum, $\overline{X}$ was calculated from the set of spectra constituting the calibration samples. For each individual spectrum, $\mathbf{x_i}$, the parameters $\mathbf{a_i}$ and $\mathbf{b_i}$ were estimated by regression onto $\overline{X}$ **.** The estimated parameters $\mathbf{a_i}$ and $\mathbf{b_i}$ representing the offset or additive parameter and the slope or multiplicative parameter of the regression line were then used for correction of the spectrum according to the following formula;

Common amplification: $Mnew(i,k) = \frac{M(i.k)}{bi}$ (CAMO, 1986-2005)

Then each sample was corrected so that all the samples appear to have the same scatter level as the reference (Martens and Naes, 1989).

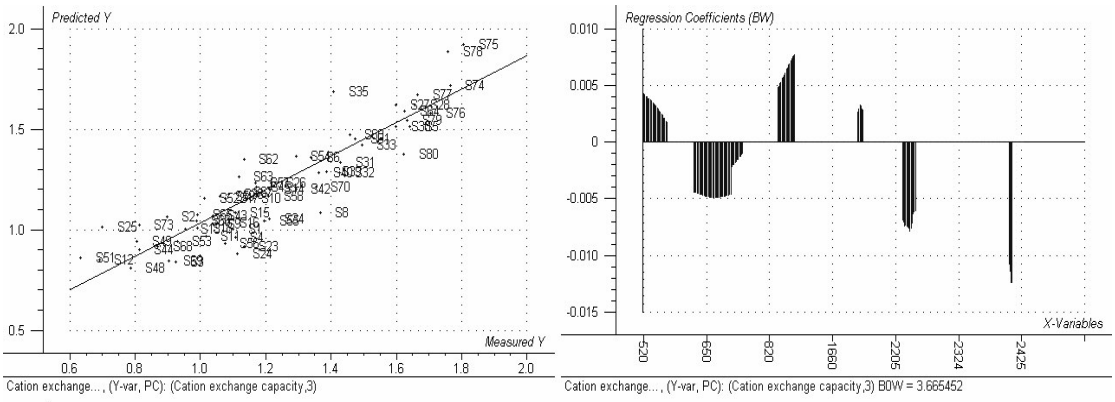

Figure 6-6: Results of data driven PLSR modeling for CEC; regression overview of prediction showing the predicted versus measured CEC and significant regression coefficients.

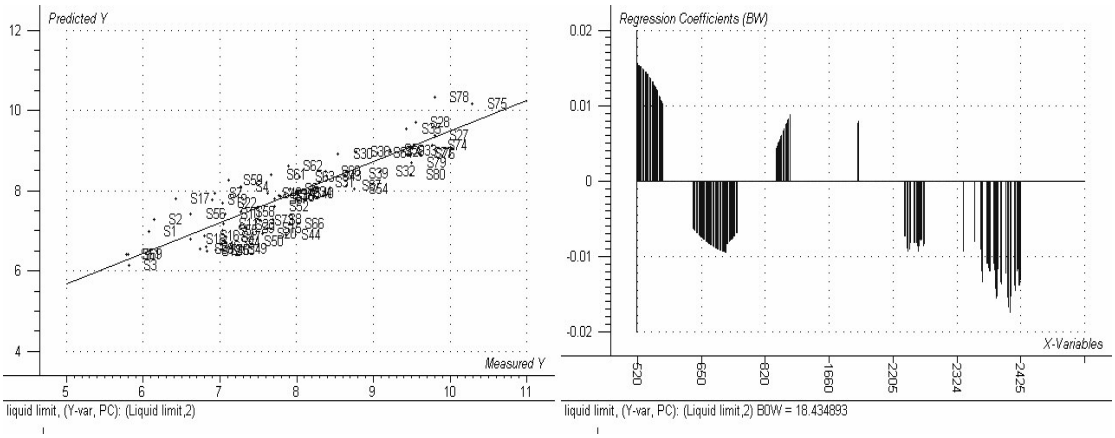

Figure 6-7: Results of data driven PLSR modeling for LL; regression overview of prediction showing the predicted versus measured LL and significant regression coefficients.

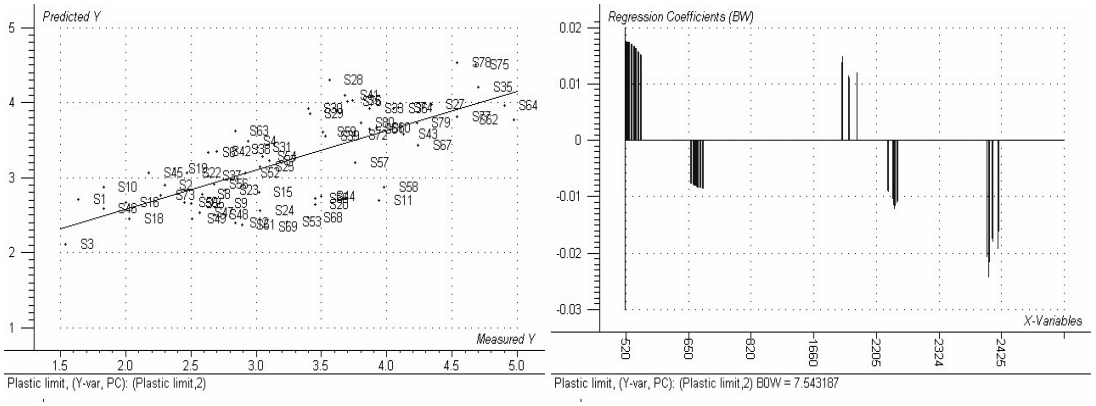

Figure 6-8: Results of data driven PLSR modeling for PL; regression overview of prediction showing the predicted versus measured PL and significant regression coefficients.

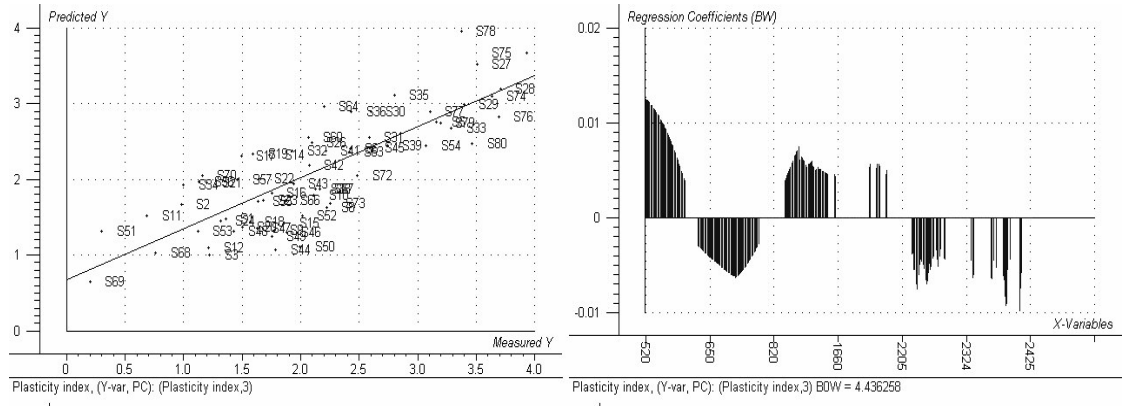

Figure 6-9: Results of data driven PLSR modeling for PI; regression overview of prediction showing the predicted versus measured PI and significant regression coefficients.

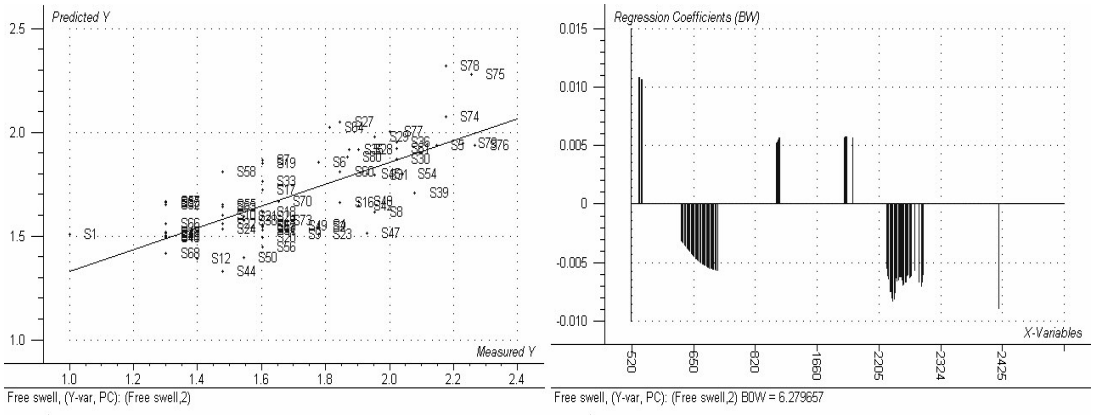

Figure 6-10: Results of data driven PLSR modeling for Fs; regression overview of prediction showing the predicted versus measured FS and significant regression coefficients.

Substantial part of the variation in the X-space (variation in the spectral parameters) is used to explain the variation in the Y-spaces (variation in the engineering parameters). This gives an

indication that a large portion of the spectral characteristics of the soil spectra are directly relevant to the engineering parameters of interest. Cases where substantial portion of the X–blocks does not participate in modeling the parameters in the Y-block are attributed to either lack of common variance or large errors (Geladi and Kowalski, 1986).

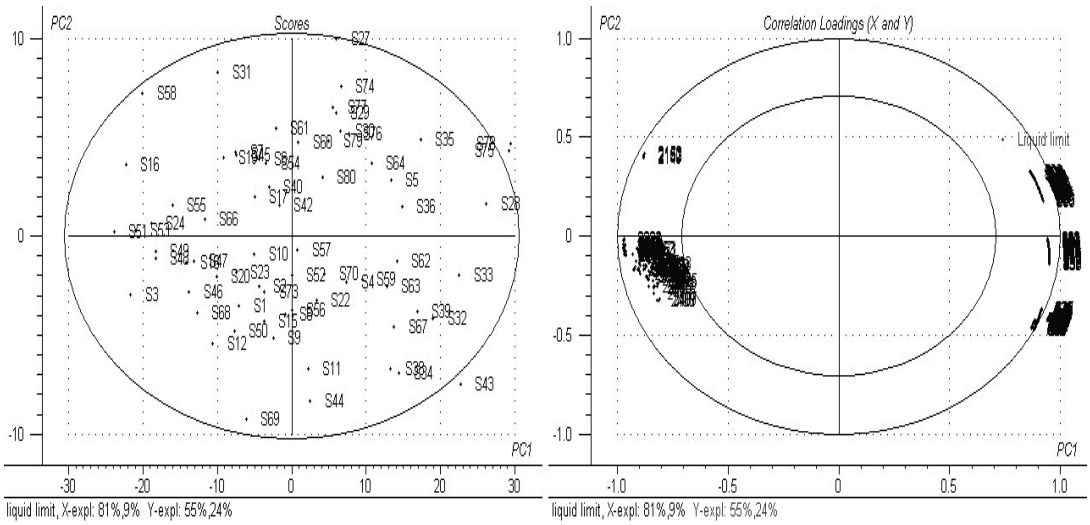

Figure 6-11: Score plot of the engineering parameter liquid limit with a circle (Hotelling T2 Ellipse) showing the 95% confidence interval; and loading plot showing the trend and contribution of spectral parameters to explain LL. The figures below the bottom line show the variation in X that was used to model Y (81%, 9%), and the variation in Y that is explained (55%, 24%) using two PLS factors.

It is possible to code the samples on the score, loading and regression plots by a relevant categorical variable of interest. We coded the samples using the Casagrande soil plasticity classes and the mineralogical groups that were obtained from the spectral interpretation results. Figure 6.12 shows regression overview of liquid limit coded with these classes. This exhibits some informative and interesting patterns and characteristics in the data set. The coded regression plots reveal that the samples are aligned in accordance with their respective plasticity and mineralogical classes. The highly expansive classes plot on the upper parts of the regression plot, and the lowest on the bottom part of the regression plot forming a relatively uniform clustering in each class. However, some samples from the smectite and mixture groups seem to disperse among other classes. This can be attributed to the possibility of variation in the amount of smectite mineral content with respect to other constituents within the soil samples.

Among the wavelength regions that are identified as spectrally significant for the prediction of the engineering parameters of interest from the soil spectral data, some fall in the VNIR and some in the SWIR wavelength regions. Those in the VNIR portion of wavelength regions can be attributed to the possibility of the presence of Fe-oxide minerals and organic matter within the soil samples. The soil spectra show differences in slopes and also exhibit absorption features that are known to be diagnostic of Fe-oxide minerals (Crowley et al., 2003) for example goethite. The differences on slopes that are apparent in the visible part of the spectral regions might be associated with organic matter. Presence of organic matter in soils can increase the expansion potential of soils. As far as Fe-oxides are concerned, presence of amorphous Fe-oxides can have the same amplifying effect on soil

expansion potential. Table 6.1 gives summary of correlation coefficients between slope parameter in the VNIR and the five engineering parameters for all the eighty soil spectra.

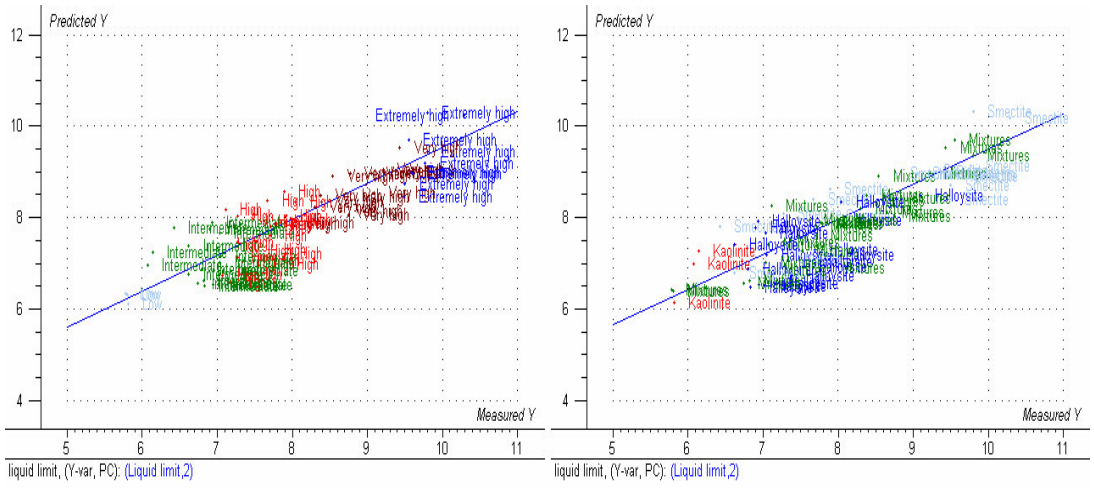

Figure 6-12: Regression overview of LL showing predicted versus measured LL with the samples classified according to their classes of plasticity from the Casagrande plasticity chart and mineralogical identification from the spectral interpretation.

VIS/NIR ~400 nm to 800 nm	Slope
LL	-0.57
PL	-0.48
PI	-0.42
FS	-0.41
CEC	-0.63

Table 6-1: Correlation coefficients between slope parameter in the VINR and the five engineering parameters.

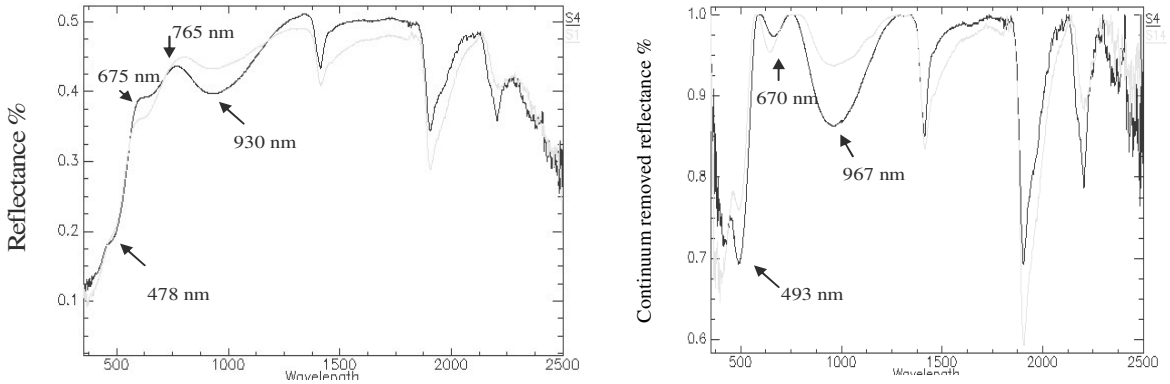

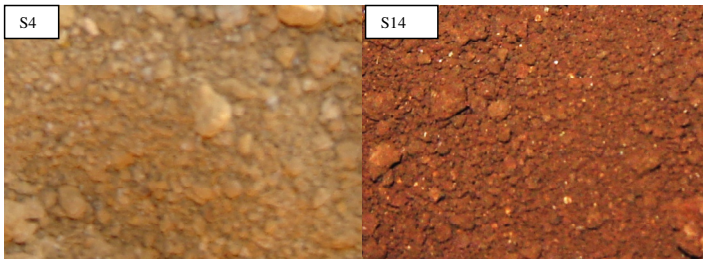

Figure 6-13: Spectra of soil samples showing presence of iron oxide mineral (goethite) and pictures of the respective soil samples (note the reddish brown and red colours).

The significant wavelength regions in the SWIR mostly coincide with the known wavelength regions for being spectrally active in relation to clay mineral related properties. For example Clark (1999) mentioned that the absorption features at ~2200 nm–2300 nm are diagnostic of clay minerals. He also attributed the cause of the absorption features at these specified wavelengths to the combination of OH stretching and bending with Al, Mg, or Fe ions.

6.3. Spectral re-sampling

Spectral re-sampling is important to compare and link the spectral signatures of materials measured by a laboratory or field spectrometers with those that are acquired by imaging devices (Scholte, 2005; Van der Meer, 1999b). Van der Meer (1999b) explained that this involves reducing the higher spectral resolution of the laboratory or field spectra into a coarser spectral resolution of the imagining devices. We re-sampled the laboratory spectra acquired by the ASD fieldspec spectrometer into the spectral resolution of a multispectral imaging device, Advanced Spaceborne Thermal Emission and Reflection Radiometer, ASTER. Besides the availability of ASTER images of the study area at different times, the large and continuous areal coverage of ASTER data are of interest.

Spectral re-sampling of the laboratory spectra into ASTER bands resulted in a limited, broad and wider spectral bands with little spectral details (lower spectral resolution) as compared to the many, narrow and contiguous spectral bands with detailed spectral features (Van der Meer, 2004b) that were available from the laboratory spectral data. Figure 6.14 shows the original ASD fieldspec acquired soil spectra re-sampled into ASTER spectral resolution.

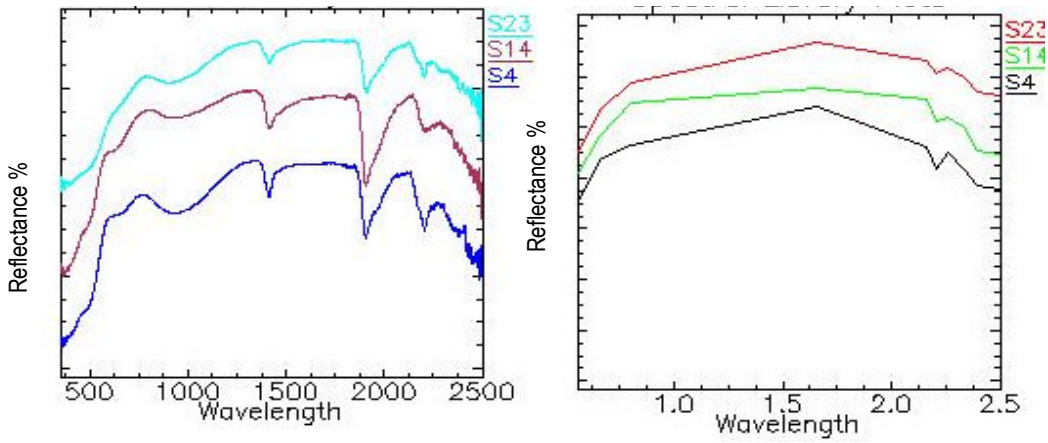

Figure 6-14: Reflectance spectra of the original ASD filedspec laboratory acquired spectra and the re-sampled spectra of same samples respectively, showing loss of some subtle spectral details that were very good for visual spectral interpretation.

It can be seen from the spectra that subtle variations in the spectral features are now broadly under-sampled and absorption features are flattened. These subtle variations were very good in enabling the discrimination of various clay mineral types possible. The absorption feature at ~2200 nm is still present on the re-sampled spectra. But it is not as detailed and well resolved as what was apparent on the original laboratory spectra of the soil samples. However, it still shows variation in shape, depth intensity, symmetry and also position to a certain extent. The shoulders to the right and left of this absorption feature show different shapes (curvatures) per the spectra of different soil samples. As previously mentioned, this absorption feature is related to the presence and the associated bonding characteristics of hydroxyl with ions (Clark, 1999) within the soil samples. The fact that this absorption feature is present after the re-sampling process can be attributed to characteristic features of the soil samples i.e. hydroxyl bearing or clayey in nature. It can also be linked to the importance of the ~2200 nm wavelength position of the ASTER bands for a clay related mineralogical composition indications. The change in slopes among the spectra of the different soil samples in the VNIR region is also somehow retained in the re-sampled spectra. This in turn can give an indication of the possibility of the ASTER VNIR bands to quantitatively characterize expansive soils. However, it was not possible to identify and differentiate the various clay minerals by visual spectral interpretation for the re-sampled spectra lacked distinctive spectral features. Hence we proceeded into the data driven PLSR analysis to establish a link between the re-sampled soil spectra and the engineering parameters.

6.3.1. Predicting engineering parameters from re-sampled soil spectra

We used the data driven PLSR analysis method to predict engineering parameters from the re-sampled soil spectra. Among the spectral pre-processing techniques that were previously discussed and applied on the laboratory acquired soil spectra multiplicative scatter correction (MSC) was applied.

Since the number of wavelengths is reduced, the number of variables to deal with was small (nine) which in turn provides with a better control and faster computation time. The results of the PLSR modelling for the re-sampled spectra are presented in the figures below.

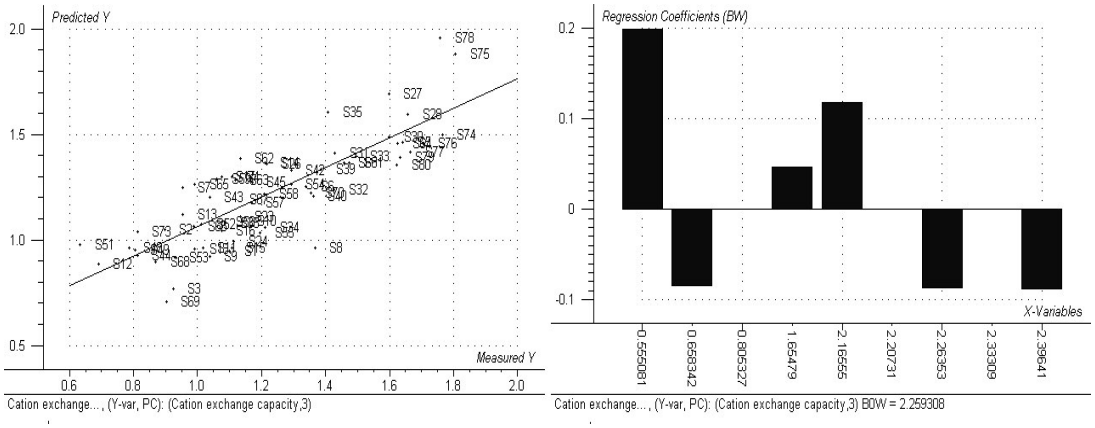

Figure 6-15: Results of data driven PLSR modeling (of the re-sampled spectra) for CEC; regression overview of prediction showing the predicted versus measured CEC, and significant regression coefficients.

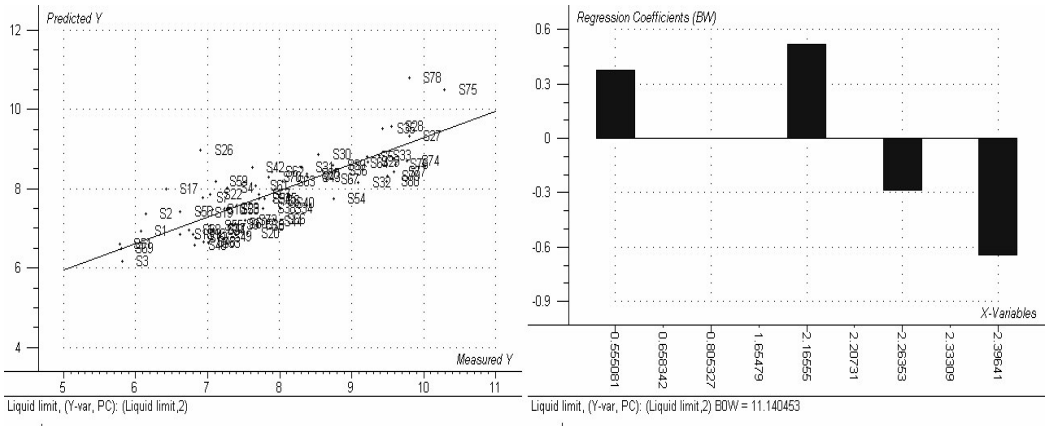

Figure 6-16: Results of data driven PLSR modeling (of the re-sampled spectra) for LL,; regression overview of prediction showing the predicted versus measured LL, and significant regression coefficients.

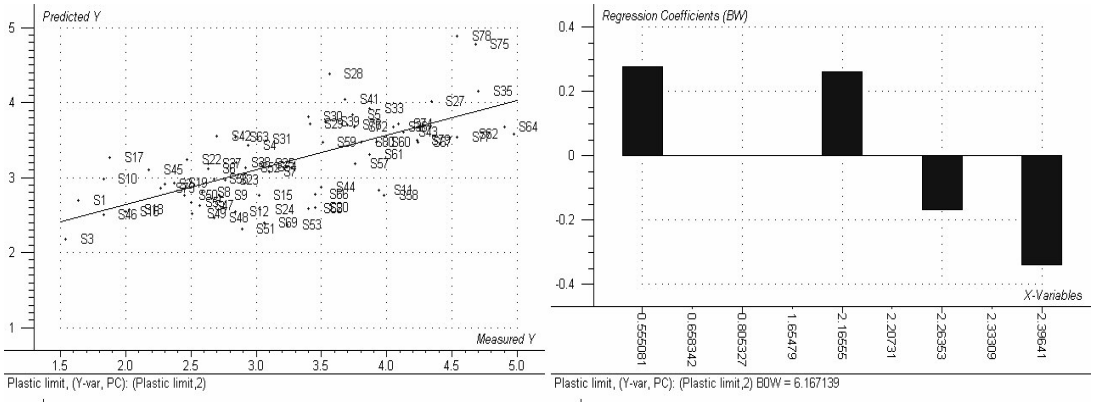

Figure 6-17: Results of data driven PLSR modeling (of the re-sampled spectra) for PL; regression overview of prediction showing the predicted versus measured PL, and significant regression coefficients.

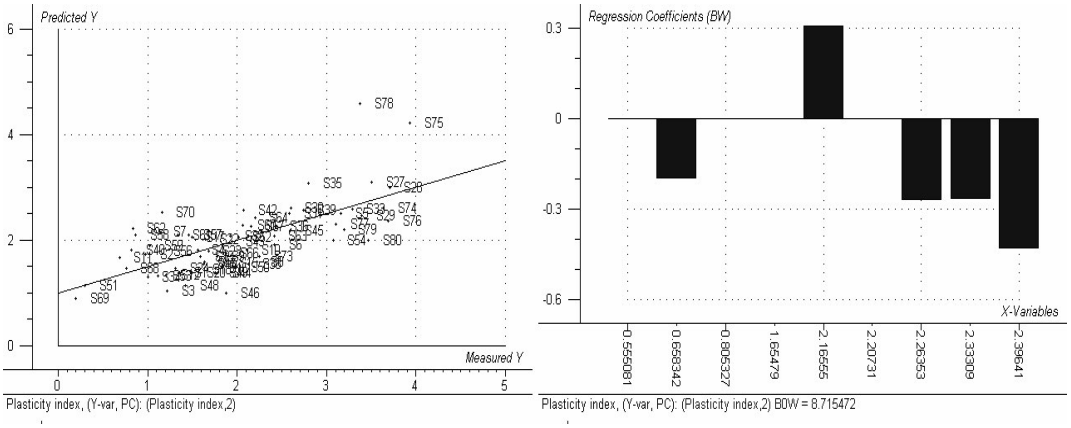

Figure 6-18: Results of data driven PLSR modeling (of the re-sampled spectra) for PI; regression overview of prediction showing the predicted versus measured PI, and significant regression coefficients.

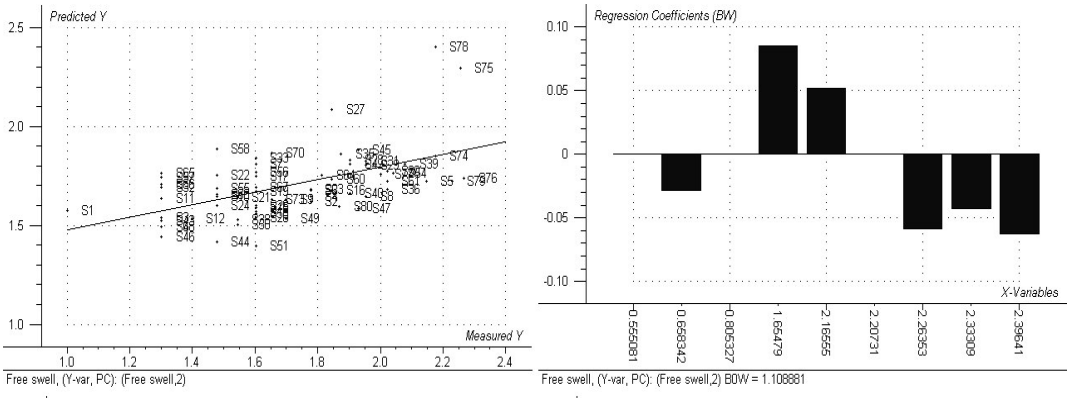

Figure 6-19: Results of data driven PLSR modeling (of the re-sampled spectra) for Fs; regression overview of prediction showing the predicted versus measured FS, and significant regression coefficients.

The overall prediction ability of the models can be considered as good. Some of the results are very much encouraging to consider extrapolation of the results to ASTER image data. More than half of the variation in the engineering parameters for example of CEC and LL are accounted for by the variation in the spectral parameters from the re-sampled spectra. While a coefficient of determination of 0.71 is obtained for the cation exchange capacity (CEC), liquid limit (LL) gave a coefficient of determination of 0.69. As far as plasticity index (PI) is concerned, about half of its variation is explained. Nearly half of the variation in Plasticity limit (PL) is explained by ASTER spectral parameters. Free swell (Fs) is found to be the least explained. A coefficient of determination of 0.52, 0.48 & 0.34 were found for plasticity index, plastic limit and free swell respectively.

In general the results gave an indication of the possibility that ASTER data can be useful in mapping engineering parameters of expansive soils. However, the question of to what extent this can be applicable will lead to some other considerations. It should be noted that spectral data acquired under laboratory conditions can be different from what can be acquired by imaging devices. For example the spatial resolution of the imaging devices has an important role on the spectral signatures of objects. It is unlikely that one can find a purely homogenous pixel (Tsai and Philpot, 1998) from ASTER spatial resolution. There are also other effects that can commonly induce different types of influences on the spectral responses of soils that can be captured on image data. For example atmospheric effects, variation in topography, differences in illumination and vegetation cover etc. Changes in surface conditions was also found to influence soil reflectance to a large extent (Farshad and Farifteh, 2002). Hence correlations that might be lower than those that are presented here might be found while working on the image data. On the other hand, ASTER data coupled with the possibility of generating DEM can help in enhancing terrain features whose occurrences are related with the presence of potentially expansive soils. Kariuki (2003) was able to map gilgai micro-relief from image data. This, together with the higher spatial resolution of ASTER can help in mapping expansive soils and specific engineering parameters. Farshad and Farifteh (2002) mentioned a number of advantages of ASTER in this respect and indicated the suitability of ASTER data for studying soil properties.

Summery of results of knowledge driven PLSR modeling (of absorption feature parameters in the SWIR)

		Calibration				Validation				
Engineering parameter	Correlation coefficients	RMSC	SEC	Bias	Offset	Correlation coefficients	RMSEP	SEP	Bias	Offset	Spectrally active absorption feature parameters
CEC	0.87	0.14	0.14	0.000	0.30	0.85	0.15	0.15	0.000	0.31	position, depth, width & area 1900 nm; depth &area 1400 nm;position & width 2200 n position, depth, width & area 1900 nm; depth, width &area 1400 nm;position, depth, width & nm
LL	0.87	0.54	0.55	0.005	1.94	0.86	0.56	0.57	0.003	2.09	
PL	0.71	0.57	0.58	0.000	1.59	0.68	0.60	0.60	0.000	1.67	position, depth & area 1900 nm; depth, width &area 1400 nm; position, depth &width 22
PI	0.84	0.46	0.46	0.000	0.60	0.83	0.47	0.48	0.000	0.65	position, depth & area 1900 nm; depth &area 1400 nm; position, depth, width & area220
FS	0.67	0.21	0.21	0.000	0.93	0.64	0.22	0.22	0.001	0.97	position & depth 1900 nm; depth 1400 nm; position & width 2200 nm

Summery of results of data driven PLSR modeling (of all the spectral bands within the ASTER band passes)

		Calibration				Validation				
Engineering parameter	Correlation coefficients	RMSEC	SEC	Bias	Offset	Correlation coefficients	RMSEP	SEP	Bias	Offset	Spectrally active spectral regions (nm)
CEC	0.92	0.12	0.12	0.000	0.19	0.90	0.12	0.12	0.000	0.21	520-560,630-777,834-860,2145-2164,2217-2247,2405-2412
LL	0.89	0.52	0.52	0.000	1.70	0.87	0.54	0.55	0.000	1.84	520-560,637-778,837-860,2149-2163,2223-2242,2247-2264,2335-2425
PL	0.74	0.54	0.55	0.000	1.44	0.71	0.57	0.57	0.000	0.71	520-545,653-674,2149-2153,2160-2162,2223-2250,-2366,2335-2425
PI	0.84	0.46	0.47	0.000	0.62	0.81	0.50	0.50	0.003	0.68	520-583,630-797,838-1655,-2150,-2165-2181,2219-2282,-2332-2394,2407-2412
FS	0.74	0.19	0.19	0.000	0.74	0.71	0.20	0.20	0.000	0.80	532-537,630-690,-854-860,2149-2155,-2160,-2218-2296

Summery of results of data driven PLSR modeling (of the re-sampled spectra)

		Calibration				Validation				
Engineering parameter	Correlation coefficients	RMSEC	SEC	Bias	Offset	Correlation coefficients	RMSEP	SEP	Bias	Offset	Spectrally active spectral bands
CEC	0.84	0.15	0.15	0.000	0.35	0.82	0.16	0.17	0.000	0.36	B1,B2,B4,B5,B7,B9
LL	0.83	0.62	0.63	0.000	2.50	0.80	0.66	0.67	0.003	2.62	B1,B5,B7,B9
PL	0.69	0.59	0.6	0.000	1.65	0.66	0.62	0.62	0.001	1.72	B1,B5,B7,B9
PI	0.72	0.62	0.62	0.000	0.96	0.68	0.65	0.65	0.004	0.99	B2,B5,B7,B8,B9
FS	0.58	0.23	0.23	0.000	1.13	0.53	0.24	0.24	0.002	1.16	B2,B4,B5,B7,B8,B9

Table 6-2 Summary of the results of the PLSR modelling for the five engineering parameters using a knowledge driven approach (using absorption feature parameters) and data driven approaches (on all spectral bands within the ASTER band passes, and the re-sampled spectra).

6.3.2. Extrapolation of model results to image data

In the previous sections we have shown that engineering parameters can be predicted using a multivariate statistical modelling technique, PLSR. We have used absorption feature parameters, full spectral band sets and finally also the ASTER band sets to derive models for predicting the engineering parameters. The results that are found using the ASTER band sets encouraged extrapolation of the model results to ASTER image data. Hence, in this section we explore whether the results can be extrapolated to the spatial and spectral resolution of ASTER. For this purpose we used an ASTER scene acquired on March, 2005 and calibrated to surface reflectance by NASA JPL. ASTER band sets and characteristics are shown in appendix D table 0.3.

First, a spatial subset was created that covers the study area. Next, a minimum distance to means classification (MDC) was applied to stratify the ASTER data into soil, vegetation, agricultural lands and urban areas. The 'soil' areas were included for further analysis while the other classes being non-soil surfaces were masked and excluded from further analysis. Then, the parameter loadings for the various ASTER VNIR and SWIR bands were used to predict the five engineering parameters of interest using the ASTER reflectance data and the following models (see also regression models in section 6.2.1 & appendix E for raw regression coefficients).

CEC=2.26+1.564*b1-2.252*b2+2.751*b4+7.773*b5-5.207*b7-3.796*b9
LL=11.14+2.923*b1+35.117*b5-16.937*b7-27.596*b9
PI=8.72-5.524*b2+21.324*b5-16.447*b7-14.265*b8-18.581*b9
PL=6.17+2.111*b1+16.237*b5-9.387*b7-14.587*b9
FS=1.11-0.775*b2+5.973*b4+3.540*b5-3.538*b7-2.264*b8-2.689*b9
Where the b1….b9 refer to ASTER bands 1…9 (the TIR bands were excluded from the analysis).

The parameter images were density sliced into approximately four classes ranging from low, medium, high and very high, for better visualization. The results are presented in figure 6:20.

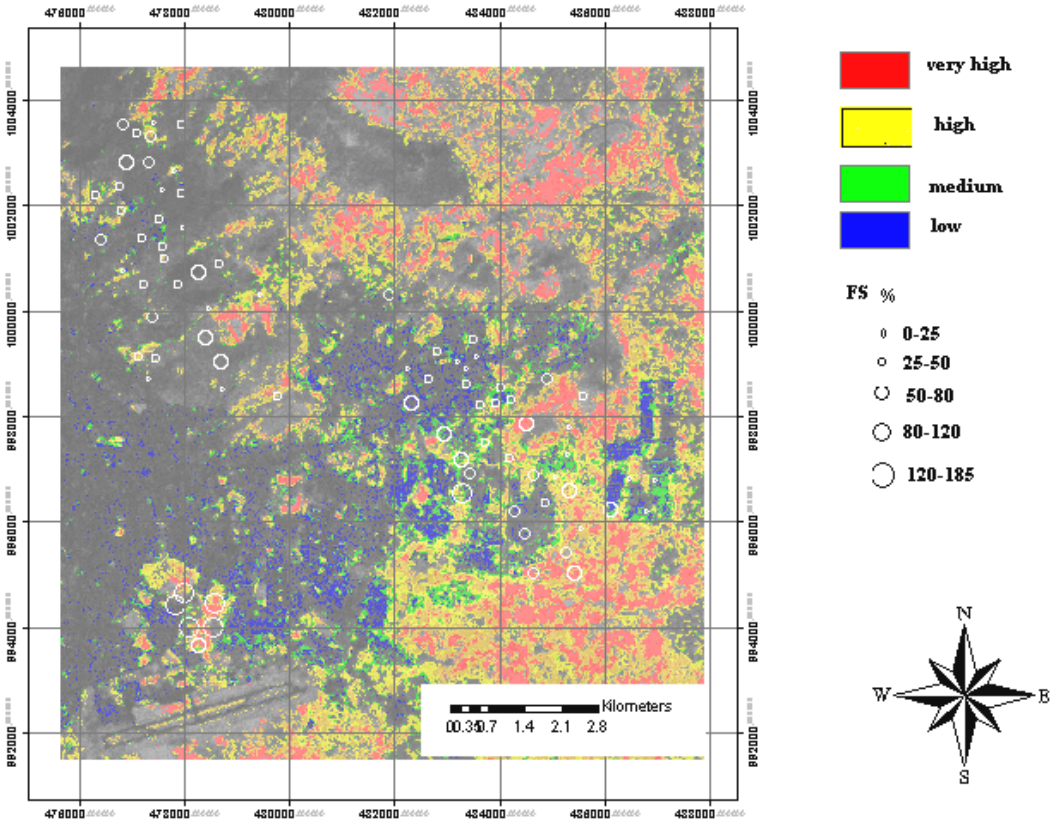
very high
high
medium
low
FS %
0-25
25-50
50-80
80-120
120-185
Kilometers
0 0.35 0.7 1.4 2.1 2.8
N
W
B
S

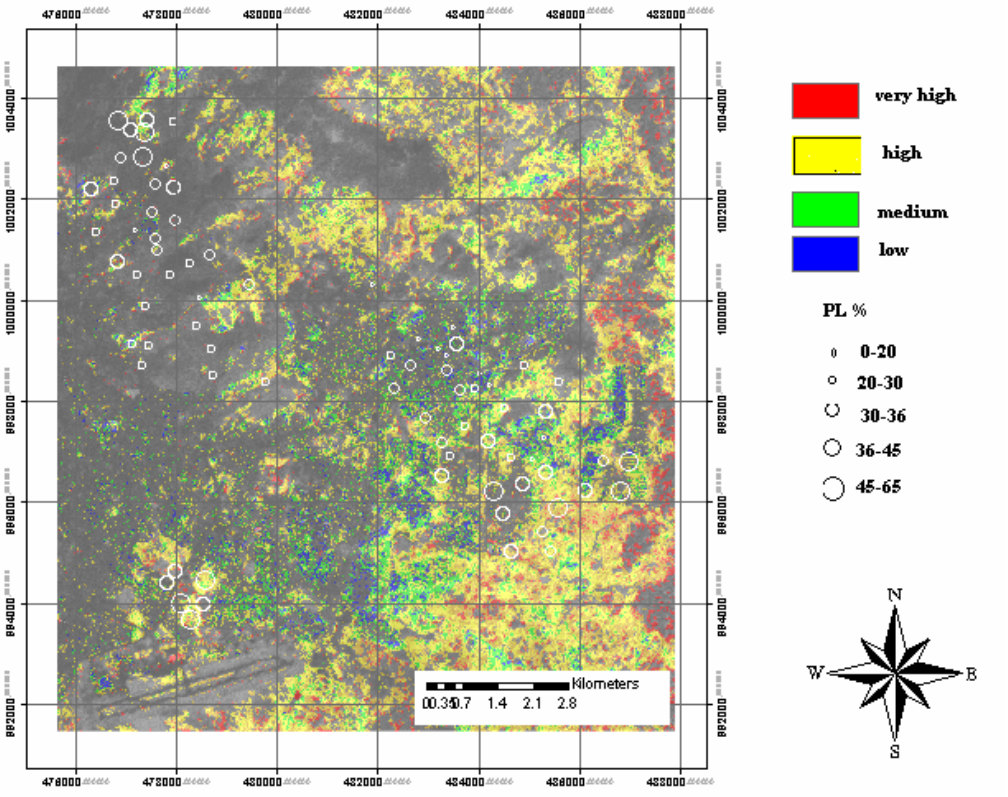
very high
high
medium
low
PL %
0-20
20-30
30-36
36-45
45-65
Kilometers
0 0.35 0.7 1.4 2.1 2.8
N
W
B
S

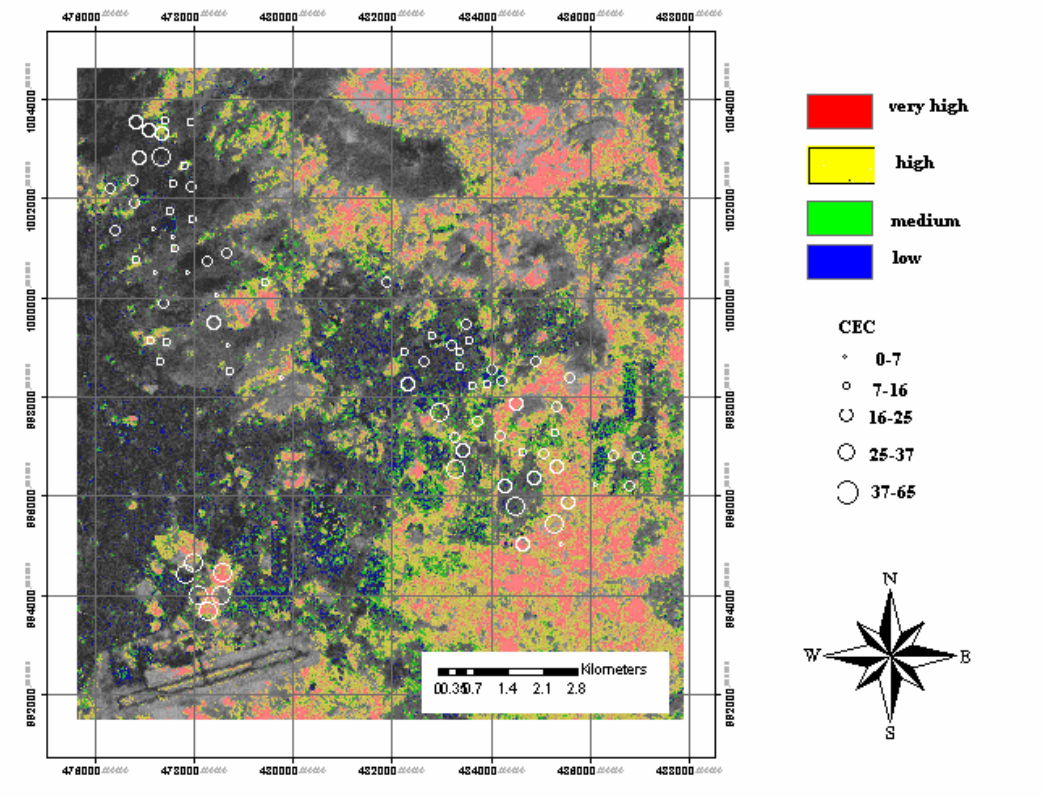
very high
high
medium
low
CEC
0-7
7-16
16-25
25-37
37-65
N
W
E
S
Kilometers
0 0.35 0.7 1.4 2.1 2.8

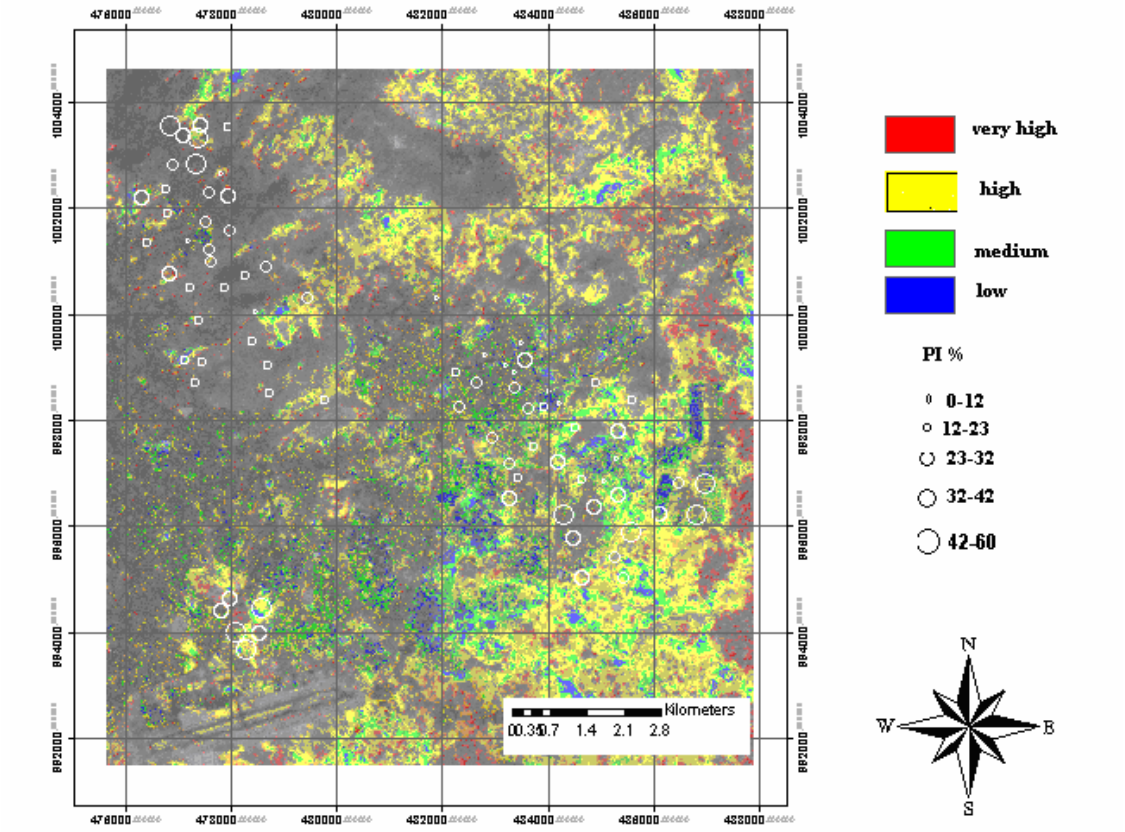
very high
high
medium
low
PI %
0-12
12-23
23-32
32-42
42-60
N
W
E
S
Kilometers
0 0.35 0.7 1.4 2.1 2.8

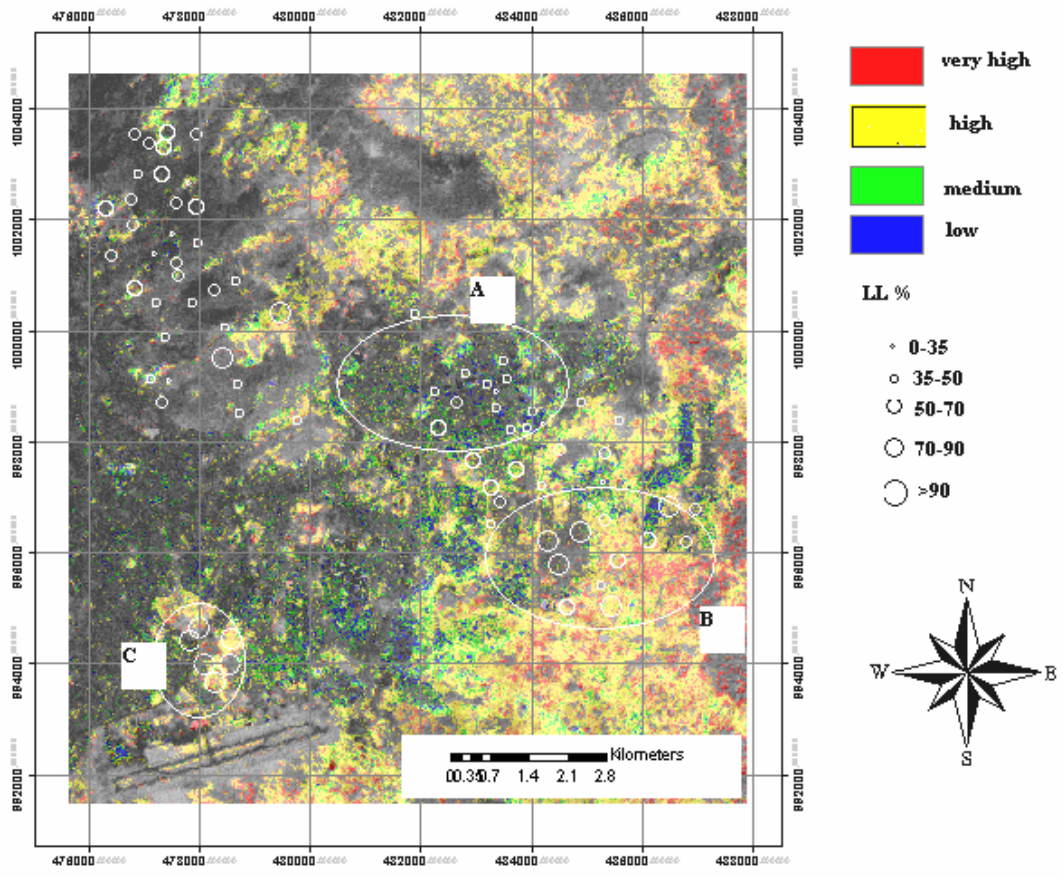

Figure 6-20: Engineering parameter maps (of FS, PL, CEC, PI and LL respectively). VNIR band 3 image used as a background and the different colours indicating the relative increase in values of the respective engineering parameters

It seems that the extrapolation give promising results. We were able to recognize certain extent of spatial pattern on the parameter maps. Predicted values of engineering parameters in areas where highly expansive soils were noted to be distributed seem to correspond with higher values in the parameter images (see the circled portions denoted by letters B and C in the LL map). Also lower and intermediate values in the parameter images seem to show some correspondence with the observed low and intermediate soil expansion potential (see the circled portion denoted by letter A in the LL map. However, in areas where vegetation cover was found to be dense, the pattern is lost. While masking out the vegetation resulted in zero values (total information loss), working without masking the vegetation resulted in a more or less uniform values in most portion of the images. The observed spatial pattern seem to be in agreement with the results of engineering geological studies conducted by the Geological Survey of Ethiopia and Addis Ababa university (AAU, 2004; GSE, 1990; Lulseged, 1990). They observed soils of highly expansive potential towards the south and southwest of the Bole international airport and low to intermediate soil expansion potential in the central parts of the study area (see also chapter 3 & 4). Looking at the spatial variations in the soils plasticity nature (figure 4.11) as well as the spatial variations in all the five engineering parameters (figures 4.3 to 4.7) also revealed some similarities with the observed spatial patterns. Information is obscured in vegetated areas. However, this approach in general needs in depth exploration and more experimental work which can lead to a further detailed study for verification.

We also performed scatter plot analysis to visualize how the parameter maps relate among one another. Then, a comparison was made with the correlations that were obtained from a correlation analysis of pairs of engineering parameters (see table 5.2 on page 45).

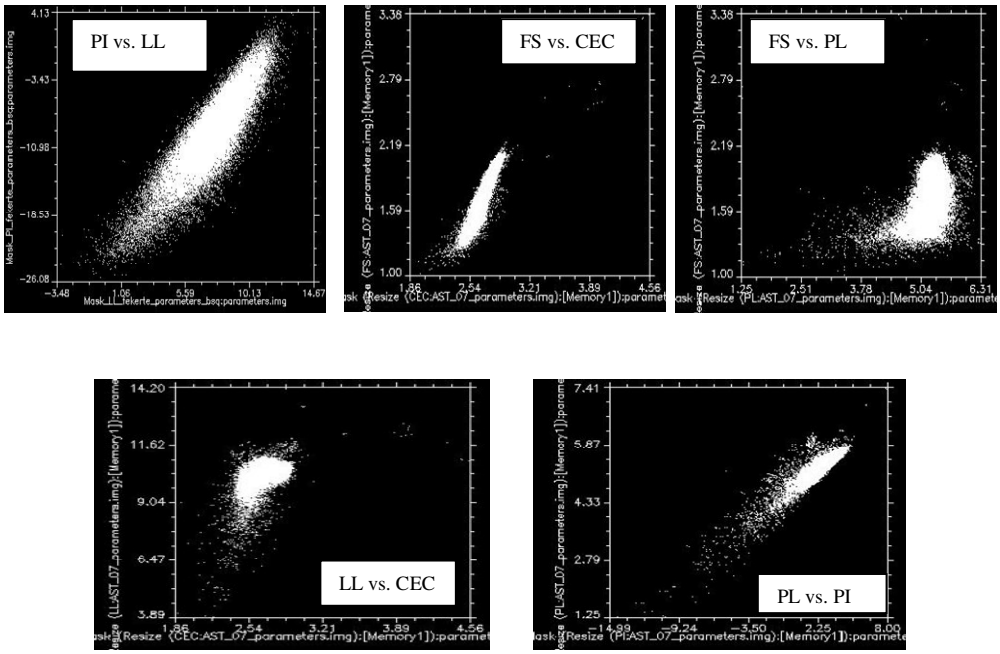

Figure 6-21: Scatter plots showing the correlations between PI versus LL; FS versus CEC; FS versus PL, LL versus CEC, and PL versus PI in the Y and X directions respectively.

The first three scatter plots showed the expected kind of correlations which resembled the correlations obtained from the bivariate correlations of the laboratory data of engineering parameters (table 5.2). The latter two, on the contrary exhibited correlations opposite from what was expected between the correlations of the respective parameters.

As far as the spectral reflectance curves from the image data are concerned, they were noted to be different from those obtained under the laboratory conditions. This was expected due to the problem of mixed pixels, atmospheric and topographic effects, moisture contents and surface textures of the soils etc.

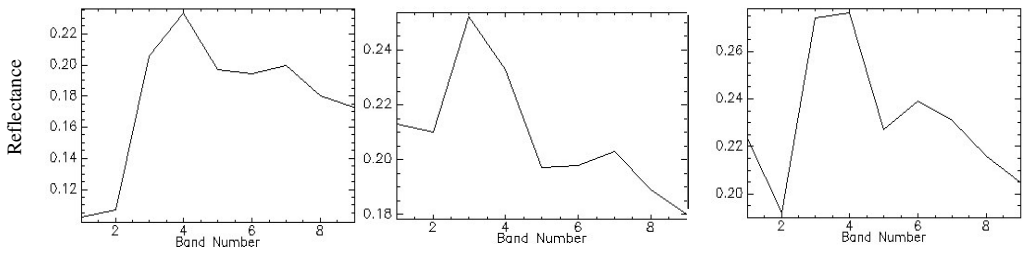

Figure 6-22: Spectra from the ASTER image data.

7. Discussion, Conclusions and recommendations

7.1. Disscussion

Characteristic differences among the spectra of the different soil samples were noted and used in differentiating the various clay mineral types that might be present within the soil samples (section 4.3.2). This was possible based on variations in shapes of the spectral curves; variations in the slopes of spectral curves; types, shape, number, positions and intensity of absorption bands; variation in reflectance intensities etc between the different soil spectra. Results from spectral interpretations indicate the potential of spectroscopy in complementing the conventional geotechnical engineering testing methods. For instance, where there is a limitation from grain sizes (sand and silt dominated soil) of soil samples which might lead to underestimation of their expansion potential. Presence of large amount of sand and silt fraction in soil samples can result in deceiving results for example about the Atterberg limits of the soil samples (figure 4.14). In this case mineralogical identification from spectral interpretation was found to give complementing information (chapter 4). However, after re-sampling the original ASD fieldspec acquired soil reflectance spectra into ASTER spectral resolution, it was not possible to discriminate various clay mineral types within the soil samples by visual spectral interpretations. This is because of the loss of subtle spectral details (see figure 6.14) due to the coarser spectral resolution of ASTER.

Results of the analysis of absorption feature parameters versus engineering parameters by grouping the soil samples into mineralogical composition classes found from the spectral interpretation showed the influence of mineralogical composition on both parameters (figure 5.6 & figure 5.8). Scatter plots (figure 5.7) revealed that the magnitude of the linear associations between absorption feature parameters and engineering parameters varies in accordance with the mineralogical compositions of the soil samples. These gave an indication that mineralogy is a key factor in controlling expansive soils engineering parameters as well as their reflectance characteristics. This is in agreement with previous observations and findings (e.g. Kariuki, 2003) in this respect. Kariuki (2003) found, among other things, the importance of mineralogy of soils in governing their expansion potential as well as their reflectance characteristics.

Apart from the qualitative information that was obtained from the spectral interpretations (chapter 4 & 5); we also established empirical relations between engineering and spectral parameters using PLSR modelling techniques (chapter 6). The model results gave a good indication of the potential of spectroscopy to provide with reliable quantitative estimates of a number of engineering parameters. Summary of the results of the PLSR modelling for the five engineering parameters using different approaches are presented in table 6.2. The prediction accuracy and performance of the models were assessed by various numerical and graphical means of evaluating PLSR models. Among the numerical means were the estimation error (RMSEC and RMSEP), interference error (bias both at the calibration and validation stages), the precision of the prediction over the whole samples (SEC

and SEP), and offset (showing the offset of the calibration and prediction regression lines from an ideal 1:1 line) etc. Of the graphical means are uncertainty limits and stability plots which show the significance and stability of different variables with respect to each other. Outlier plots which are means to help in detecting samples showing differences from the rest of the population (outlying or influential samples) and residual plots that show variable residuals and patterns both in the X and Y blocks were also used.

The results of the knowledge driven approach on overall gave high prediction ability for the engineering parameters with good prediction accuracy. High correlation coefficients were found with low estimation and interference errors, negligible bias, and small offsets from the ideal 1:1 regression lines. CEC and LL followed by PI were among the highly predicted. The models were able to explain seventy percent and above of the variations in these three engineering parameters. What was accounted for the variations in PL and FS is found to be less than 50 %. Among the absorption feature parameters calculated from the ~1400 nm, ~1900 nm and ~2200 nm absorption bands; Position and depth of the absorption feature at ~1900 nm, depth at ~1400 nm, and position and width at ~2200 nm were found to be significant for the prediction of all the five engineering parameters. In all cases these absorption feature parameters show similar trends of relations with the engineering parameters. The absorption feature position at the ~1900 nm was found to be negatively correlated with the engineering parameters. The rest of the absorption features; depth at ~1900 nm, depth at ~1400 nm, position and width at ~2200 nm showed positive relationships.

The overall trends of the relationships (for example the positive relationship with depth at the ~1900 nm, the negative relationship with position at ~1900 nm, the positive relationship with area at the ~1400 nm, and the positive relationship with position at the ~2200 nm) match Kariuki's observations; which he established a relationship between soil expansion potential and absorption feature parameters based on experimenting on clay mineral mixtures with variable smectite and kaolinite contents.

The results of the data driven PLSR, on the other hand gave higher prediction abilities for all the five engineering parameters. Again higher prediction abilities were found for CEC, LL and PI, followed by PL and FS. The additional spectral information from other wavelength regions has contributed for the higher prediction abilities of the models. For example, looking at the regression coefficients (spectral bands) on figures 6.6 - 6.10 and the summary of spectrally active wavelength regions with respect to the engineering parameters (table 6.2) reveal that the VNIR spectral region contribute significantly for the prediction of the engineering parameters. While the ~520 - 560 nm spectral bands gave positive correlations; the ~630 - 700 nm and the ~830 – 860 nm bands gave negative correlations. The wavelength regions in the VNIR spectral region are mentioned to be influenced by and associated with spectral features of organic matter and properties related to Fe-bearing minerals (Ben Dor and Banin, 1994). Hence, the significance of these wavelength regions in modelling the engineering parameters can be associated with presence of organic matter and Fe-oxide minerals that might be among the constituents of the soil samples. Figure 6.13 shows spectra of soil samples showing diagnostic absorption features related to Fe. Table 6.1 gives correlation coefficients between slope parameter calculated from the VNIR wavelength region and the five engineering parameters. Besides, the overall dark spectra and strongly convex shapes (Ben Dor and

Banin, 1994) exhibited by some soil spectra can be due to the influence of organic matter that might be present within the soil samples.

In the SWIR spectral region, the identified wavelength regions as significant predictors for the engineering parameters of interest mainly fall between ~2200 – 2300 nm. Spectral features in these wavelength regions are associated with the combination of fundamental OH stretching and bending with Al, Mg, or Fe ions; and are mentioned to be diagnostic of clay minerals (Clark, 1999). Looking back at table 2.3 indicate that the spectral regions at ~2160– 2170 nm and the~2200 nm can be attributed to AlOH features, ~2290 nm to FeOH features, ~2340 nm to FeOH/ MgOH features, and ~2384 to FeOH features respectively.

Even though slight differences are apparent among the significant predictors (spectral bands) for the various engineering parameters, the overall trends of the relations are similar. Relatively few wavelength regions were found to be significant for the prediction of some engineering parameters e.g. PL and FS, but those also fall within the same spectral regions as is apparent for the others.

When it comes to the re-sampled spectra, it was expected that the loss of subtle spectral variations might result in loss of significant information which in turn can lead to lower prediction ability. But unlike this expectation the results under the laboratory conditions indicate the possibility of ASTER data to provide with quantitative estimates of certain engineering parameters of expansive soils. Examples are CEC, LL and to some extent PI. PL and FS gave poor correlations with the spectral parameters. The wavelength regions that are identified through the PLSR analysis as significant to the explanation of the engineering parameters are again mostly similar. Similar overall trends of relationships between wavelength regions and engineering parameter of interest were exhibited. For example the three bands of ASTER in the SWIR region; bands 5, 7 and 9 are identified to be significant predictors for all the engineering parameters. These three bands are situated in wavelength regions (see also appendix D) that are also mentioned to be spectrally active with respect to clay minerals related spectral characteristics (table 2.3).

In all cases, the models gave lower errors in terms of root mean square errors, standard calibration and prediction errors, bias, and offset. The regression fit was also good since most of the samples fall within the 95 % confidence interval. The trends of the relationships between the engineering and the spectral parameters showed similarities with the trends of relations observed between the knowledge driven and data driven PLSR modelling approaches.

As far as extrapolation of the PLSR models to ASTER image data is concerned, the results gave an indication of the possibility of ASTER data to be used in mapping engineering parameters. The observed general spatial patterns and the overall trends of the variation in soil expansion potential seem in agreement with information from literature as well as field observation made.

7.2. Conclusions

In this thesis research, the main aim was in finding empirical relations between engineering parameters of potentially expansive soils and their reflectance spectra in an attempt to rationalize the geotechnical assessment of their properties. Conventional geotechnical testing methods are expensive, time consuming and it is impossible to get a continuous representation of sites under investigation. Hence, supporting these methods with a cheaper, faster and yet reliable method is of utmost concern to professionals in the field. Employing remote sensing methods, especially reflectance spectroscopy was found to have a potential in contributing to supporting conventional geotechnical testing methods (e.g. Chabrillant and Goetz, 1997-2000; Kariuki, 2003; Van der Meer, 1999a). This can contribute towards a better understanding of the properties of expansive soils as well as for more reliable results and efficiency of the geotechnical investigation of such soils.

We were able to spectrally discriminate the different soil samples using the distinct spectral characteristics and absorption features that they exhibited (chapter 4). Hence, the soil samples were grouped into three mineralogical classes namely; kaolinites, mixtures and smectites (summarized in appendix A, table 0-3). This was achieved by comparing the soil spectra with available spectral libraries from different sources. Also by using manuals prepared to help in spectral interpretation of minerals and literature on clay mineral related spectral characteristics. On the other hand, the soil samples were also classified into five classes of plasticity characters. This is by using the Casagrande plasticity chart which is a classification method based on Atterberg limit results (summarized in appendix A, table 0-3).

Different statistical tools and techniques were used to explore and visualize the structure of the data. Univariate analysis helped to observe the spread and variability of the data. Bivariate correlations gave the magnitude and trends of linear relationships between pairs of engineering versus absorption feature parameters (see table 5.2, table 5.3 and table 6.1). Use of box plots illustrated the influence of mineralogical composition on absorption feature parameters and engineering parameters. The relations between the ~1900 nm absorption band and the five engineering parameters are presented as examples (see figure 5.6 and figure 5.8). Scatter plots (figure 5.7) revealed that the magnitude of the linear associations between the absorption feature parameters and the engineering parameters varies in accordance with the mineralogical compositions of the soil samples etc.

Apart from the general qualitative classifications and analyses, geotechnical engineers are also interested in the quantitative estimates of soil expansion potential. This is because these numerical values are needed for decisions regarding the design parameters of structures. Besides, they are also directly used in construction specifications. Owing to such relevance, we developed models that enable to quantitatively characterize some specific engineering parameters of expansive soils from their reflectance spectra. Empirical relationships were established between expansive soil engineering parameters and their reflectance spectra which in turn helped to identify characteristic spectral features that can be diagnostic of engineering parameters of expansive soils. This was achieved by linking engineering parameters and absorption feature parameters (absorption feature position, depth, width and area) that were calculated from known absorption bands in the SWIR spectral region (~1400 nm, ~1900 nm and ~2200 nm absorption bands) with respect to clay mineral

related spectral characteristics, and by simple wave length approaches. The later was a data driven approach in which we used the entire spectral band sets of the ASD fieldspec acquired laboratory soil reflectance spectral data that also fall within the ASTER band sets in the VNIR and SWIR. After running the PLSR analysis, significant spectral parameters (absorption feature parameters and wavelength regions) that contribute to the prediction of the given engineering parameters were identified.

Absorption feature parameters are found to be useful in determining engineering parameters of expansive soils from their reflectance spectra. The ~1900 nm water absorption band was observed to be highly correlated with the engineering parameters of the expansive soils, followed by the ~1400 nm water and hydroxyl absorption feature. The ~2200 nm hydroxyl absorption feature gave smaller magnitude of correlation when used alone. However, it was identified as significant when used with absorption feature parameters calculated from other wave length regions. The results that we obtained from this approach are supported by the observations made by other researchers. An example is Kariuki's (2003) observations on synthetic clay mineral mixtures and soils obtained from Kenya and Spain. He established a one-to-one link between properties related with soil expansion potential and absorption feature parameters. Apart from the similarities in the trends of the relationships, the magnitudes of the one-to-one relationships that Kariuki has obtained were higher than what we were able to obtain. The results are also different in terms of models empirical equations, which gave an indication that models developed for one particular environment can not be universally applicable. This can be attributed to the effects of different environmental specific soil forming factors that are responsible in controlling the nature and properties of soils (see also section 5.1.3).

A multivariate data analysis method, PLSR is found to be a useful and suitable method for analyzing soil spectral data in modelling its possible relationship with respect to engineering parameters that are indicators of soil expansion potential. The PLSR analysis approach helped to model engineering parameters of expansive soils by grasping the common variation between engineering parameters and the spectral parameters. This ability of the PLSR analysis to model the common structure in the predictors and response variables, helped to exclude some irrelevant variations from the spectral features. Hence, it uncovered the potential of spectroscopy in providing with a possibility of explaining variations in soil expansion potential from their respective reflectance spectra. In this approach, of the entire spectral band sets of the ASD fieldspec spectrometer, those that also fall within the ASTER band sets were selected and used to model the engineering parameters of interest. This helped on the later stages, i.e. when modelling the engineering parameters from the spectral data that are re-sampled in to ASTER spectral resolution, to note how the lowering of the spectral resolution influenced the prediction.

Good prediction ability was obtained for engineering parameters; CEC, LL and PI in all the approaches. But, all showed decreased prediction ability when it comes to the re-sampled spectra. CEC, LL and PI were found to show strong relationships with the spectral parameters. On the other hand, PL and FS exhibited relatively lower magnitude of relations with the spectral parameters. In general the results of the PLSR modelling still gave good prediction ability for the re-sampled laboratory spectra. The results were also generally encouraging to consider extrapolation of the PLSR models to ASTER image data. But, spectral data acquired under laboratory conditions can be

different from those that can be acquired by imaging devices for various reasons (section 6.3.1). Extrapolating the results of PLSR models developed from the re-sampled spectra, gave a general indication of the possibility of ASTER data to be used in mapping engineering parameters of expansive soils. However, this needs a more rigorous and further detailed analysis.

In all cases, either in the one-to-one simple linear regression analysis, or the knowledge driven and data driven PLSR analysis, CEC showed very strong relationship with the spectral parameters. However, LL which is also governed by the mineralogy and amount of clay fractions within the soil samples, show a bit less strong relationship as compared to that exhibited by the CEC. This is can be attributed to the differences in the testing procedures and specifications of the two tests (chapter 4).

The results in general confirm that spectroscopy has a great potential in contributing to the geotechnical investigation of expansive soils. This is both in the identification and subsequent quantitative characterization. Apart from supplying a great deal of information within a short period of time and of being cheaper, the accuracy of spectroscopic measurements are also reliable. Besides continuous sampling of sites is possible to avoid under-sampling which can lead to large economical losses due to failure of civil engineering infrastructure. Hence, spectroscopy can play an important role especially in identifying sites that might need due attention and further detailed geotechnical assessment with respect to the presence of potentially expansive soils.

7.3. Recommendations

- X-ray diffraction (XRD) analysis should preferably be incorporated for comparison of mineralogical identification using spectral interpretations. This will help in identifying the different soil constituents that contributed to the characteristic spectral features. Also to identify the sources of irrelevant information relative to the material of interest i.e. non clay response, and the sources of diluting effects on the engineering tests. On the other hand this can contribute towards the developing of soil spectral libraries for future use and easier comparison.

- Incorporating some additional tests for example determination of silica, clay contents and organic matter contents of soil samples can add significant information to the interpretation and analysis of the soil spectral characteristics and model results. It has been found that the ratio of silica to clay fractions, and presence of organic matter in soils have influence on soils plasticity characteristics (e.g. Perloff and Baron, 1976); also on soil spectral characteristics (e.g. Van der Meer, 2004; Kariuki, 2003) .

- Adding more samples to the dataset can result in improved prediction ability and a better representation especially of the less decomposed soil samples of sandy and silty nature; also soils obtained from forested areas which might have higher organic contents.

- Since promising indications are seen upon extrapolating the PLSR models to ASTER image data in an attempt to map engineering parameters, a more rigorous and detailed work should be considered for future prospect to explore the potential of ASTER in this respect.

- In this thesis research, we focused on the problems and engineering difficulties associated with expansive soils. However, expansive soils are not necessarily evil. They also have some useful engineering applications as landfill liner, drilling mud and construction materials (mainly for making bricks). The use and suitability of these soils is dependent on their mineralogy and their relative abundance for extraction and supply. This in general focuses on identifying the mineralogical composition and constituents of the soils, also on quantifying their hydraulic conductivity. The hydraulic conductivity of such soils is influenced among other things by the mineralogical content and grain size distribution of the soils. Since the amount of light scattered and absorbed by minerals is dependent on the grain size (Clark, 1999), there will be a possibility of quantifying grain size distribution of these soil samples from their reflectance spectra. On the other hand it would be of great interest to see if whether it is possible to link soils hydraulic conductivity with their respective reflectance spectra for this will have a contribution towards the economical, successful, more timely and efficient way of investigating the engineering properties of such soils. It would be of interest especially in areas of rapidly growing urban areas where there is a need to locate such types of soils of potential engineering use especially as land fill liner.

References

AASHTO, 2002, Standard Specifications for Transportation Materials and Methods of Sampling and Testing; The materials book, AASHTO.

AAU, 2004, Soils of the Bole area, Engineering characteristics of soils of Addis Ababa: Addis Ababa.

Analytical Spectral Devices, I.A., 1999, Technical Guide, in H. C. David, eds., Analytical Spectral Devices, Inc. (ASD)

ASTM, 1989, Annual book of ASTM standards: section 4 construction: soil and rock, building stones; geotextiles: Philadelphia, American Society for Testing and Materials (ASTM), 996 p.

AusSpec International, 2005, The Spectral Geologist Users guide manual: Sydney, AusSpec International.

Bell, F.G., 1983, Engineering Properties of Soils and Rocks: London, ButterWorths.

Ben Dor, E., and Banin, A., 1994, Visible and Near-Infrared (0.4-1.1µm) analysis of Arid and Semiarid Soils: Remote Sensing of Environment, v. 48, p. 261-274.

Berhanu, D., 1983, The Vertisols of Ethiopia: Their Properties, Classification and Management, World Soil Resources Reports: Rome, FAO, p. 31-54.

Bowles, J.E., 1984, Physical and Geotechnical properties of soils, Mc Graw Hill Inc.

British Standard Institution, B., 1981, Code of practice for Site investigations BS 5930: 1981: London, British Standard Institution.

CAMO, 1986-2005, The Unscarmbler 9.2.

Chabrillant, s., and Goetz, A.F.H., 1997-2000, Identification and Mapping of Expansive Clay Soils in the Western US: Using Field Spectrometry and AVIRIS Data. http://cires.colorado.edu/cses/research/soils/expansive/

Chen, F.H., 1988, Foundation on Expansive Soils, Elsevier Science Publishers.

Christopher, C.D., and Mustard, J.F., 1999, Effects of very fine particle size on reflectance spectra of Smectite and Palagonitic soil: Icarus, v. 142, p. 557-570.

Clark, R.N., 1999, Spectroscopy of Rocks and Minerals, and Principles of Spectroscopy, *in* Rencz, A., ed., Chapter 1 in: Manual of Remote Sensing: New York, John Wiley and Sons, Inc.

Crowley, J.K., Williams, D.E., Hammarstrom, J.M., Piatak, N., Chou, I.-M., and Mars, J.C., 2003, Spectral reflectance properties (0.4-2.5 µm) of secondary Fe-oxides, Fe-hydroxides, and Fe-sulphate-hydrate minerals associated with sulphide-bearing mine wastes: Geochemistry; Exploration, Environment, Analysis, v. 3, p. 219-228.

CSA, 2004, the 1994 population and housing census of Ethiopia: Addis Ababa, Ethiopia, Addis Ababa City Council.

Davies, A.M.C., 2001, Uncertainty testing in PLS regression, Spectroscopy Europe, Norwich Near Infrared Consultancy.

Day, R.W., 2001, Soil Testing Manual: Procedures, Classification Data, and Sampling Practices, Mcgraw-Hill.

Tamiru, A., 2001, Geological map of Addis Ababa: Addis Ababa, Addis Ababa university department of Geology and Geophysics.

EMA, 1988, National Atlas of Ethiopia: Addis Ababa, Ethiopian Mapping Agency.

EMSB, 2000, Annual report, Environmental Management and Safety Branch: Addis Ababa, Ethiopian Roads Authority.

ENVI 4.2, 2005, Spectral library.

ERSDAC, 2001, ASTER User's Guide; Part I General Ver 3.1, Earth Remote Sensing Data Analysis Centre.

Ethiopian Roads Authority, E., 2001, Maintenance Action Plan 2001-2005: Addis Ababa.

Farshad, A., and Farifteh, J., 2002, Remote Sensing and modelling of topsoil properties, a clue for assessing land degradation: Thailand.

Fitzpatrick, E.A., 1980, SOILS; their formation, classification and distribution, Longman Inc.

Geladi, P., and Kowalski, R.B., 1986, Partial Least Squares Regression: A tutorial: Analytica Chimica ACTA, v. 185, p. 1-17.

Gillott, J.E., 1968, Clay in Engineering Geology: Amsterdam, Elsevier publishing company.

Goetz, A.F.H., Chabrillant, s., and Lu, Z., 2001, Field Reflectance Spectrometry for Detection of Swelling Clays at Construction Sites: Field Analytical Chemistry and Technology, v. 5(3), p. 143-155.

Gourley, C., Newill, D., and Schreiner, H.D., 1993, Expansive soils: TRL's research strategy, First International Symposium on Engineering Characteristics of Arid Soils: City University, London, Overseas Centre, Transport Research Laboratory, Crowthorne, Berkshire, UK.

Gray, J., and Murphy, B., 2002, PARENT MATERIAL AND SOIL DISTRIBUTION: Australian Association of Natural Resource Management, v. 5, p. 3-12.

GSE, 1990, Engineering Geological Mapping of Addis Ababa: Addis Ababa, Geological Survey of Ethiopia and the Ethiopian Ministry of Mines and Energy.

Hawkins, A.B., 1986, Site investigation practice: assessing BS 5930, Geological Society Special Publication, v 2: London, The Geological Society of London, p. 423.

Head, K.H., 1980, Soil classification and compaction tests: London, Pentech press limited.

Herve, A., 2003, Partial Least Squares (PLS) Regression, University of Texas at Dallas.

Hocking, R.R., 2003, Methods and Applications of Linear Models Regression and the analysis of variance, Wiley series in probability and statistics.

Jeffrey, R.J., Paul, G.L., Keith, A.H., and Edwin, M.W., 1998, Infrared Measurements of Pristine and Disturbed soils 1. Spectral contrast differences between field and laboratory data: Remote Sensing of Environment, v. 64, p. 34-46.

Johnson, A.I., and Pettersson, C.B., 1988, Geotechnical applications of remote sensing and remote data transmission: Cocoa Beach, FL, 31 Jan.-1 Feb. 1986: Philadelphia, American Society for Testing and Materials (ASTM), 277 p. p.

Kariuki, P.C., 2003, Spectroscopy and Swelling Soils An Integrated Approach, PhD thesis: Enschede, The Netherlands, ITC.

Kezdi, A., 1980, Hand book of soil mechanics, soil testing: Amsterdam, Elsevier scientific publishing company.

Kooistra, L., 2004, Incorporating spatial variability in ecological risk assessment of contaminated river floodplains, PhD thesis: Nijmegen, The Netherlands, Katholieke Universiteit Nijmegen.

Lambe, T.W., and Whitman, R.V., 1979, Soil Mechanics, SI Version: New York, Jhon Wiley & Sons.

Lulseged, A., 1990, Engineering geological characteristics of the clay soils of bole area; their distribution and practical importance: Addis Ababa, Addis Ababa University.

Martens, H., and Naes, T., 1989, Multivariate Calibration, John Wiley & Sons, INC.

McSweeney, K., 1999, Soil Morphology, Classification and Mapping, University of Wisconsin - Madison, Department of Soil Science.

Mekonnen, T., 2004, In depth assessment of pavement failure founded on expansive sub-grade in Ethiopia, MSC thesis: Addis Ababa, Addis Ababa University.

Mitchell, J.K., 1993, Fundamentals of Soil behaviour, John Wiley & Sons, Inc.

Nelson, J.D., and Miller, D.J., 1992, Expansive Soils Problems and Practice in Foundation and Pavement Engineering, John Wiley & Sons, Inc.

Netterberg, F.D., 2001, Addis Ababa-Jimma road project Preliminary report on cracking problem: Addis Ababa, Ethiopian Roads Authority.

NSW, 2004, Cation exchange capacity, Soil types, structure and condition, State of New South Wales, department of Primary Industries.

Perloff, W.H., and Baron, W., 1976, Soil mechanics Principles and Applications, John Wiley & Sons, Inc.

Pontual, S., Merry, N., and Gamson, P., 1997, G-Mex Spectral Interpretation Field Manual: Sydney, AusSpec International.

Rogers, J.D., Olshansky, R., and Rogers, R.B., 2000, Damage to Foundations from Expansive Soils, p. 6.

Scholte, H.K., 2005, Hyperspectral Remote Sensing and Mud Volcanism in Azerbaijan, Phd thesis: Delft, The Netherlands, Delft University of Technology.

Seed, B.H., Woodward, R.J., and Lundgren, R., 1962, Prediction of swelling potential for compacted clays: Journal of the soil mechanics and foundations division, American society of civil engineers, v. 88, p. 53-87.

SINET, 1987, Ploughing for Progress: Ethiopia: SINET Science and Technology, v. 1, p. 209-217.

Spectral International INC SII, 2005, PIMA application, http://www.pimausa.com/pima2.html Clay minerals.

Thomas, P.J., 1998, Quantifying Properties and Variability of Expansive Soils in Selected map Units PhD thesis: Blacksburg.

Tsai, F., and Philpot, W., 1998, Derivative Analysis of Hyperspectral Data: Remote Sensing of Environment, v. 66, p. 41-51.

TSG Professional, 2005, The Spectral Geologist: Sydney, AusSpec International.

USGS, 2003, USGS digital spectral library, USGS.http://www.usgs.org

Van der Meer, F.D., 1995, Spectral Reflectance of Carbonate Mineral Mixtures and Bidirectional Theory: Quantitative Analysis techniques for Application in Remote Sensing: Remote Sensing Reviews, v. 13, p. 69-94.

Van der Meer, F.D, 1999a; Can we map swelling clay with remote sensing? International Journal of Applied Earth Observation & Geoinformation (JAG), v. 1, p. 27-35.

Van der Meer, F.D, 1999b, Physical principles of optical remote sensing, *in* Stein, A., Van der Meer, F.D., and Gorte, B., eds., Spatial Statistics for Remote Sensing, Volume 1, Kluwer Academic publishers.

Van der Meer, F.D, 2004a, Analysis of spectral absorption features in hyperspectral imagery: International Journal of Applied Earth Observation & Geoinformation, v. 5, p. 55-68.

Van der Meer, F.D, 2004b, Remote sensing image analysis: including the spatial domain, *in* Van der Meer, F.D., and De Jong, S.M., eds., Remote sensing and digital image processing: Dordrecht etc., Kluwer Academic publishers, p. 539 p.

Verhoef, P.N.W., 1992, The Methylene Blue Adsorption Test Applied to Geo-materials: Delft, Delft University of Technology.

Wilson, M.J., 1987, Handbook of Determinative Methods in Clay Mineralogy: Glasgow etc.; New York, Blackie; Chapman and Hall, 308 p. p.

Wold, S., Eriksson, L., Johan, T., and Nouna, K., 2004, The PLS method- Partial Least Squares projection to latent structures and its application in industrial RDP (research, development, and production): Prague.

Wold, S., Sjostrom, M., and Eriksson, L., 2001, PLS-regression: a basic tool of Chemometrics: Chemometrics and Intelligent Laboratory Systems, v. 58, p. 109-130.

Appendices

Appendix A: Summary of the laboratory results of the five engineering parameters.

X-COORD (UTM)	Y-COORD (UTM)	Sample number	LL %	PL %	PI %	FS %	CEC meq/100 g
485,076,352	996,840,726	S1	36.8	16.4	20.4	10.0	12.6
484,645,014	996,893,186	S2	37.7	23.0	14.7	60.0	7.9
485,305,621	997,275,949	S3	33.7	15.4	18.3	20.0	8.4
484,924,801	998,700,334	S4	52.8	29.4	23.4	60.0	12.8
483,286,558	996,537,029	S5	84.8	37.4	47.4	140.0	43.8
483,463,550	996,925,549	S6	62.6	26.3	36.3	60.0	21.8
483,395,330	998,602,082	S7	48.0	31.0	17.0	40.0	9.0
484,532,338	997,869,849	S8	59.2	25.9	33.3	90.0	23.3
483,949,909	998,262,278	S9	53.9	27.2	26.7	50.0	10.9
484,038,720	998,554,497	S10	50.0	18.3	31.7	30.0	13.8
483,586,067	999,138,934	S11	49.7	39.4	10.3	20.0	10.4
482,283,102	998,909,594	S12	46.6	28.4	18.2	25.0	4.9
483,382,920	998,916,719	S13	NP	NP	NP	4.0	9.0
483,226,859	999,048,937	S14	41.7	15.7	26.0	10.0	16.3
482,671,178	998,722,851	S15	58.1	30.2	27.9	40.0	12.8
481,903,866	1,000,321,350	S16	46.3	20.0	26.3	70.0	11.9
483,516,046	999,450,050	S17	41.2	18.8	22.4	40.0	11.9
482,838,119	999,224,704	S18	43.8	20.3	23.5	40.0	9.8
477,913,569	1,000,511,980	S19	47.6	23.7	23.9	40.0	-
477,630,404	1,001,229,937	S20	57.0	34.5	22.5	40.0	-
477,215,921	1,001,384,084	S21	32.0	14.0	18.0	35.0	-
477,253,601	1,000,507,161	S22	49.4	24.7	24.7	30.0	-
477,428,301	999,893,315	S23	52.8	27.6	25.2	60.0	13.6
478,693,673	1,000,913,423	S24	50.0	30.3	19.7	30.0	13.0
479,467,832	1,000,324,240	S25	34.5	30.3	4.2	10.0	5.0
484,233,107	998,328,516	S26	47.6	16.2	31.4	40.0	16.5
484,492,327	995,783,423	S27	96.0	43.4	52.6	70.0	39.6
485,264,487	995,426,269	S28	91.2	35.6	55.6	80.0	45.4
485,442,020	995,042,713	S29	85.0	34.1	50.9	90.0	-
482,947,298	997,677,303	S30	73.0	34.0	39.0	105.0	39.8
482,358,115	998,273,336	S31	68.9	30.1	38.8	90.0	26.9
485,581,597	995,878,319	S32	82.6	53.7	28.9	20.0	26.7
484,878,721	996,355,889	S33	88.0	38.7	49.3	40.0	31.2

X-COORD (UTM)	Y-COORD (UTM)	Sample number	LL %	PL %	PI %	FS %	CEC meq/100 g
486,810,693	996,199,687	S34	64.2	49.2	15.0	10.0	16.3
484,297,795	996,208,337	S35	89.0	47.0	42.0	75.0	25.6
486,126,234	996,248,819	S36	77.0	40.5	36.5	105.0	-
478,418,422	999,494,926	S37	84.8	26.3	58.5	100.0	34.7
476,839,622	1,001,916,596	S38	60.4	28.5	31.9	35.0	12.2
476,920,586	1,002,834,189	S39	76.4	35.3	41.1	120.0	24.4
476,859,863	1,003,529,131	S40	64.5	52.2	12.3	80.0	23.0
476,333,596	1,002,199,970	S41	70.0	36.8	33.2	40.0	13.4
476,428,054	1,001,349,847	S42	58.1	27.0	31.1	80.0	19.6
476,867,667	1,000,776,124	S43	70.4	41.3	29.1	20.0	10.9
477,643,574	1,000,998,775	S44	61.8	35.0	26.8	30.0	6.5
478,291,286	1,000,735,642	S45	60.7	21.8	38.9	85.0	14.8
478,493,697	1,000,060,941	S46	46.5	18.3	28.2	20.0	-
478,736,589	999,032,275	S47	50.1	25.7	24.4	85.0	-
478,743,336	998,526,249	S48	48.2	26.8	21.4	20.0	6.1
477,163,012	999,130,277	S49	51.4	25.1	26.3	50.0	6.4
479,789,123	998,384,562	S50	54.4	24.5	29.9	35.0	-
477,493,929	999,119,320	S51	33.4	28.9	4.5	40.0	4.3
477,344,907	998,727,041	S52	59.4	29.2	30.2	20.0	10.3
483,649,175	998,227,353	S53	49.2	32.4	16.8	40.0	8.5
483,275,246	997,173,745	S54	76.6	30.5	46.1	110.0	19.6
483,755,374	997,504,518	S55	49.5	25.0	24.5	30.0	15.7
485,598,434	998,374,661	S56	43.8	26.8	17.0	40.0	11.9
485,327,836	997,795,307	S57	59.5	37.6	21.9	20.0	14.7
484,211,138	997,205,940	S58	52.8	39.8	13.0	30.0	16.2
486,468,693	996,840,115	S59	50.5	35.1	15.4	10.0	11.5
484,665,657	995,030,769	S60	70.2	39.2	31.0	70.0	28.7
485,334,523	996,583,494	S61	58.8	38.7	20.1	105.0	29.8
486,970,857	996,780,571	S62	62.2	49.7	12.5	10.0	13.6
476,793,117	1,002,361,583	S63	64.6	28.4	36.2	30.0	13.1
477,344,285	1,002,832,667	S64	82.0	49.0	33.0	65.0	42.3
477,845,989	1,002,651,299	S65	26.0	14.5	11.5	20.0	9.8
477,619,869	1,002,286,209	S66	62.6	34.5	28.1	20.0	9.7
477,966,115	1,002,234,390	S67	74.8	42.4	32.4	40.0	13.1
478,020,290	1,001,590,432	S68	45.4	34.0	11.4	20.0	7.4
477,553,917	1,001,731,758	S69	33.6	30.6	3.0	30.0	8.0
477,134,652	1,003,372,986	S70	61.7	44.3	17.4	45.0	22.6
477,384,327	1,003,318,811	S71	79.6	60.5	19.1	60.0	36.0

X-COORD (UTM)	Y-COORD (UTM)	Sample number	LL %	PL %	PI %	FS %	CEC meq/100g
477,457,879	1,003,584,809	S72	74.8	37.5	37.3	20.0	9.9
477,958,271	1,003,533,843	S73	56.5	22.7	33.8	45.0	6.5
478,012,291	994,630,270	B1(S74)	95.4	40.9	54.5	150.0	58.2
478,604,716	994,429,221	B2(S75)	105.8	46.8	59.0	180.0	64.1
478,556,464	993,981,551	B3(S76)	92.4	37.0	55.4	185.0	50.8
478,309,844	993,651,830	B4(S77)	92.0	45.4	46.6	100.0	46.3
478,100,753	994,002,996	B5(S78)	96.0	45.4	50.6	150.0	57.4
477,856,813	994,418,498	B6(S79)	90.2	42.3	47.9	170.0	43.0
485,264,487	995,426,269	28B(S80)	90.0	38.0	52.0	74.0	42.0

Table 0-1: Summary of the laboratory results (of the engineering parameters) for the 80 soil samples (0-30 cm depth) for which the reflectance spectra is also available.

X-COORD (UTM)	Y-COORD (UTM)	Sample number	LL %	PL %	PI %
484,924,801	998,700,334	S4b	65.0	29.2	35.8
483,395,330	998,602,082	S7b	45.0	31.0	14.4
484,532,338	997,869,849	S8b	48.7	14.3	34.4
483,949,909	998,262,278	S9b	49.0	24.6	24.4
477,913,569	1,000,511,980	S19b	46.0	24.0	22.0
477,913,569	1,000,511,980	S19b	47.4	25.4	22.0
477,253,601	1,000,507,161	S22b	59.8	26.8	33.0
484,878,721	996,355,889	S33b	89.0	39.3	49.7
476,920,586	1,002,834,189	S39b	79.1	41.0	38.1
476,428,054	1,001,349,847	S42b	57.2	22.1	35.1
478,743,336	998,526,249	S48b	41.6	23.5	18.1
483,275,246	997,173,745	S54b	74.5	31.0	43.5
485,334,523	996,583,494	S61b	56.8	29.7	27.1
477,553,917	1,001,731,758	S69b	33.0	28.2	4.8
477,384,327	1,003,318,811	S71b	81.0	59.3	21.7
477,457,879	1,003,584,809	S72b	73.0	35.5	37.5
478,604,716	994,429,221	B2(S75)b	106.0	47.4	58.6
477,856,813	994,418,498	B6(S79)b	91.2	44.6	46.6

Table 0-2: Summary of the laboratory results (of the engineering parameters) of some samples from the 30 – 60 cm depth.

ID	Plasticity	Mineralogy	ID	Plasticity	Mineralogy
S1	Intermediate	Kaolinite	S41	Very high	Mixtures
S2	Intermediate	Kaolinite	S42	High	Mixtures
S3	Low	Kaolinite	S43	Very high	Mixtures
S4	High	Smectite	S44	High	Mixtures
S5	Very high	Smectite	S45	High	Mixtures
S6	High	Smectite	S46	Intermediate	Mixtures
S7	Intermediate	Halloysite	S47	Intermediate	Mixtures
S8	High	Mixtures	S48	Intermediate	Halloysite
S9	High	Halloysite	S49	High	Halloysite
S10	High	Mixtures	S50	High	Halloysite
S11	Intermediate	Halloysite	S51	Low	Mixtures
S12	Intermediate	Halloysite	S52	High	Mixtures
S13	Low	Mixtures	S53	Intermediate	Halloysite
S14	Intermediate	Smectite	S54	Very high	Mixtures
S15	High	Halloysite	S55	Intermediate	Mixtures
S16	Intermediate	Halloysite	S56	Intermediate	Halloysite
S17	Intermediate	Smectite	S57	High	Mixtures
S18	Intermediate	Smectite	S58	High	Mixtures
S19	Intermediate	Halloysite	S59	High	Mixtures
S20	High	Halloysite	S60	Very high	Mixtures
S21	Low	Mixtures	S61	High	Smectite
S22	Intermediate	Halloysite	S62	High	Smectite
S23	High	Smectite	S63	High	Halloysite
S24	High	Smectite	S64	Very high	Smectite
S25	Low	Mixtures	S65	Low	Mixtures
S26	Intermediate	Halloysite	S66	High	Halloysite
S27	Extremely high	Mixtures	S67	Very high	Mixtures
S28	Extremely high	Mixtures	S68	Intermediate	Mixtures
S29	Very high	Mixtures	S69	Low	Mixtures
S30	Very high	Mixtures	S70	High	Mixtures
S31	Very high	Mixtures	S71	Very high	Smectite
S32	Very high	Halloysite	S72	Very high	Mixtures
S33	Very high	Smectite	S73	High	Mixtures
S34	Very high	Halloysite	S74	Extremely high	Smectite
S35	Very high	Mixtures	S75	Extremely high	Smectite
S36	Very high	Smectite	S76	Extremely high	Smectite
S37	Very high	Halloysite	S77	Extremely high	Smectite
S38	Very high	Mixtures	S78	Extremely high	Smectite
S39	Very high	Mixtures	S79	Extremely high	Smectite
S40	High	Mixtures	S80	Extremely high	Smectite

Table 0-3: Summary of soil classification using the Casagrande plasticity chart & mineralogical classes from spectral interpretations.

Appendix B: Some examples of Atterberg limits test results

Sample Number 1 (S1)					
	Atterberg limits				
	LL			**PL**	
Container number	P1	P2	P3	P4	P5
Number of blows	31.0	26.0	17.0		
Weight of container + wet soil gm	33.3	36.5	34.3	16.3	15.6
Weight of container. gm	9.4	9.5	9.3	9.2	9.2
Weight of container + dry soil gm	27.0	29.26	27.4	15.3	14.7
Weight of water gm	6.3	7.24	6.9	1.0	0.9
Weight of dry soil gm	17.6	19.76	18.1	6.1	5.5
Moisture content %	35.8	36.6	38.1	16.4	16.4
PI=LL-PL	36.8	16.4	**20.4**		

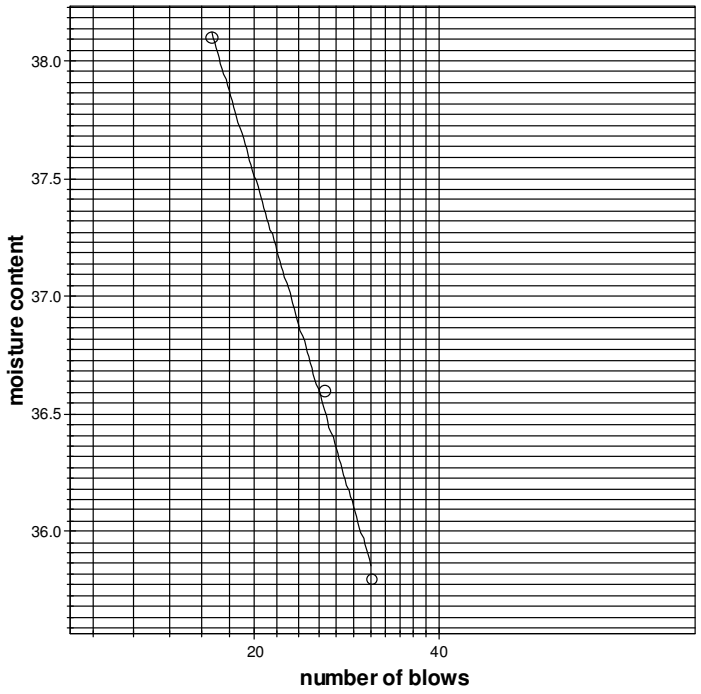

Sample number 3 (S3)					
	Atterberg limits				
	LL			**PL**	
Container number	Q25	Q26	Q27	Q28	Q29
Number of blows	29.0	22.0	16.0		
Weight of container + wet soil gm	33.1	31.16	35.9	13.0	12.5
Weight of container. gm	9.5	9.5	9.7	9.1	9.6
Weight of container + dry soil gm	27.3	25.6	28.9	12.5	12.1
Weight of water gm	5.8	5.6	7.0	0.5	0.4
Weight of dry soil gm	17.8	16.1	19.2	3.4	2.5
Moisture content %	32.6	34.5	36.5	14.7	16.0
PI=LL-PL	33.7	15.4	**18.3**		

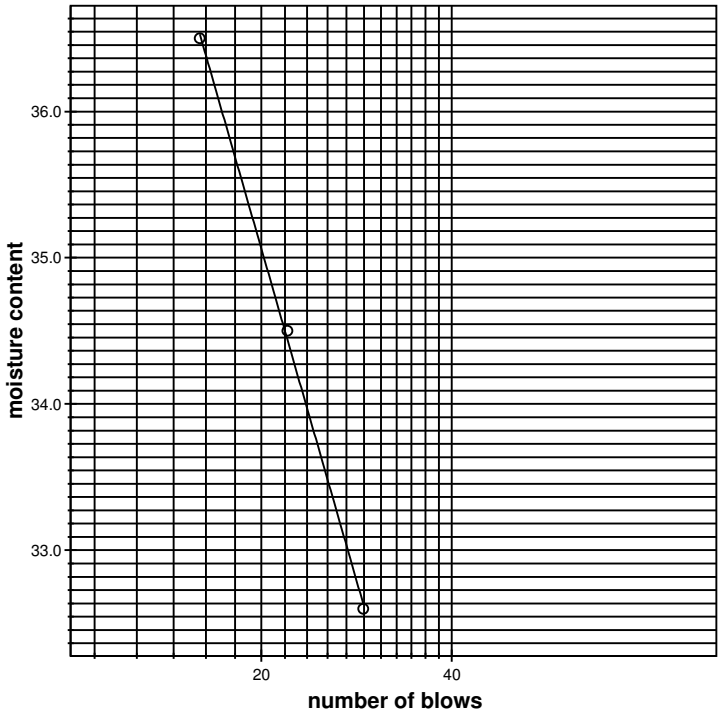

Sample number 10 (S10)					
	Atterberg limits				
	LL			**PL**	
Container number	F1	F2	F3	F4	F5
Number of blows	28.0	23.0	16.0		
Weight of container + wet soil gm	40.6	39.6	38.8	14.9	15.2
Weight of container. gm	9.4	9.7	9.4	9.6	9.5
Weight of container + dry soil gm	30.5	29.6	28.6	14.1	14.3
Weight of water gm	10.1	9.9	10.2	0.8	0.9
Weight of dry soil gm	21.1	19.9	19.2	4.5	4.8
Moisture content %	48.0	49.9	53.1	17.8	18.8
PI=LL-PL	50.0	18.3	**31.7**		

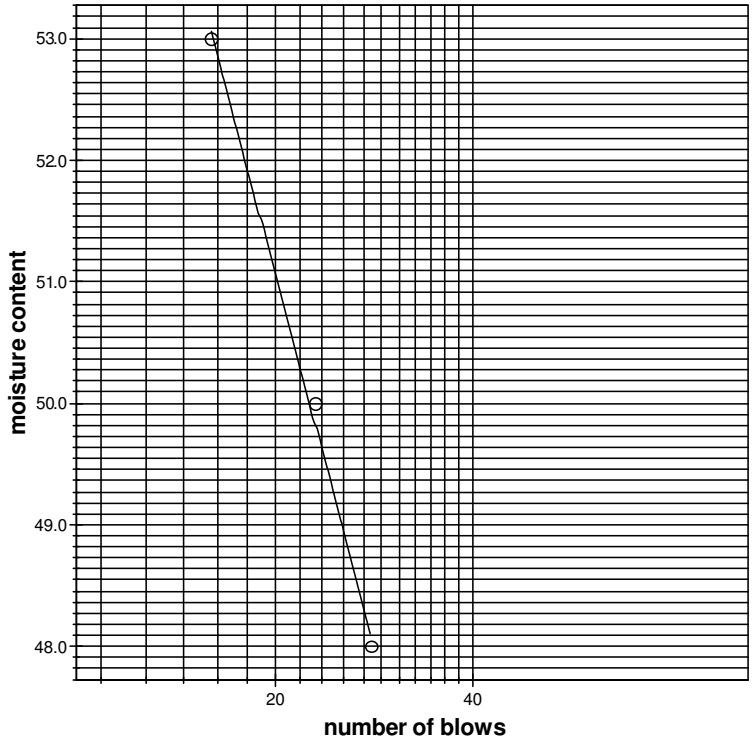

Sample number B2 (S75)					
	Atterberg limits				
	LL			**PL**	
Container number	A1	A2	A3	A4	A5
Number of blows	35	24	16		
Weight of container + wet soil gm	32.6	34.1	35.8	26.6	26.1
Weight of container. gm	22.2	22.3	22.3	22.1	22.1
Weight of container + dry soil gm	27.5	28.3	29.1	25.2	24.8
Weight of water gm	5.0	5.76	6.7	1.41	1.3
Weight of dry soil gm	5.4	5.97	6.78	3.05	2.7
Moisture content %	93.7	96.5	98.8	46.2	47.4
10% increase. for correcting oven drying	103.0	106.1	108.7		
PI=LL-PL	96.5	46.8	49.8		
PI=LL-PL	105.8	46.8	**59.0**		

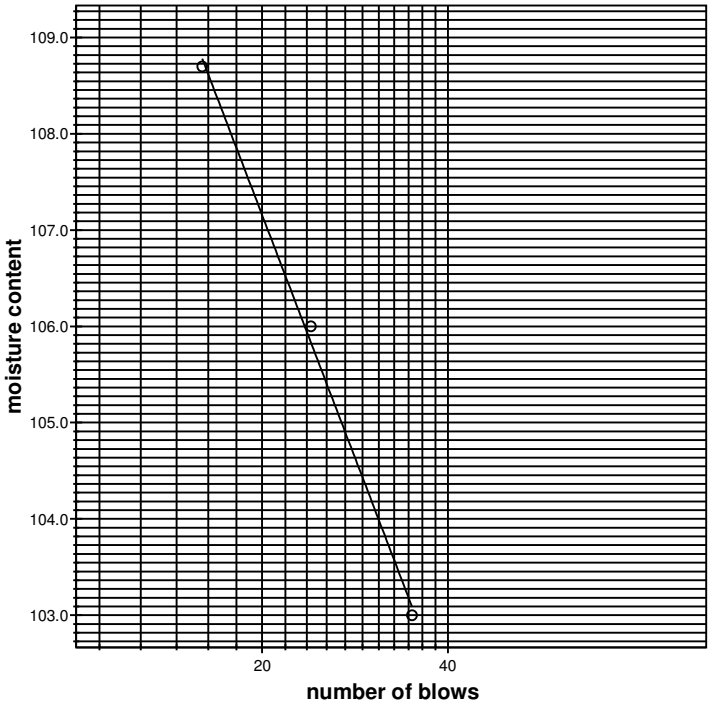

Appendix C: Summary of soil description

Sample number	Description
S1	(moist) stiff reddish brown silty clay
S2	(moist)stiff reddish brown silty clay
S3	(moist) stiff reddish brown silty clay
S4	(moist) greyish to pinkish brown clayey silt
S5	(moist) soft black clay**
S6	(moist) black silty clay**
S7	(moist) firm brownish red clayey silt
S8	(moist) stiff brownish red clayey silt
S9	(moist) soft brownish red silty clay
S10	(moist) stiff brownish red silty clay
S11	(moist)stiff reddish brown silty clay
S12	(moist) stiff reddish brown silty clay
S13	loose sandy silt with some gravel & boulders
S14	(moist) stiff silty clay
S15	(moist) stiff silty clay
S16	(moist) stiff silty clay
S17	very stiff coarse silty clay
S18	(moist) firm silty clay
S19	(moist) soft brown silty clay
S20	poorly graded clayey gravel
S21	loose sandy silt with some boulders
S22	(moist) firm silty clay
S23	(moist) firm silty clay
S24	(moist) firm silty clay
S25	(moist) stiff coarse silty clay
S26	(moist) stiff silty clay
S27	(moist) stiff black clay**
S28	(moist) stiff black clay**
S29	(moist) stiff black clay**
S30	(moist) stiff black clay**
S31	(moist) firm clayey silt
S32	(moist) soft greyish brown clay
S33	(moist) soft greyish brown clay
S34	(moist) firm clayey silt
S35	(moist) soft yellowish brown clay
S36	(moist) firm black clay**
S37	(moist) firm black clay**
S38	(moist) stiff reddish brown clay
S39	(moist) stiff brown clay
S40	(moist) stiff brown clay

Sample number	Description
S41	(moist) dense brown clayey silt
S42	(moist) firm brown clayey silt
S43	(moist) firm red silty clay
S44	(moist) stiff red silty clay
S45	(moist) firm dark brown clayey silt
S46	(moist) very stiff silty clay
S47	(moist) very stiff silty clay
S48	(moist) very stiff silty clay
S49	(moist) very stiff silty clay
S50	(moist) very stiff silty clay
S51	(moist) soft clayey silt
S52	(moist) stiff reddish silty clay
S53	(moist) stiff brown silty clay
S54	(moist) firm brown clay
S55	(moist) stiff brown silty clay
S56	(moist)stiff brown silty clay
S57	(moist) stiff brown silty clay
S58	(moist) stiff black clay**
S59	(moist) stiff dark brown clay**
S60	(moist) stiff black clay**
S61	(moist)stiff black clay**
S62	(moist) soft clayey silt
S63	(moist) firm silty clay
S64	(moist) stiff reddish brown clay
S65	(moist) stiff coarse silty clay
S66	(moist) firm brownish red clayey silt
S67	(moist) firm brownish red clayey silt
S68	(moist) firm reddish brown clayey silt
S69	(moist) firm reddish brown clayey silt
S70	(moist) firm reddish brown clayey silt
S71	medium dense poorly graded clayey gravel
S72	Saprolite (weathered basalt)*
S73	Saprolite (weathered basalt)*
B1(S74)	(moist) stiff black clay**
B2 (S75)	(moist) stiff dark grey clay
B3 (S76)	(moist) stiff black clay**
B4 (S77)	(moist) stiff black clay**
B5 (S78)	(moist) stiff dark grey clay

* indicating soil with original relicts of parent rock (discontinuities)

** indicating black cotton soils

The identification and naming is based on the British standard field soil identification procedures (British Standard Institution, 1981).

Appendix D: The Advanced Spaceborne Thermal Emission and Reflection Radiometer, ASTER

The Advanced Spaceborne Thermal Emission and Reflection Radiometer, ASTER covers a wide spectral range in the VNIR, SWIR and TIR regions of the electromagnetic spectrum and has a high spatial and radiometric resolution, and stereoscopic capability (ERSDAC, 2001). Apart from the five bands in the thermal infrared portion, ASTER has nine bands situated in the visible, near infrared and short wave infrared region of the electromagnetic spectrum. Some of the ASTER bands in the SWIR wavelength region are situated in the wavelength regions that are well known to be related with characteristic absorption features of clay minerals in the SWIR portion (table 2.3 on page17) of the electromagnetic spectrum. However, ASTER band widths are on the order of 10 nm and are very coarse when compared with the laboratory acquired input spectra. The ranges of wavelength regions covered by ASTER bands together with their respective characteristics are shown on the following table and figure.

Characteristic	VNIR	SWIR	TIR
Spectral Range	1*: 0.52 - 0.60 µm Nadir looking	4: 1.600 - 1.700 µm	10: 8.125 - 8.475 µm
	2: 0.63 - 0.69 µm Nadir looking	5: 2.145 - 2.185 µm	11: 8.475 - 8.825 µm
	3N: 0.76 - 0.86 µm Nadir looking	6: 2.185 - 2.225 µm	12: 8.925 - 9.275 µm
	3B: 0.76 - 0.86 µm Backward looking	7: 2.235 - 2.285 µm	13: 10.25 - 10.95 µm
		8: 2.295 - 2.365 µm	14: 10.95 - 11.65 µm
		9: 2.360 - 2.430 µm	
Ground Resolution	15 m	30m	90m
Data Rate (Mbits/sec)	62	23	4.2
Cross-track Pointing (deg.)	±24	±8.55	±8.55
Cross-track Pointing (km)	±318	±116	±116
Swath Width (km)	60	60	60
Detector Type	Si	PtSi-Si	HgCdTe
Quantization (bits)	8	8	12

*the numbers indicate the band number

Table 0-4: Summary of some of the characteristics of ASTER band passes in the VNIR, SWIR and TIR region of the electromagnetic spectrum; in van der Meer (2004b).

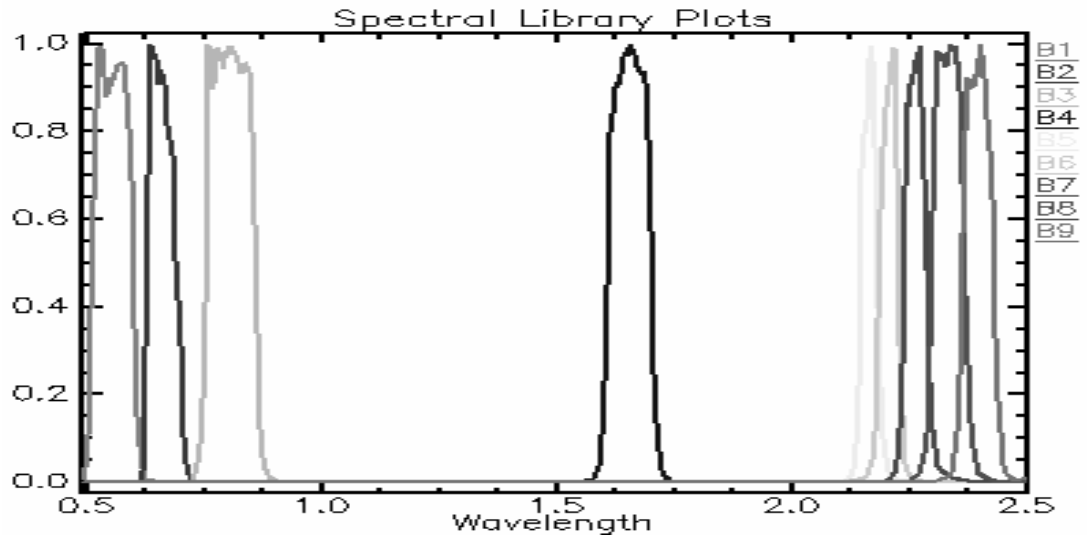

Figure 0-1: ASTER band passes in the 500 nm to 2500 nm wavelength range.

Appendix E: Raw regression coefficients of PLSR models

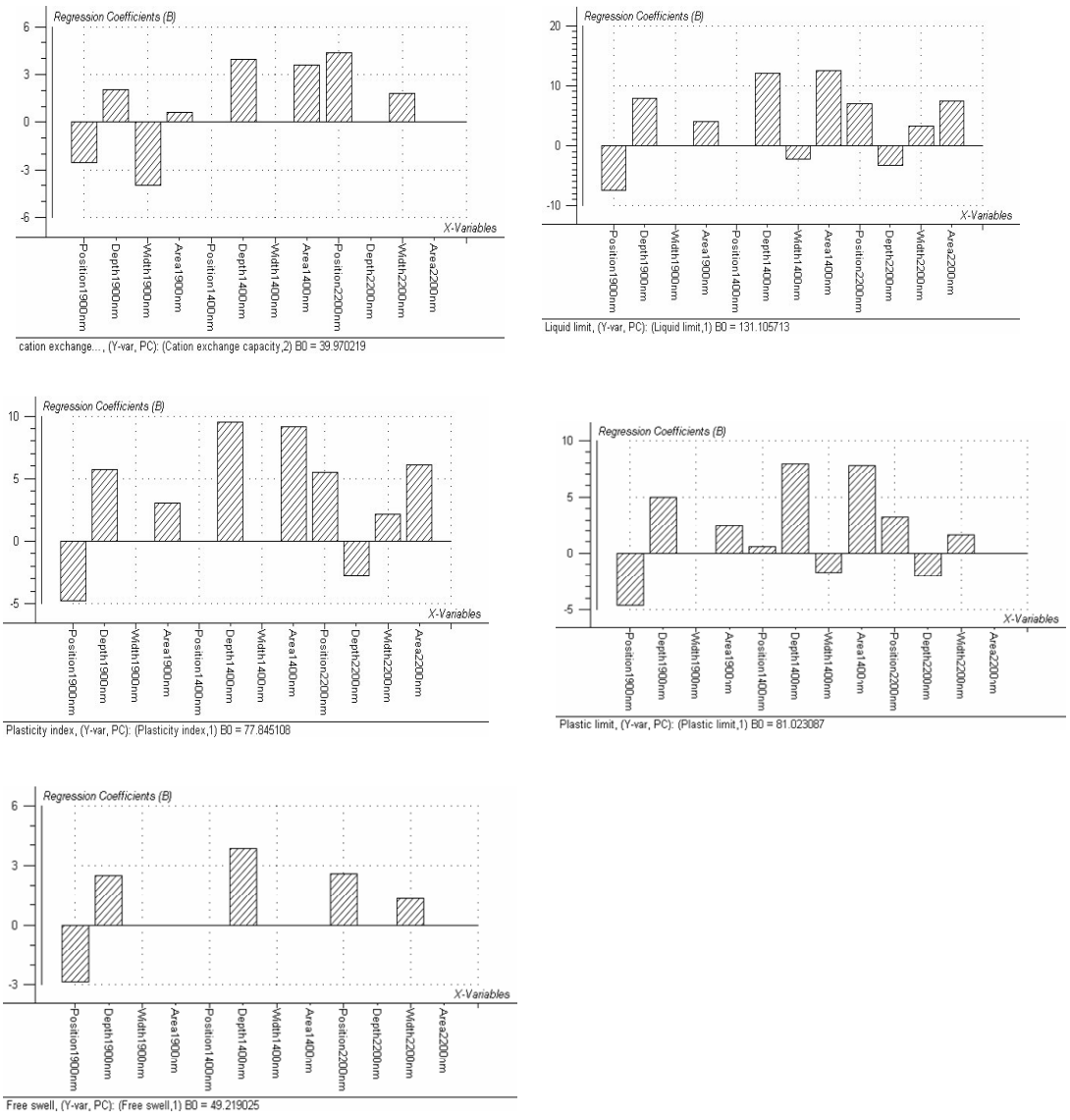

Figure 0-2: Raw regression coefficients calculated for the five engineering parameters from the knowledge driven PLSR prediction; CEC, LL, PI, PL and FS respectively.

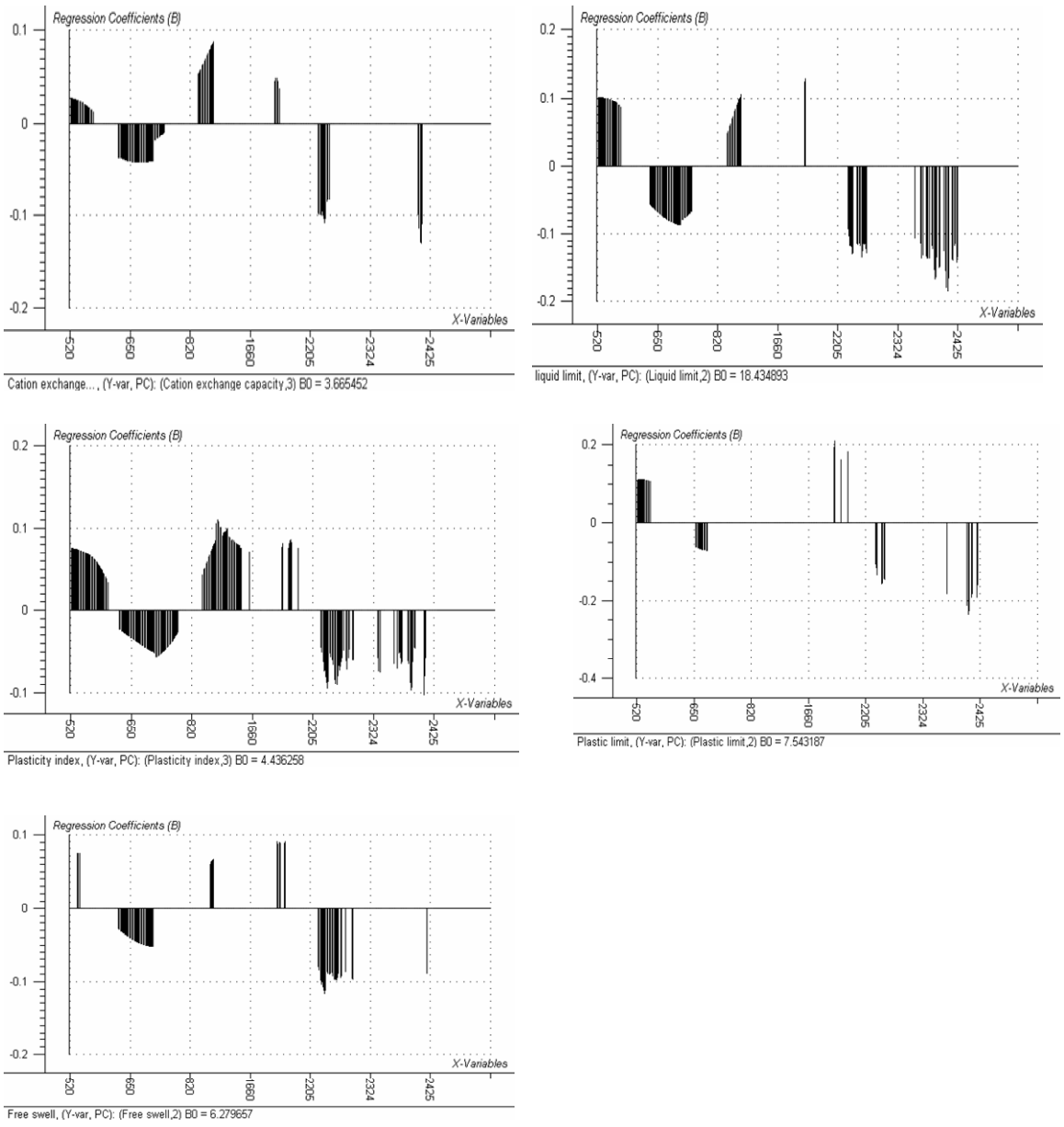

Figure 0-3: Raw regression coefficients calculated for the five engineering parameters from the data driven PLSR prediction; CEC, LL, PI, PL and FS respectively.

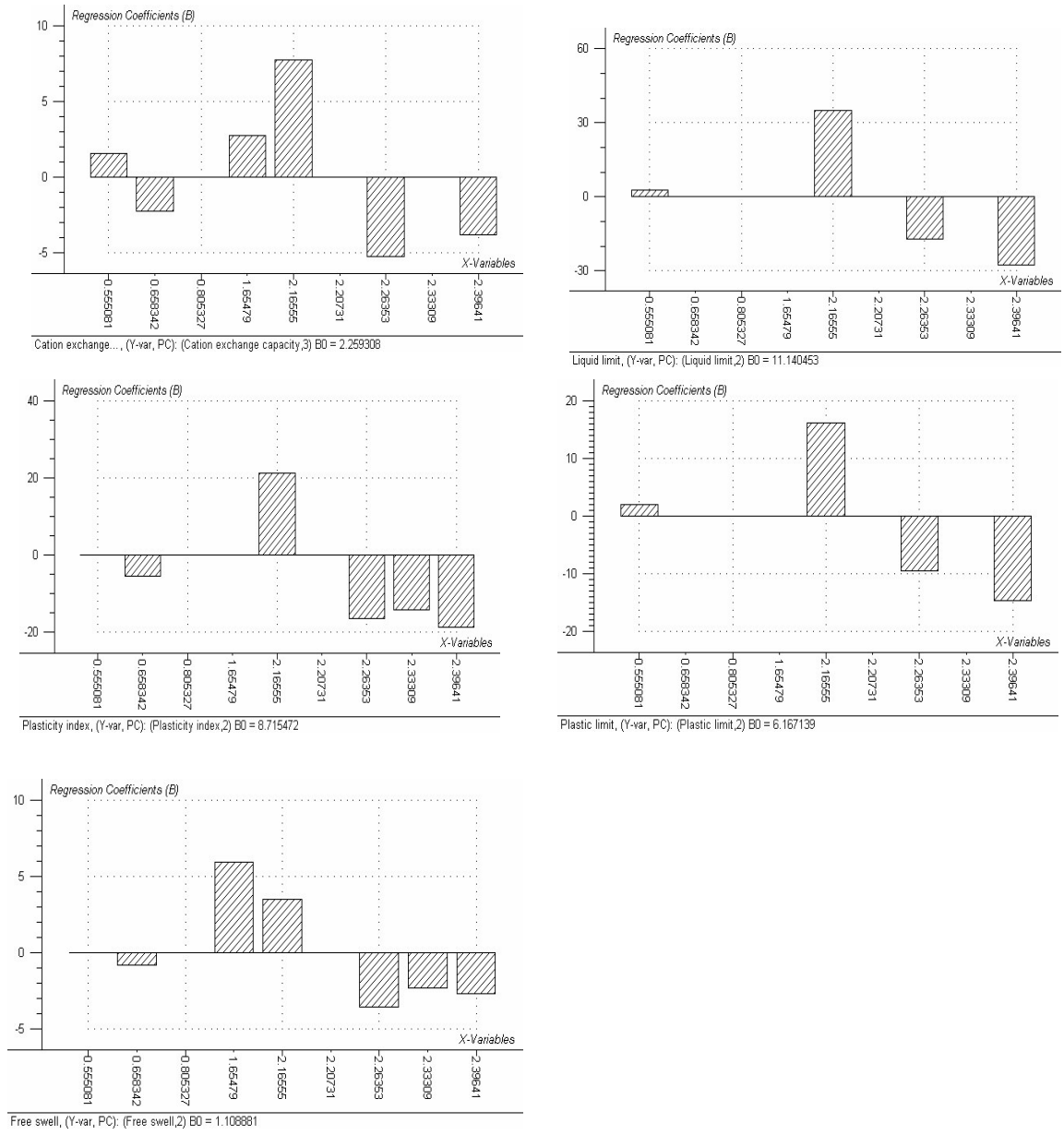

Figure 0-4: Raw regression coefficients calculated for the five engineering parameters from ASTER band sets PLSR prediction; CEC, LL, PI, PL and FS respectively.